Reaction of Transition Metal Complexes via Silicon Hypervalent Structure

（ケイ素超原子価構造を経由する遷移金属錯体の反応）

理学研究科

物質分子系専攻

2009 年 3 月

福本　晃造

（Kozo Fukumoto）

Contents

List of Abbreviations

TMS	Trimethylsilyl, Me_3Si
OTf	Trifluoromethanesulfonate, OSO_2CF_3
Bn	Benzyl, $C_6H_5CH_2$
n-Hex	*n*-hexyl, C_6H_{13}
cyclo-Hex	*cyclo*-hexyl, C_6H_{11}
nbd	2,5-norbornadiene
Cp	Cyclopentadienyl, η^5-C_5H_5
Cp*	Pentamethylcyclopentadienyl, η^5-C_5Me_5
py	Pyridine

List of Complexes

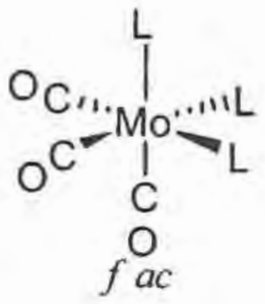

f ac

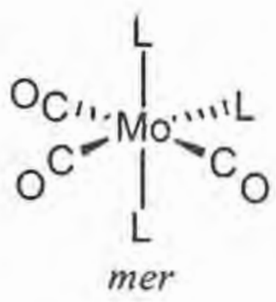

mer

No. of Compounds	L
fac-**2.1**	CH_3CN
fac- or *mer*-**2.2**	$P(OMe)_3$
fac- or *mer*-**2.3**	$P(OEt)_3$
fac- or *mer*-**2.4**	$P(OPh)_3$
fac- or *mer*-**2.5**	$P(NMeCH_2CH_2NMe)(OMe)$

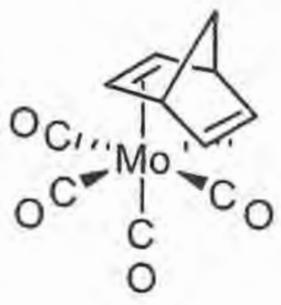

cis-**2.6**

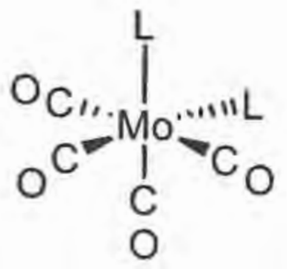

cis

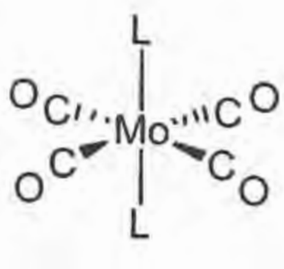

trans

No. of Compounds	L
cis- or *trans*-**2.7**	$P(OMe)_3$
cis- or *trans*-**2.8**	$P(OPh)_3$
cis- or *trans*-**2.9**	$PPh_2(OMe)$

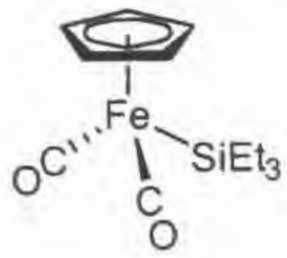

3.1

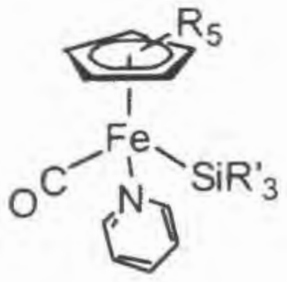

No. of Compounds	R, R'
3.3	R = H, R' = Et
3.5	R = Me, R'$_3$ = Me$_2$Ph
3.7	R = H, R' = Ph

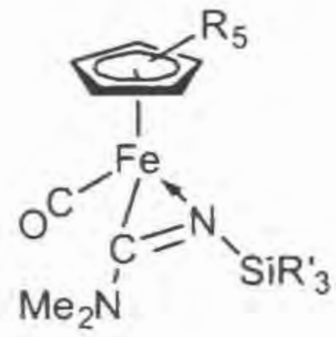

No. of Compounds	R, R'
3.4	R = H, R' = Et
3.6	R = Me, R'$_3$ = Me$_2$Ph

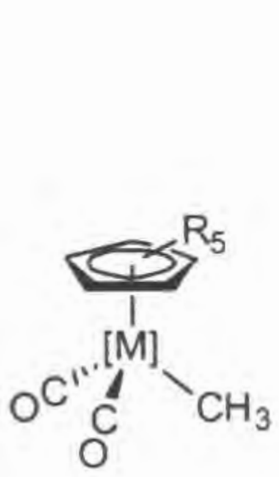

No. of Compounds	[M]	R_5
3.8	Fe	Me_5
3.9	Fe	H_4Me
3.2	Fe	H_5
3.10	Fe	H_4I
3.11	Mo(CO)	Me_5
3.12	Mo(CO)	H_5

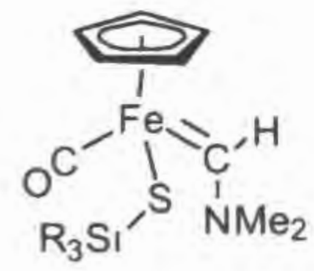

No. of Compounds	R
3.13	R = Et
3.14	R = Ph

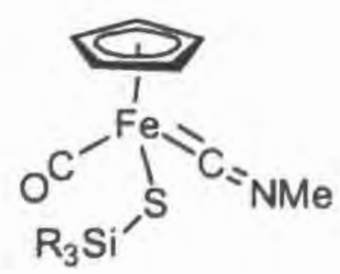

No. of Compounds	R
3.15	R = Et
3.16	R = Ph

Chapter 1.

General Introduction

Chapter 1.

General Introduction

1-1 Prologue

Silicon situating just below carbon in the periodic table has pronounced capacity for the enlargement of the coordination sphere. Compounds of silicon with coordination number greater than four have been known since the beginning of the 19th century, when Gay-Lussac[1.1] and J. Davy[1 2] first observed, independently, the formation of the $[SiF_6]^{2-}$ ion and of the adduct of SiF_4 with ammonia. The formation and structure of hypercoordinate silicon compounds continue to be an area of lively interest,[1 3-1 5] which has been reviewed.[1 6-1 14] In recent year, interest in hypercoordinate silicon compounds has grown considerably, because of their unexpected reactivity. Interest in this field started with studies of nucleophilic activation at silicon. It was shown that some reactions, such as racemization of optically active silicon compounds, hydrolysis and alcholysis of tetracoordinate chlorosilanes, are highly accelerated by nucleophiles (Scheme 1-1).[1 15] These studies suggested that a pentacoordinate intermediate reacts with nucleophiles faster than does the starting tetracoordinate silane. The enhanced reactivity of pentacoordinate silicon compounds in nucleophilic substitutions was demonstrated experimentally[1 16] and was supported by calculations.[1 17-18]

In contrast to the well-developed organosilicon chemistry concerning

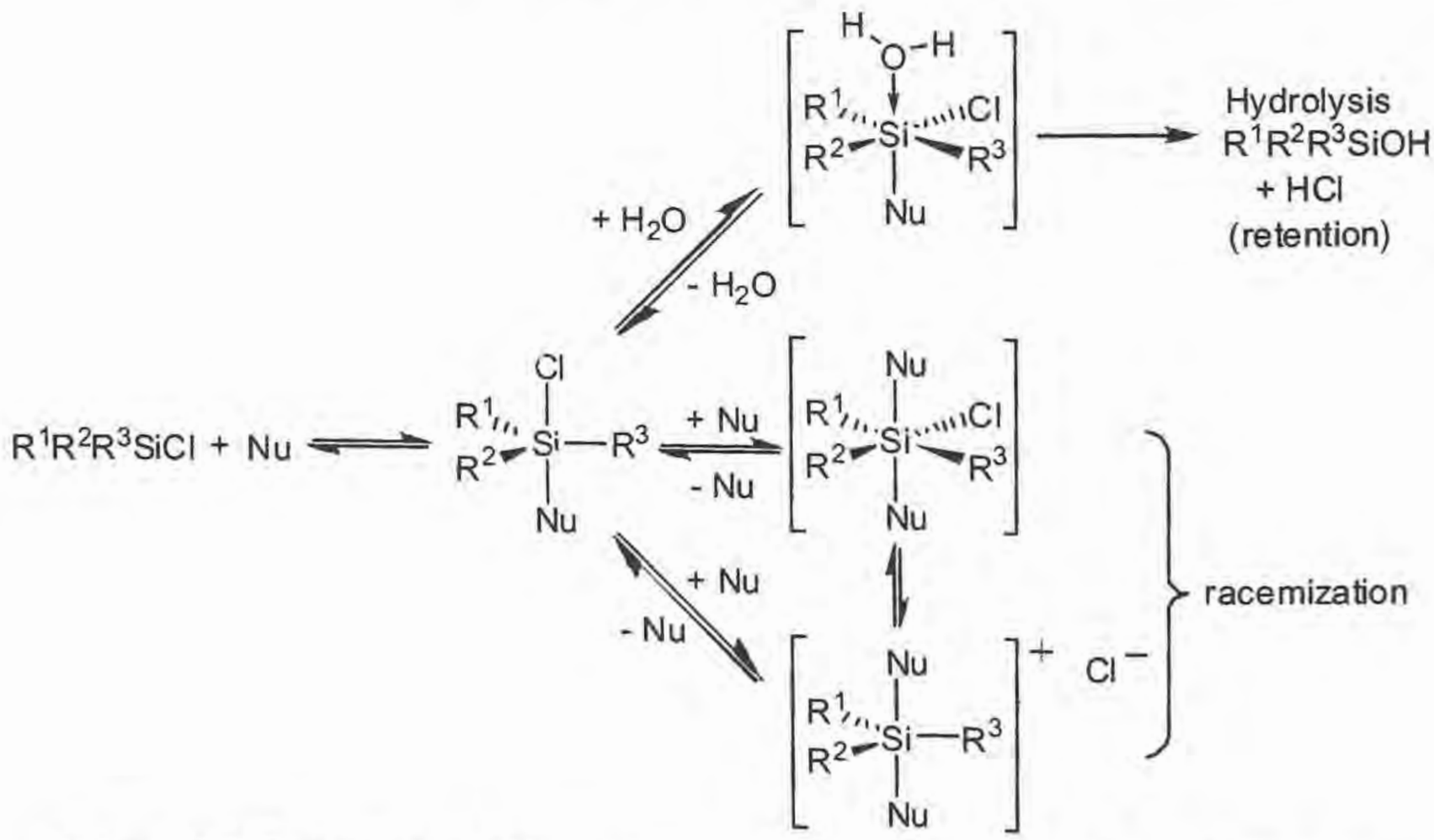

Scheme 1-1. Racemization of hypercoordinate silane and hydrolysis of chlorosilane.

hypervalent silicon structures, the role of hypervalency of silicon in coordination chemistry of transition metals is much less investigated. In this thesis, I describe the first example of trialkylhalosilane catalyst for geometrical isomerization of octahedral transition metal complexes where a hypervalent silicon compound with O→Si interaction plays a crucial role. I also describe unprecedented N-CN bond cleavage of cyanamide (R_2N-CN) where the formation of a hypervalent silicon compound with N→Si interaction in a coordination sphere of a transition metal is a trigger of the N-CN bond activation.

It might be pertinent to take a cursory look at examples of N→Si and O→Si interaction to afford pentacoordinate silicon compounds and summarize briefly findings about pentacoordinate silicon compounds.

1-2 Preparation of Pentacoordinate Silicon Compounds

Pentacoordinate silicon species may be prepared according to the following general methods[1 12]:

(1) By addition of an anion to an organosilane (e.g., eq. 1-1)[1 19] or to a spirosilane (e.g., eq. 1-2)[1 19-1 20] to give an anionic pentacoordinate silicon complex.

$$\underset{(n = 1\text{-}3)}{Ph_nSi(OMe)_{4-n}} + MeO^-[K, 18\text{-crown-6}]^+ \longrightarrow [Ph_nSi(OMe)_{5-n}]^-[K, 18\text{-crown-6}]^+ \qquad (1\text{-}1)$$

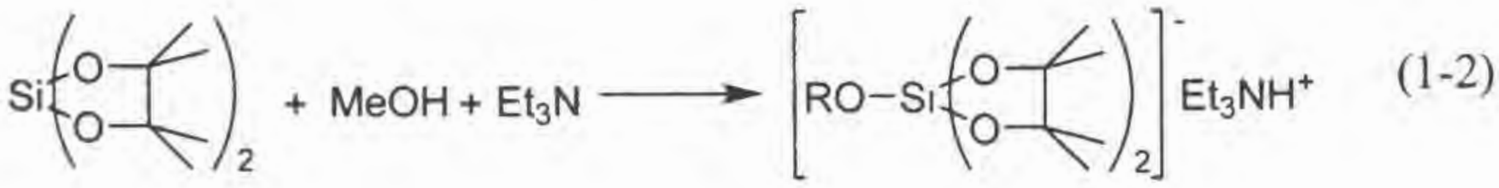

(1-2)

(2) By inter- or intramolecular coordination of a neutral donor to silicon, giving a neutral or a cationic pentacoordinate silicon complex, depending on the nature of the substituents (e.g., Figure 1-1).[1 21-1 26]

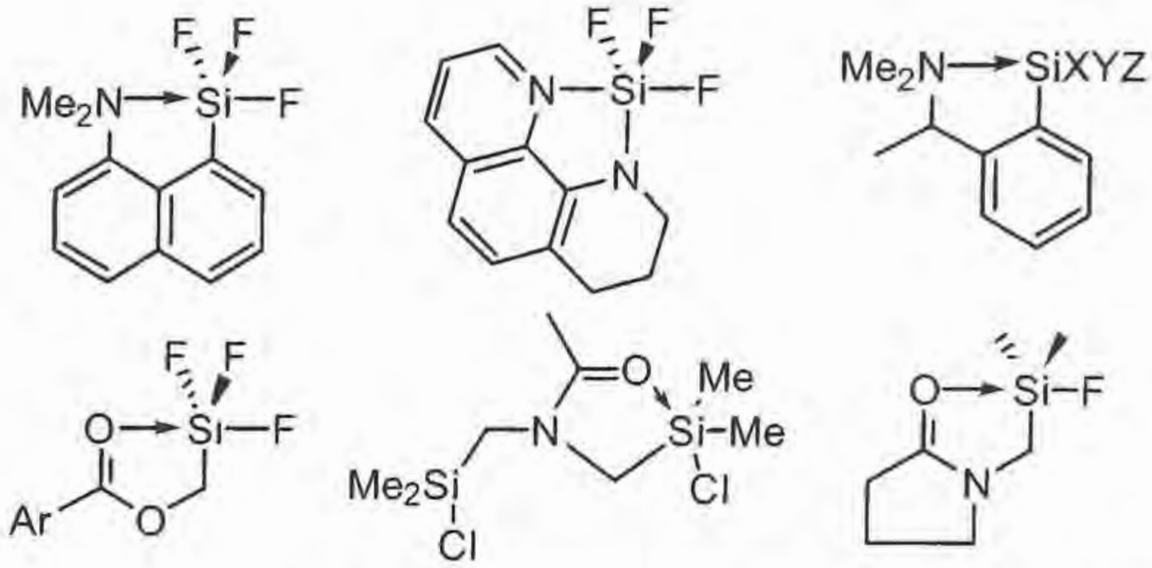

Figure 1-1. Oragenosilicon compounds donated by a neutral donor.

(3) By substitution of an organosilane: (a) by a bidentate ligand to give an anionic or a cationic pentacoordinate complex according to the nature of the bidentate ligands (e.g., eq. 1-3)[1 19] or (b) by triethanolamine or another trialkanolamine to give silatranes, or by tris(2-aminoethyl)amine to give triazasilatranes (e.g., eq. 1-4).[1 20, 1 27]

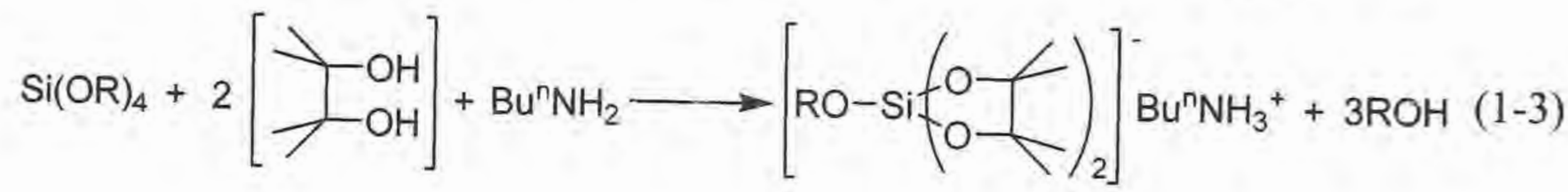

(1-3)

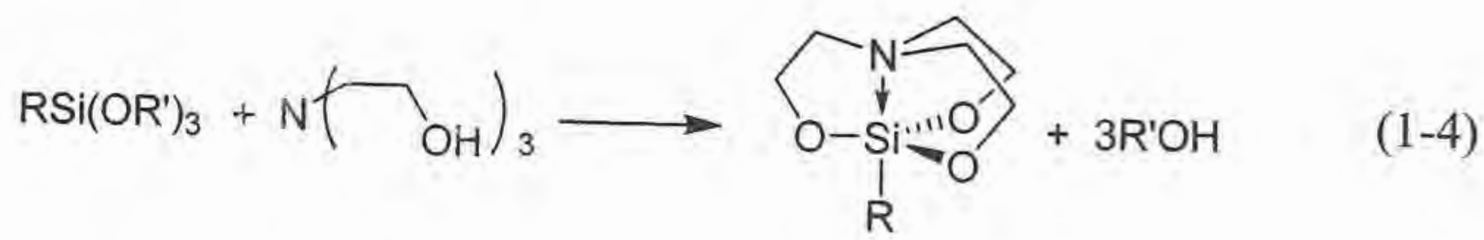

(1-4)

1-3 N→Si Coordination to an Organosilane

Numerous neutral pentacoordinate silicon compounds have been preparated. For example, intramolecular chelation of a donor atom to the silicon atom can be facilitated (Figure. 1-2).[1 28]

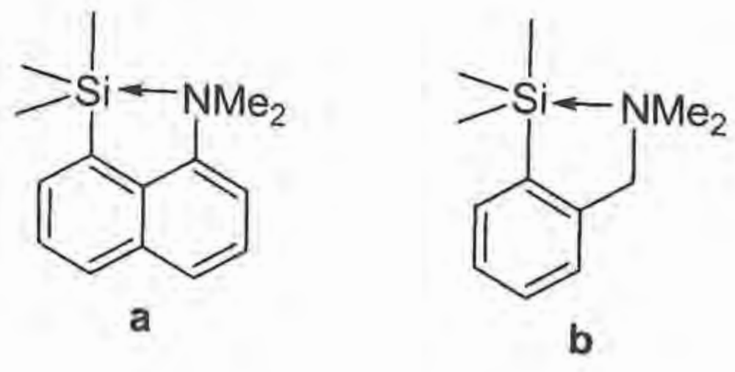

Figure 1-2. Chelate ligands on N→Si intramolecular coordination .

Variable temperature ^{1}H NMR studies[1 29] of monofunctional and bifunctional

derivatives **c**, **d** and **e** showed two signals for diastereotopic N-methyl groups at low temperature thus indicating intramolecular coordination of N→Si. The bond energies were calculated to lie in the range 38.4-72 kJ mol^{-1}, the stability of the chelated form depends on X in the order: OR < H < F, SF < OAc, Cl, Br. ^{19}F NMR studies of fluorosilanes **f** established the apicophilicity of X related to fluorine.[130] Resonance due to axial fluorine is found at relatively low field, and an upfield shift indicates occupation of an equatorial site.[131] The experiments showed fluorine to be more apicophilic than H, OR and NR_2, but less than Cl.[130] However, fluorine appears to be more apicophilic than chlorine in compound **g**.[132]

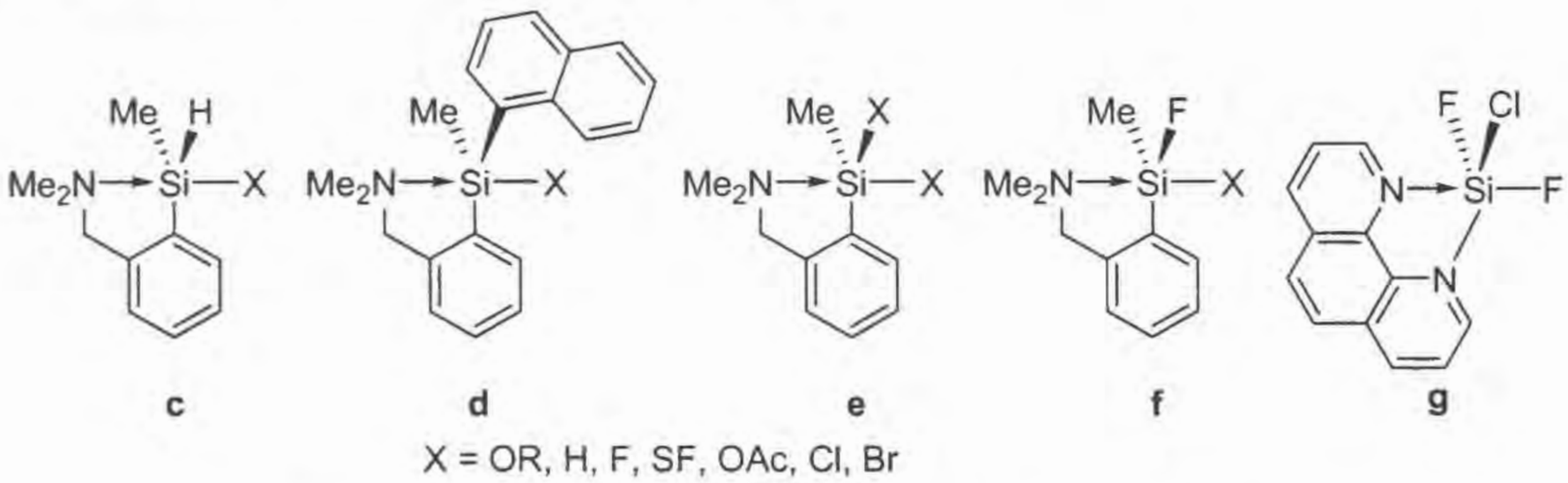

Figure 1-3. Pentacoordination silane stabilized by N atom.

1-4 O→Si Coordination to an Organosilane

In 1970, Boer and van Remoortere determined, by X-ray crystallography, the structure of compound **h**.[133] They found that one silicon atom is pentacoordinated with a distorted trigonal bipyramidalal geometry, the axial sites being occupied by the two oxygen atoms. The coordinative O→Si bond is longer (2.613 Å) than the covalent O-Si bond (1.670 Å).

Numerous compounds with Si-halogen bonds and O→Si coordination have been described.[134] The X-ray crystal structure determination of **i** showed that the Si(1)-Cl(1) bond at pentacoordinate silicon is 15 % longer (2.35 Å) than the Si(2)-Cl(2) bond at tetracoordinate silicon (2.05 Å) (Figure 1-4). The geometry around the silicon atom is a slightly deformed trigonal bipyramidal with an O→Si distance of 1.913 Å, which is much shorter than the O→Si coordinative bond in **h**.

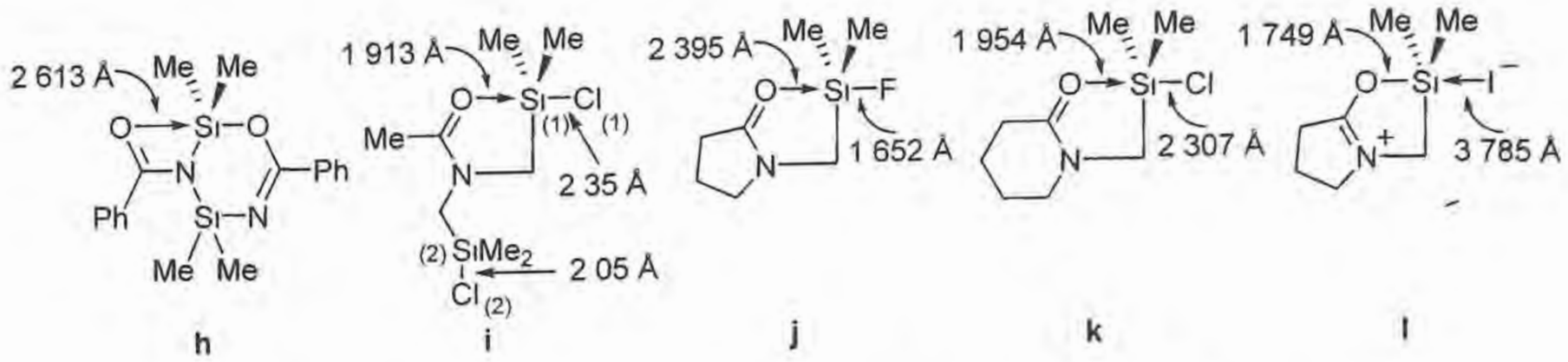

Figure 1-4. Pentacoordination silane stabilized by O atom.

The fact that in these complexes the length of the coordinative bond depends on the other equatorial ligand is particularly well illustrated for compounds **j**, **k** and **l** (Figure 1-4). Three types of compounds can be distinguished. In **j** of the first type compound, the coordinative O-Si distance is 2.395 Å, whereas the length of the Si-F bond is 1.652 Å, which is only 0.1 Å longer than an Si-F bond for tetrahedral Si.[1.35-1 36] The geometry around the silicon atom is that of a tetrahedron monocapped by the oxygen atom. In the chloro compound **k** (second type), the O→Si coordinative bond is shorter than that in the first type compound (e.g., **j**).[1 35] In this case, the geometry around the silicon corresponds to a slightly distorted bipyramidal. In the third type, including a compound **l**, the O-Si distance (1.749 Å) is much more shorter than that in **k**, whereas the opposite X-Si bonds are very long (3.734 Å for the Si-I distance in **l**).[1 35-1 37] The geometry around the silicon atom in the derivative **l** is that of inverted (compared to the first type) tetrahedron monocapped by iodide ions. The changes in the O-Si lengths and in the geometries around the silicon atoms on going from **j** to **k** and **l** mimic the course of S_N2 substitution at silicon occurring with inversion of configuration. **j** represents the initial attack of the oxygen at the silicon, **k** the transition state, and **l** the final attack close to the "reaction product."[1 38]

1-5 References

1.1 Gay-Lussac, J.L.; Thenard, L. J. *Mémores des Physique et de Chimie de la Société d'Arcueil* **1809**, *102*, 317.

1.2 Davy, J. *Phil. Trans. Roy. Soc. London* **1812**, 102, 352.

1.3 (a) Corriu, R. J. P.; Guérin, C.; Moreau, J. J. E. *Top. Stereochem.* **1984**, *15*, 43. (b) Corriu, R. J. P.; Guérin, C.; Moreau, J. J. E. *The Chemistry of Organic Silicon Compounds*. Patai, S. and Rappoport, Z.; Eds. (John Wiley, Chichester, **1989**), Chapter 4.

1.4 Yamamura, M.; Kano, N.; Kawashima, T. *J. Org. Chem.* **2008**, *73*, 8244.

1.5 Dorsey, C. L.; Gabbai, F. P. *Organometallics* **2008**, *27*, 3065.

1.6 Tandura, S. N.; Voronkov, M. G.; Alekseev, N. V. *Main Group Met. Chem.* **1987**, *10*, 209.

1.7 Shklover, V. E.; Struchkov, Y. T.; Voronkov, M. G. *Russ. Chem. Rev.* **1989**, *58*, 211.

1.8 Lukevics, E.; Pudova, O.; Sturkovich, R. *Molecular Structure of Organosilicon Compounds* (Ellis Horwood, Chichester, **1989**).

1.9 Corriu, R. J. P.; Young, J. C. *The Chemistry of Organic Silicon Compounds*, Patai, S. And Rappoport, Z.; Eds (John Wiley, Chichester, **1989**), Chapter 20.

1.10 Gel'mbol'dt, V. O.; Ennan, A. A. *Russ. Chem Rev.* **1989**, *58*, 371.

1.11 Holmes, R. R. *Chem. Rev.* **1990**, *90*, 17.

1.12 Chuit, C.; Corriu, R. J. P.; Reyé, C.; Young, J. C. *Chem. Rev.* **1993**, *93*, 1371.

1.13 Chuit, C.; Corriu, R. J. P.; Reye, C. *Chemistry of Hypervalent Compounds*, Akiba, K.; Eds (Wiley-VCH, **1999**), 81.

1.14 Kira, M.; Zhang, L. C. *Chemistry of Hypervalent Compounds*, Akiba, K.; Eds (Wiley-VCH, **1999**), 147.

1.15 (a) Corriu, R. J. P.; Dabosi, G.; Martineau, M. *J. Organomet. Chem.* **1978**, *150*, 27. (b) Corriu, R. J. P.; Dabosi, G.; Martineau, M. *J. Organomet. Chem.* **1978**, *154*, 33. (c) Corriu, R. J. P.; Dabosi, G.; Martineau, M. *J. Organomet. Chem.* **1980**, *186*, 25.

1.16 Corriu, R. J. P. *J. Organomet. Chem.* **1990**, *400*, 81.

1.17 Deiters, J. A.; Holmes, R. R. *J. Am. Chem. Soc.* **1990**,*112*, 7197.

1.18 Gordon, M. S.; Carroll, M. T.; Davis, L. P.; Burggraf, . W. *J. Phys. Chem.* **1990**, *94*, 8125.

1.19 Holmes, R. R. *Chem. Rev.* **1996**, *96*, 927.

1.20 Frye, C. L. *J. Am. Chem. Soc.* **1970**, *92*, 1205.

1.21 Corriu; R. J. P.; Mazhar, M.; Poirier, M.; Royo, G. *J. Organomet. Chem.* **1986**, *306*, C5.

1.22 Klebe, G.; Hensen, K.; Fuess, H. *Chem. Ber.* **1983**, *116*, 3125.

1.23 (a) Corriu, R. J. P.: Royo, G.: de Saxé, A. *J. Chem. Soc. Chem. Commun.* **1980**, 892.
(b) Boyer, J.; Breiére, C.; Carré, F.; Corriu, R. J. P.; Kpoton, A.; Poirier, M.; Royo, G.; Young, J. C. *J. Chem. Soc. Dalton Trans.* **1989**, 43.

1.24 Voronkov, M. G.; Frolov, Yu. L.; D'yakov, V. M.; Chipanina, N. N.; Gubanova, L. I.; Gavrilova, G. A.; Klyba, L. V.; Aksamentova, T. N. *J. Organomet. Chem.* **1980**, 201, 165.

1.25 Onan, K. D.; McPhail, A. T.; Yoder, C. H.; Hillyard, R. W. *J. Chem. Soc. Chem. Commun.* **1978**, 209.

1.26 Macharashvili, A. A.; Shklover, V. E.; Struchkov, Yu. T.; Oleneva, G. I.; Kramarova, E. P.; Shipov, A. G.; Baukov, Y. I. *J. Chem. Soc. Chem. Commun.* **1988**, 683.

1.27 Verkade, J. G. *Coord. Chem. Rev.* **1994**, *137*, 233.

1.28 Jastrzebski, J. T. B.H.; van Koten, G. *Adv. Organomet. Chem.* **1993**, *35*, 241.

1.29 Corriu, R. J. P.; Royo, G.; de Saxcé, A. *J. Chem. Soc. Chem. Commun.* **1980**, 892.

1.30 Corriu, R. J. P.; Poirer, M., Royo, G. *J. Organomet. Chem.* **1982**, *233*, 165.

1.31 Breliére, C.; Carré, F.; Corriu, R. J. P.; de Saxcé, A.; Poirier, M.; Royo, G. *J. Organomet. Chem.* **1981**, *205*, C1.

1.32 Klebe, G.; Hensen, K. *J. Chem. Soc. Dalton Trans.* **1985**, 5.

1.33 Boer, F. P.; van Remoortere, F. P. *J. Am. Chem. Soc.* **1970**, *92*, 801.

1.34 Onan, K. D.; McPhail, A. T.; Yoder, C. H.; Hillyard, R. W. *J. Chem. Soc. Chem. Commun.* **1978**, 209.

1.35 Macharashvili, A. A.; Shklover, V. E.; Struchkov, Y. T.; Oleneva, G. I.; Kramarova, E. P.; Shipov, A. G; Baukov, Y. J. *J. Chem. Soc. Chem. Commun.* **1988**, 683.

1.36 Macharashvili, A. A.; Shklover, V. E.; Chernnikova, N. Y.; Antipin, M. Y.; Struchkov, Y. T.; Baukov, Y. I.; Oleneva, G. I.; Kramarova, E. P.; Shipov, A. G. *J. Organomet. Chem.* **1989**, *359*, 13.

1.37 Macharashvili, A. A.; Shklover, V. E.; Struchkov, Y. T.; Baukov, Y. I.; Kramarova, E. P.; Oleneva, G. I. *J. Organomet. Chem.* **1987**, *327*, 167.

1.38 Voronkov, M. G.; Pestunovich, V. A.; Baukov, Y. I. *Organomet. Chem. USSR* **1991**, *4*, 593.

Chapter 2.

Geometrical Isomerization of Molybdenum Complexes with Phosphites Catalyzed by Neutral or Cationic Silicon Compound

2-1 Introduction

2-1-1 Silicon Catalyst in Chemical Reactions

Organosilicon reagents are widely used, especially for organic synthesis, because of unique reactivity making highly efficient and selective organic reactions possible, ready availability, and relatively low toxicity.[21-22] In particular, they have extensively been used for carbon-carbon bond formation in the past three decades. And, several synthetically valuable named reactions have been created such as the Mukaiyama aldol reaction with silyl enolates (Scheme 2-1)[23-24], the Hosomi-Sakurai reaction with allylsilanes (Scheme 2-2)[25-26], and the Hiyama coupling with alkenyl-, alkynyl-, and arylsilanes (Scheme 2-3).[27] In these reactions, silicon compounds play important roles with the aid of a Lewis acid or a transition-metal complex, and are finally converted into other silicon compounds. In other words, these reactions require a stoichiometric amount of silicon compounds.

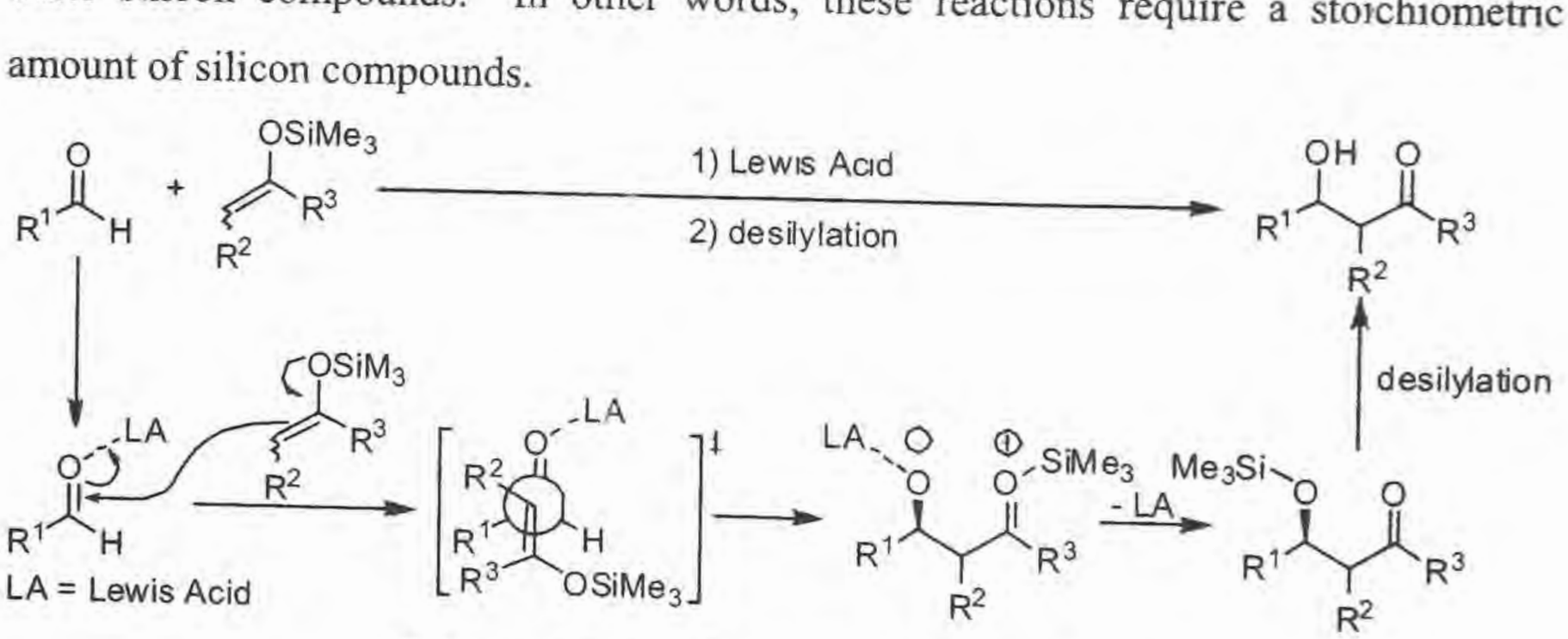

Scheme 2-1. Mukaiyama aldol reaction.

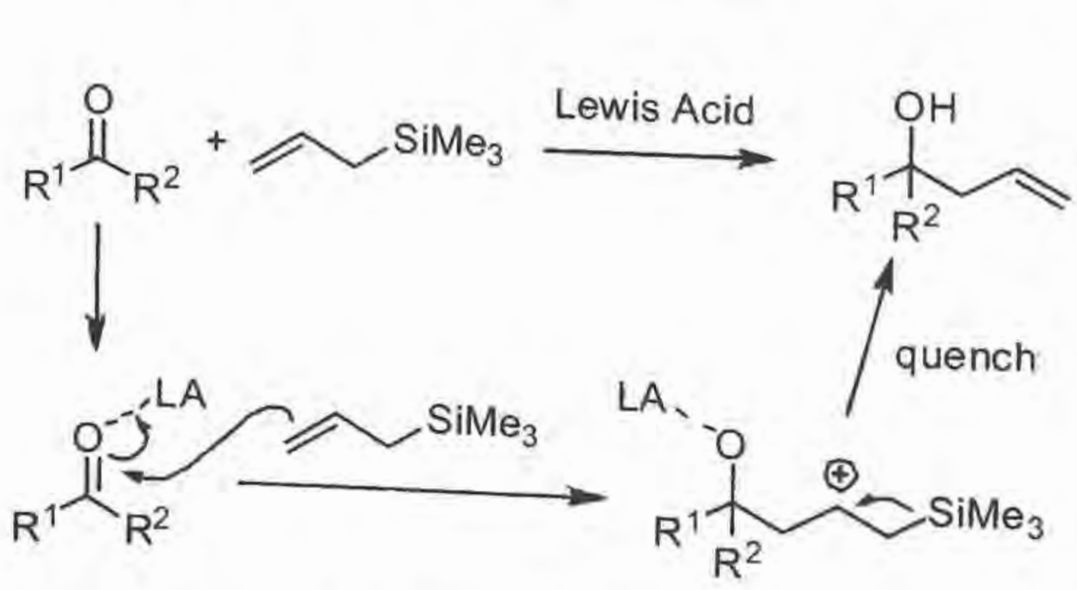

Scheme 2-2. Hosomi-Sakurai reaction.

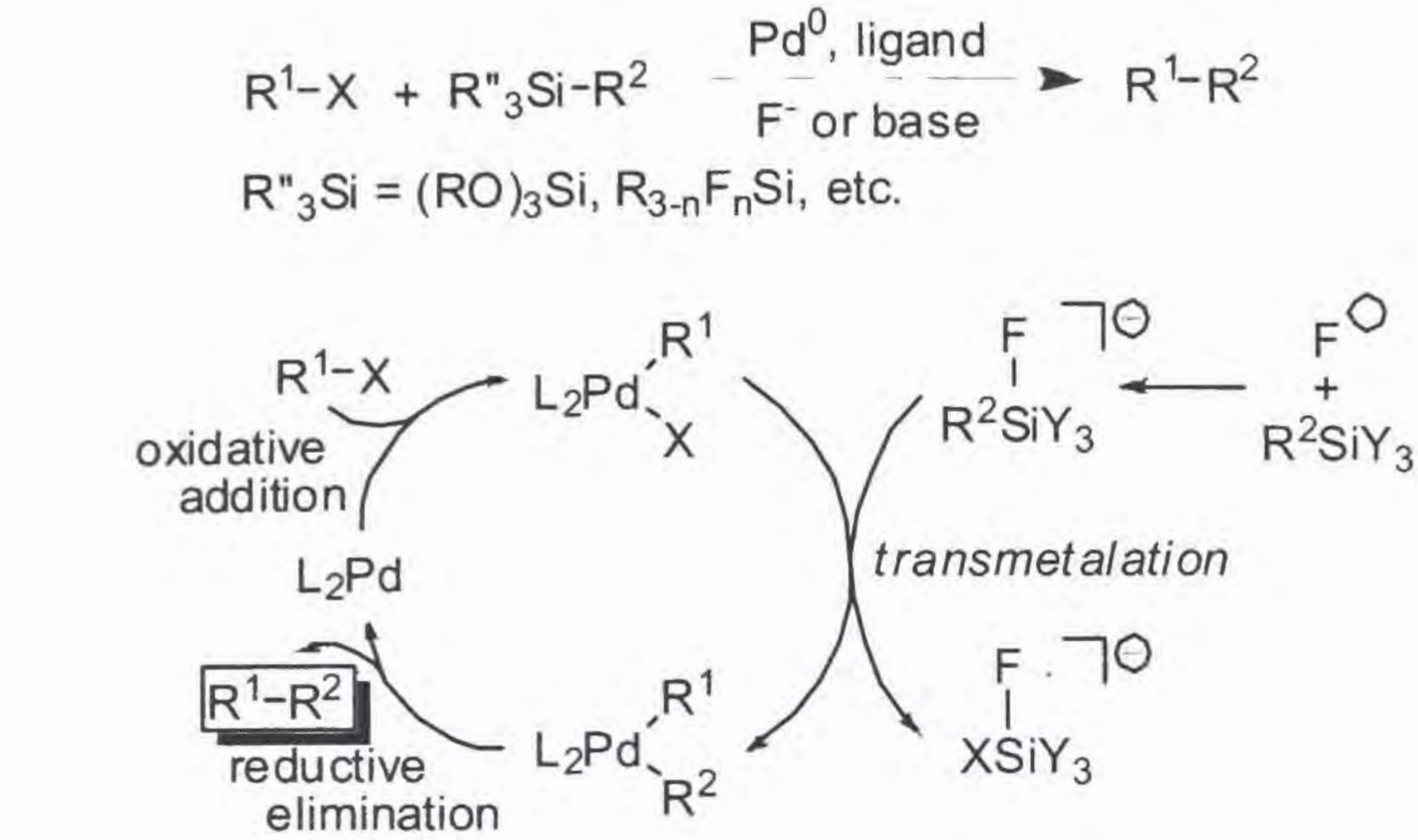

Scheme 2-3. Hiyama Coupling.

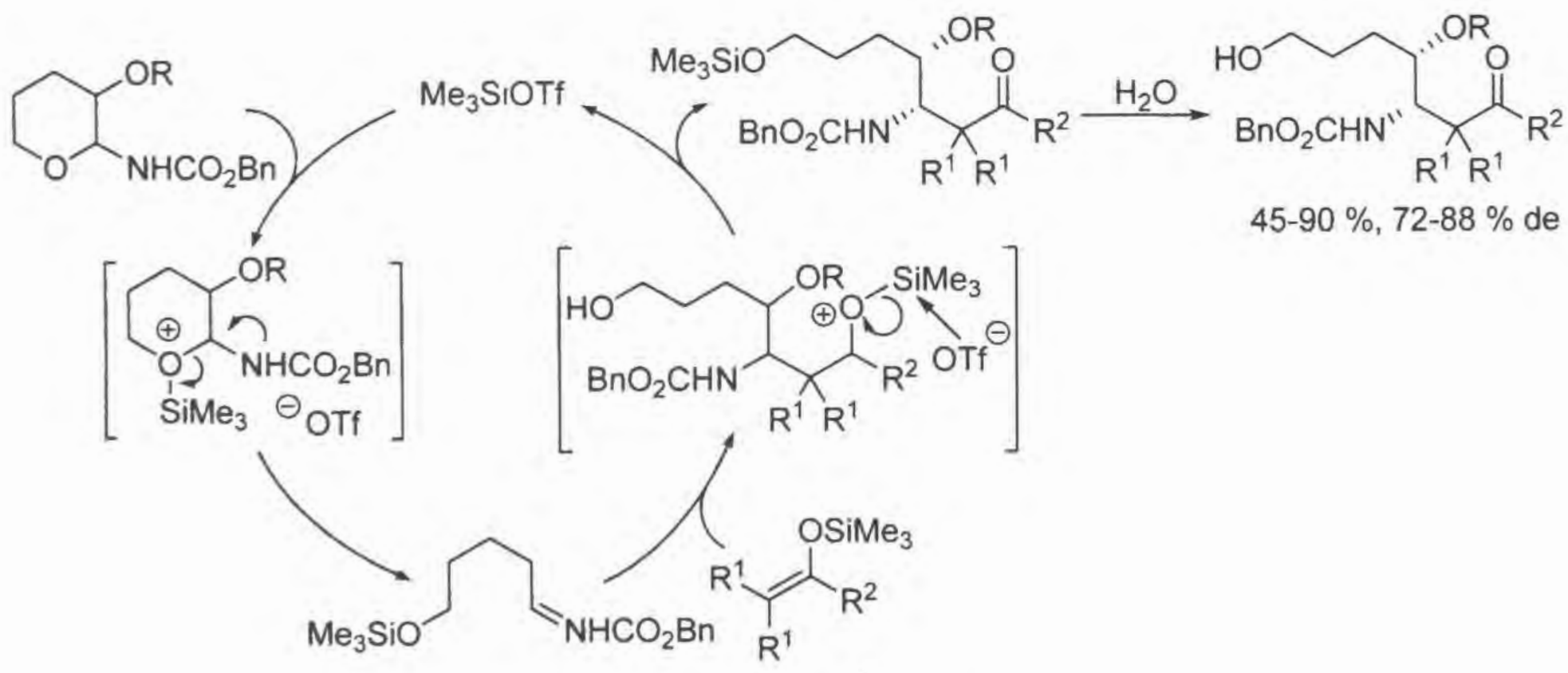

Scheme 2-4. Me_3SiOTf-catalyzed ring-opening.

Several silicon-based catalysts have been reported: R_3SiOTf, $R_3SiB(OTf)_4$, $R_3SiB(OTf)_3Cl$, $R_3Si(SO_2F)_2$, and $R_3SiN(Tf)_2$.[22] These catalysts can be described as containing R_3Si^+ and are considered to be a Lewis acid. For example, Kobayashi et al. reported the TMSOTf-catalyzed ring-opening of benzyl (3-oxytetrahydropyran-2-yl)carbamates with a silyl enolate with high 1,2-syn diastereoselectivity (Scheme 2-4)[28]. They proposed the reaction mechanism involving the coordination of Me_3Si^+ to the ring-oxygen followed by ring-opening activation to form an acyclic iminium ion intermediate. After the nucleophilic addition of a trimethylsilylated nucleophile to the iminium proton, TMSOTf is regenerated by the triflate anion attack onto the trimethylsilyl group of the nucleophile.

In contrast, no report described silane (a neutral four-coordinate silicon compound) serving as a catalyst instead of a reagent. It has been speculated that a silane is not a catalyst any more than an alkane is. In this chapter, I report the first example of a silane-catalyzed reaction. Me_3SiX (X = Cl, Br, I) and related silane compounds catalyze *fac-mer* isomerization of $[Mo(CO)_3\{P(OR)_3\}_3]$ at room temperature.

2-1-2 *fac-mer* Isomerizaiton of Phosphite Molybdenum Complexes

Tricarbonyltriphosphine or tricarbonyltriphosphite complexes of group 6 transition metals described as $M(CO)_3L_3$ (M = Cr, Mo, W; L = phosphine, phosphite) principally have two geometrical isomers: facial (*fac*) and meridional (*mer*) forms. The *fac* isomer is considered more stable electronically, as this isomer achieves stronger M to CO back-donation, but the *mer* isomer is favored from a steric point of view (Figure 2-1).

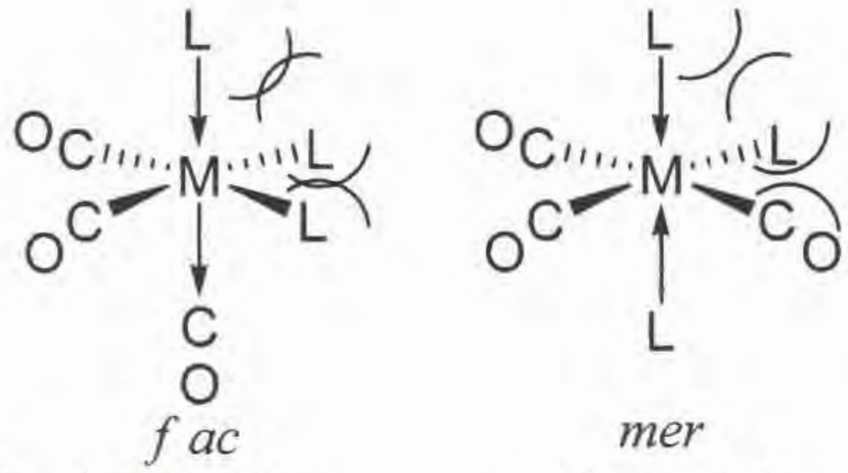

f ac *mer*

electronical effect	favorable	unfavorable
steric effect	unfavorable	favorable

Figure 2-1. Considerable effects in a favor of *fac/mer* $M(CO)_3L_3$.

$Mo(CO)_3L_3$ is known to be exclusively obtained in the substitution reaction of *fac*-$Mo(CO)_3L'_3$ (L' = weak ligand such as MeCN) with L. The *mer* isomers were obtained using isomerization of the *fac* isomer. Bond et al. reported *fac-mer* isomerization via a one-electron oxidation to produce the 17e cation species for $M(CO)_3(\eta^3\text{-}Ph_2PCH_2CH_2P(Ph)CH_2CH_2PPh_2)$ (Scheme 2-5).[29]

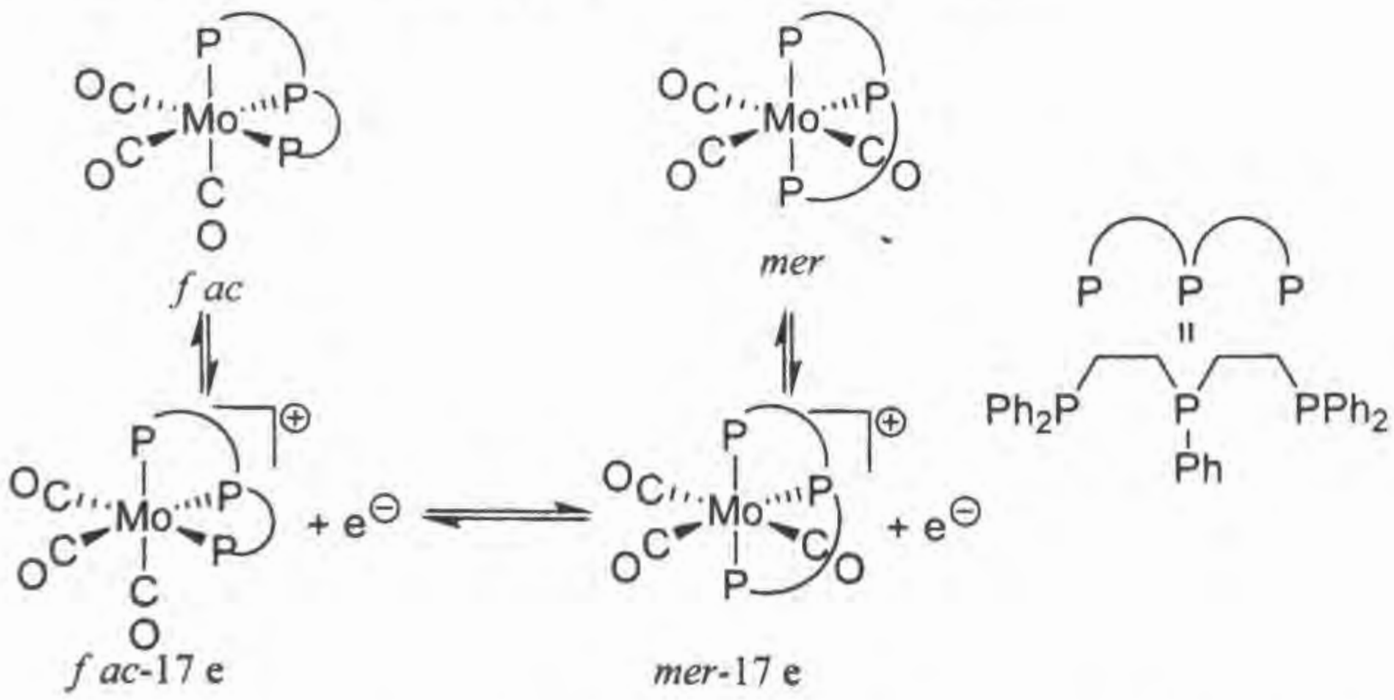

Scheme 2-5. *fac/mer* isomerization via one-electron oxidation.

Nakazawa et al. reported the related isomerization for *fac*-$M(CO)_3(bpy)\{P(NMeCH_2CH_2\dot{N}Me)(OMe)\}$ (M = Cr, Mo, W; bpy = 2,2'-bipyridine) (Scheme 2-6).[2 10] The reaction of the *fac* isomer with $BF_3 \cdot OEt_2$ gives the cationic phosphenium complex *fac*-$M(bpy)\{P(\dot{N}MeCH_2CH_2\dot{N}Me)\}^+$, which then isomerizes to the *mer* form. It does so because the phosphenium ligand shows strong π acidity, leading to an electron-deficient metal center (not complete one-electron oxidation, but partial oxidation).

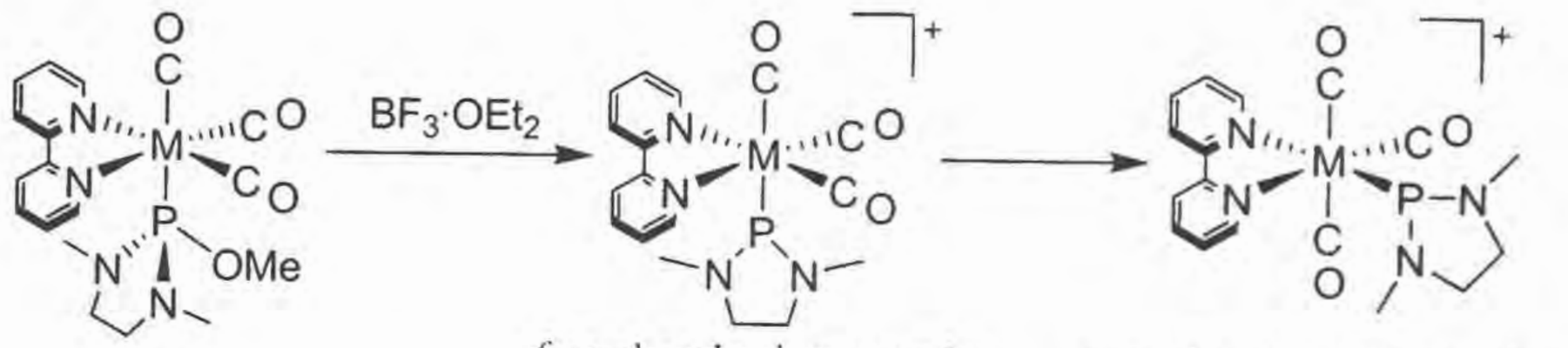

f ac-phosphenium complex *mer*-phosphenium complex

Scheme 2-6. *fac/mer* isomerization of a phosphenium complex.

Thermal *fac-mer* isomerization has been reported by Rousche et al. for *fac*-$Mo(CO)_3(\eta^2\text{-dppe})\{P(O^iPr)_3\}$[2 11] and by Howell et al. for *fac*-$M(CO)_3\{P(OR)_3\}_3$ (M = Cr, Mo, W)[2 12]. Howell et al. performed also computational calculation using the MM2 program and proposed the *fac-mer* isomerization mechanism for the $M(CO)_3\{P(OR)_3\}_3$ (Scheme 2-7). The *fac-mer* isomerization can be accomplished either by rotation of two torigonal planes consisteng of P(2)-P(3)-C(1) and P(1)-C(2)-C(3) or those consisting of P(2)-C(1)-C(3) and P(1)-C(2)-P(3). Though these faces are rendered non-equivalent due to the orientation of the $P(OR)_3$ ligands, the rotation-energy profile is independent of the choice of face pairs.

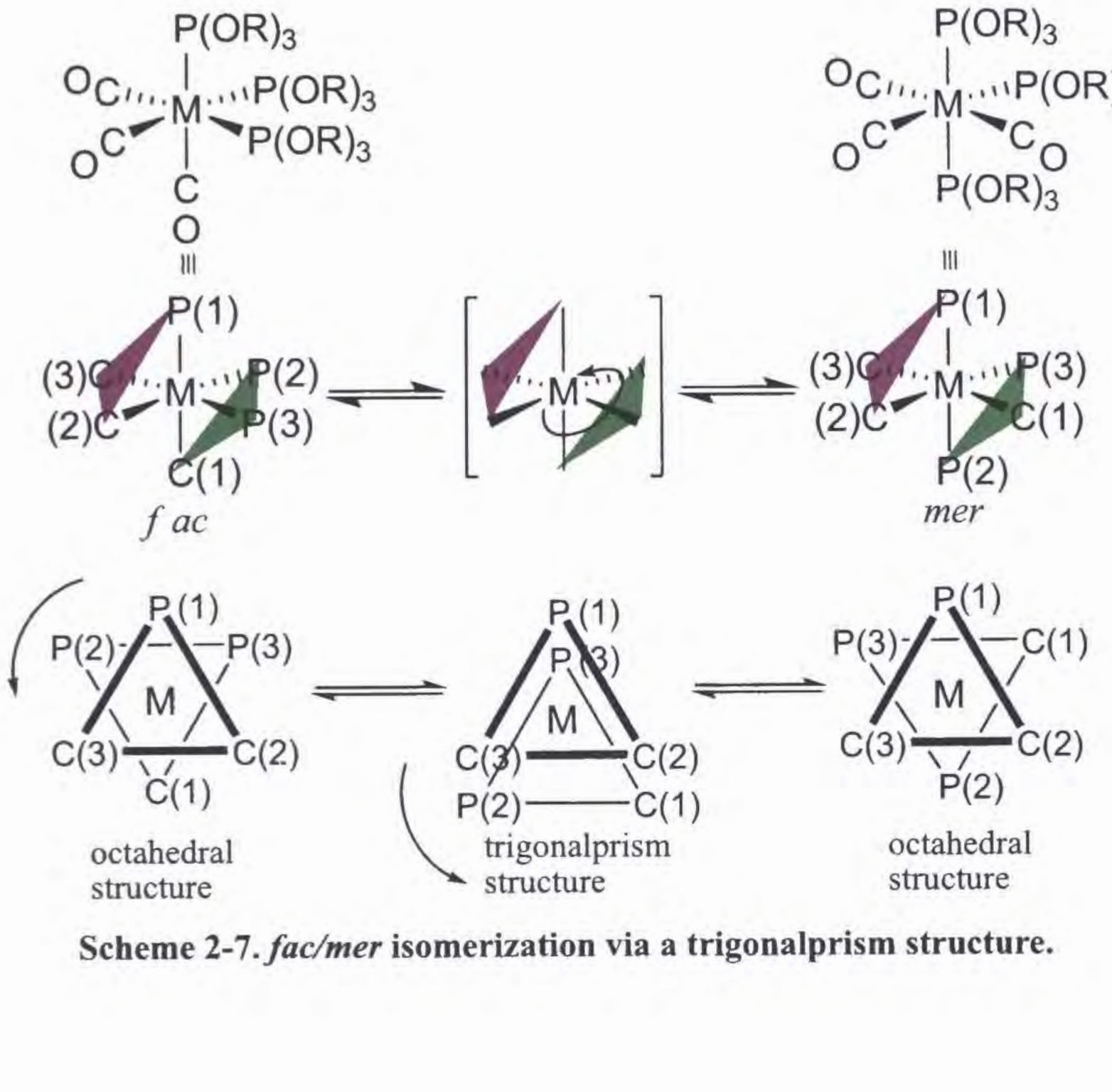

Scheme 2-7. *fac/mer* isomerization via a trigonalprism structure.

2-2 *fac-mer* Isomerization Catalyzed by Me_3SiCl

2-2-1 *fac-mer* Isomerization of $Mo(CO)_3\{P(OR)_3\}_3$ with Me_3SiCl

The reaction of *fac*-$[Mo(CO)_3\{P(OMe)_3\}_3]$ (***fac*-2.2**) with 1 equiv of Me_3SiCl in CH_2Cl_2 at room temperature was examined. The reaction was monitored by measuring the $^{31}P\{^1H\}$ NMR spectrum. A singlet at 164.8 ppm because of ***fac*-2.2** decreased with time, instead a triplet at 167.1 ppm (J_{PP} = 44.3 Hz) and a doublet at 175.3 ppm (J_{PP} = 41.7 Hz) appeared. The two new signals could be attributed to *mer*-$Mo(CO)_3\{P(OMe)_3\}_3$ (***mer*-2.3**) from the coupling patterns. After 3 h, equilibrium between ***fac*-2.2** and ***mer*-2.2** was established with the ratio of 1 : 3.4. No *fac-mer* isomerization occurred at room temperature in CH_2Cl_2 without Me_3SiCl. Next, the reactions with 0.5 equiv and 0.1 equiv of Me_3SiCl were examined. Table 2-1 (entries 1–3) shows that the final equilibrium position was independent of the amount of Me_3SiCl used, although it takes a longer time to reach the equilibrium when the amount of Me_3SiCl is reduced The equilibrium ratio resembles that obtained in thermolysis by Howell et al. (1 : 3)[2,12]. These results show that Me_3SiCl acts as a catalyst for *fac-mer* isomerization.

The corresponding isomerization catalyzed by Me_3SiCl was observed for triethylphosphite complex (***fac*-2.3**), triphenylphosphite complex (***fac*-2.4**), and diamino-substituted phosphite complex (***fac*-2.5**) (entries 4-6). In all cases, the ^{31}P NMR spectra of the reaction mixture suggested the formation of the corresponding *mer* isomers; ***fac*-2.3**: 164.8 ppm (s); ***mer*-2.3**: 167.1 ppm (t, J_{PP} = 44.3 Hz, *cis*-PP), 175.3 ppm (d, J_{PP} = 41.7 Hz, *trans*-PP); ***fac*-2.4**: 145.4 ppm (s); ***mer*-2.4**: 148.8 ppm (t, J_{PP} = 52.1 Hz, *cis*-PP), 155.7 ppm (d, J_{PP} = 52.1 Hz, *trans*-PP); ***fac*-2.5**: 146.1 ppm (s); ***mer*-2.5**: 143.9 ppm (d, J_{PP} = 46.9 Hz, *cis*-PP), 180.9 ppm (t, J_{PP} = 46.9 Hz, *trans*-PP). The isomerization of ***fac*-2.4** to ***mer*-2.4** was much slower (more than 72 h) than that of ***fac*-2.2** to ***mer*-2.2** (3 h), which might be attributed to a steric cause. The reaction of ***fac*-2.5** is noteworthy. We found that the reaction of ***fac*-2.5** with Me_3SiOTf involves abstraction of one OMe as an anion from the phosphorus to give a cationic

Table 2-1. Isomerization of *fac*-$Mo(CO)_3\{P(OR)_3\}_3$ by Me_3SiCl in CH_2Cl_2 at room temperature.

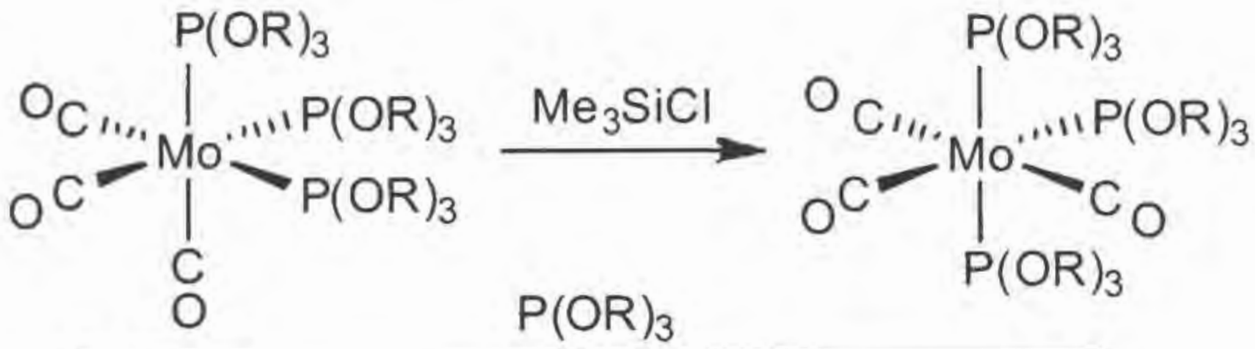

***fac*-2.2**	$P(OMe)_3$	***mer*-2.2**
***fac*-2.3**	$P(OEt)_3$	***mer*-2.3**
***fac*-2.4**	$P(OPh)_3$	***mer*-2.4**
***fac*-2.5**	$P(\overline{NMeCH_2CH_2NMe})(OMe)$	***mer*-2.5**

entry	complex	Me_3SiCl (eq)	time (h)	*fac* : *mer*
1	***fac*-2.2**	1.0	3	1 : 3.4
2	***fac*-2.2**	0.5	5	1 : 3.4
3	***fac*-2.2**	0.1	8	1 : 3.4
4	***fac*-2.3**	1.0	2	1 : 2.2
5	***fac*-2.4**	1.0	72	1 : 1.3[a]
6	***fac*-2.5**	1.0	12	1 : 0.5

[a] The isomerizatio is very slow, and the equilibrium is not attained after 72 h.The final ratio obtained by using Me_3SiOTf is 1 : 30 (see Chapter 2-3-1).

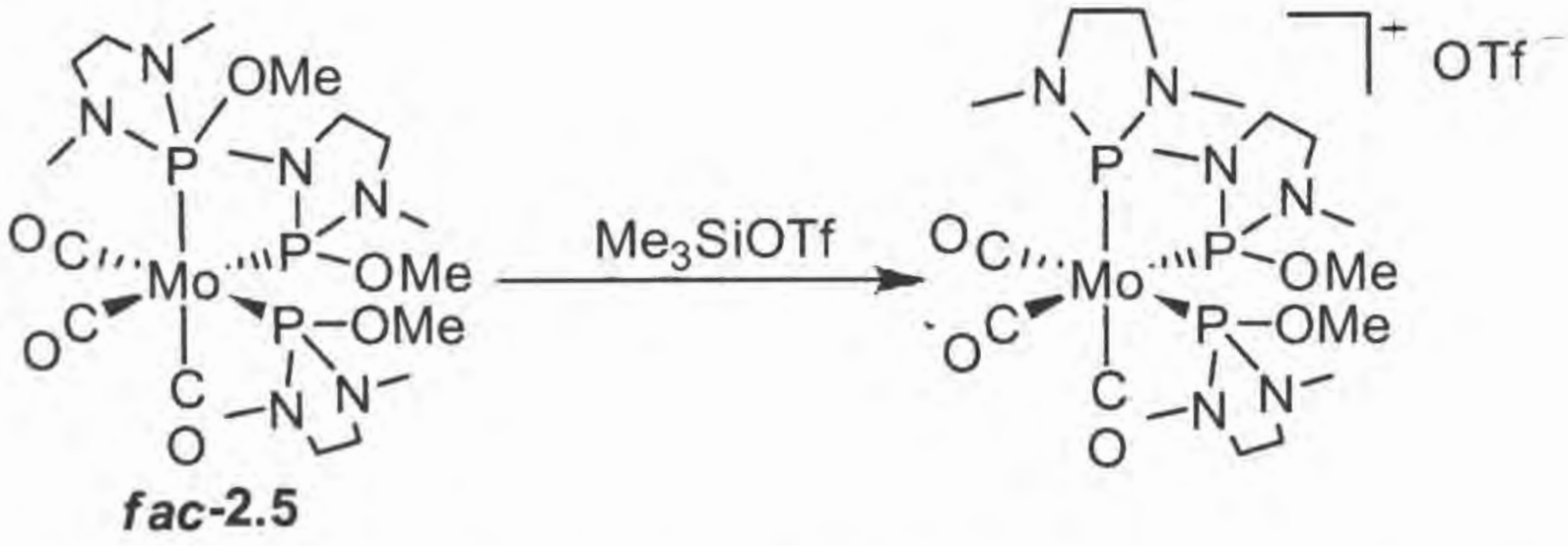

***fac*-2.5**

Scheme 2-8. Generation of a cationic phosphenium complex in the reaction with Me_3SiOTf.

phosphenium complex, *fac*-$[Mo(CO)_3\{P(\overline{NMeCH_2CH_2N}Me)(OMe)\}_2\{P(NMeCH_2)_2\}]^+$ (Scheme 2-8).[213] In contrast, based on ^{31}P NMR monitoring, the reaction of ***fac*-2.5** with Me_3SiCl generated no cationic phosphenium complex, which suggests that the pathway of the isomerization promoted by Me_3SiCl differs from that involving a cationic phosphenium complex produced by Me_3SiOTf.

2-2-2 Possibility of *fac-mer* Isomerization with Adventitious HCl

In our experiments dry CH_2Cl_2 distilled from CaH_2 was used. However, there is a possibility that adventitious HCl from Me_3SiCl hydrolysis (eq. 2-1) could be responsible for the observed isomerization. Thus, the ^{29}Si NMR of Me_3SiCl in CH_2Cl_2 was measured. No signal other than a singlet attributable to Me_3SiCl was observed, indicating no silicon compound derived from Me_3SiCl hydrolysis exist (less than 5%, if any). We observed that the isomerization of ***fac*-2.2** is completed within 8 h in the presence of 10 mol% of Me_3SiCl. If 10% of the Me_3SiCl produces adventitious HCl, then the amount of HCl would be 1 mol% based on ***fac*-2.2** in the above conditions. The CH_2Cl_2 solution of ***fac*-2.2** containing 1 mol% of HCl was prepared and monitored by the ^{31}P NMR measurement and no isomerization was observed after 10 h. These results clearly indicate that the *fac-mer* isomerization is catalyzed by Me_3SiCl but not by HCl.

$$Me_3SiCl + H_2O \longrightarrow Me_3SiOH + HCl \quad (2\text{-}1)$$

2-2-3 Plausible Mechanism for *fac-mer* Isomerization Promoted by Me_3SiCl

Scheme 2-9 presents a plausible mechanism for the *fac-mer* isomerization promoted by Me_3SiCl. The silicon atom in Me_3SiCl interacts with one oxygen in $P(OR)_3$ ligands to form an Si hypervalent structure (**α**). An interaction of tetracoordinated silicon with an oxygen in phosphite may be plausible because formation of pentacoordinated silicon compounds by coordination of a carbonyl oxygen has been reported (see Section 1.4). The interaction weakens the coordination of $P(OR)_3$•Me_3SiCl toward the central metal and makes the ligand bulky, thereby makes the trigonalprism structure in Scheme 2-7 possible leading to decrease the isomerization energy barrier, which gives its *mer* isomer (**β**). The following dissociation of the Me_3SiCl gives the mer isomer reproducing free Me_3SiCl.

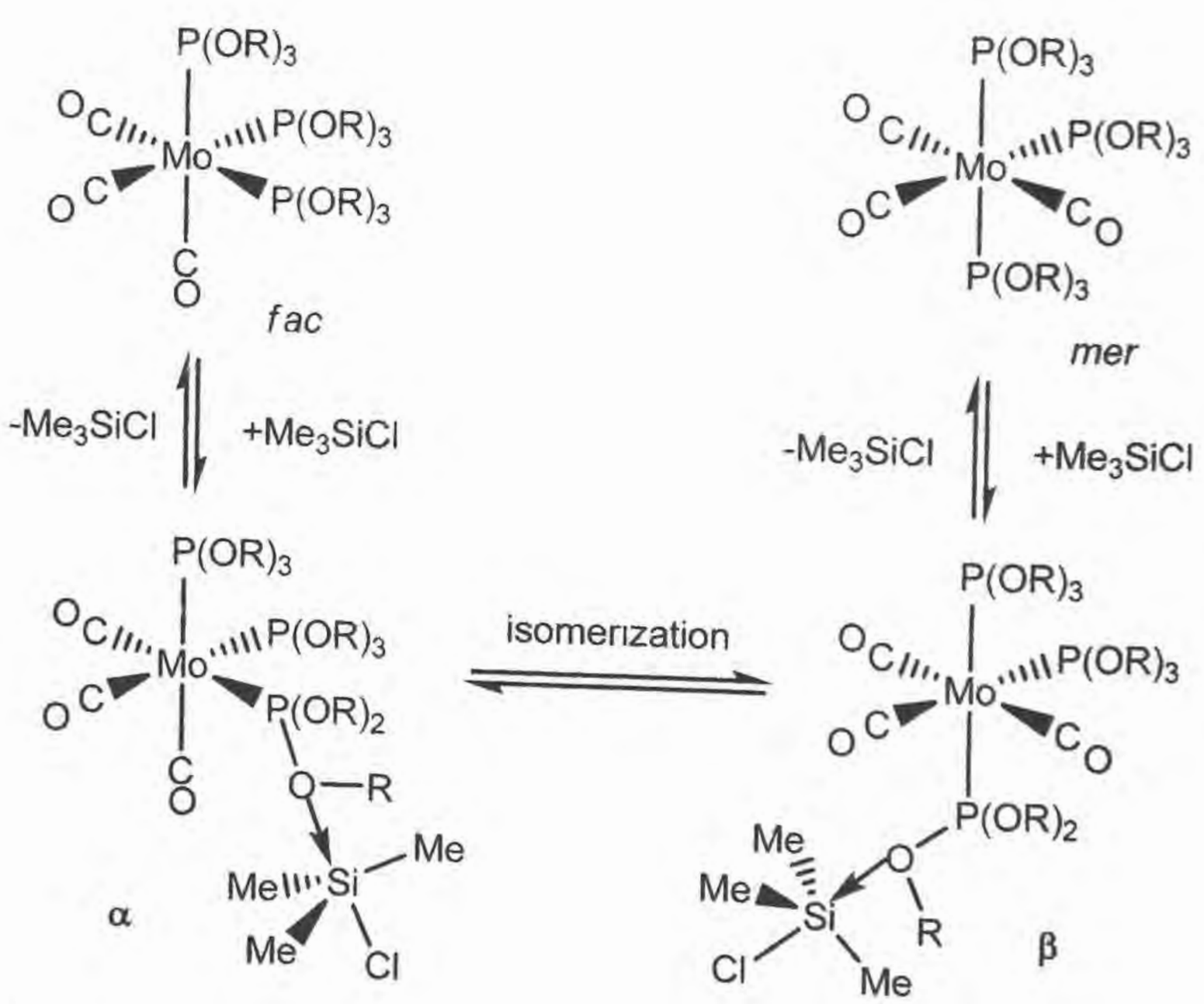

Scheme 2-9. Proposed *fac-mer* isomerization mechanism catalyzed by Me_3SiCl.

2-2-4 Observation of Pentacoordinate Silyl Complexes as Intermediates

The ^{31}P and ^{29}Si NMR measurements of a CH_2Cl_2 solution containing ***fac*-2.2** and Me_3SiCl showed no signals assignable to either **α** or **β** in Scheme 2-9. To obtain some evidence of **α** and **β**, we dissolved ***fac*-2.2** in Me_3SiCl and measured the ^{31}P and ^{29}Si NMR spectra of the solution. The ^{31}P NMR is shown in Fig. 2-2. In addition to a singlet at 166.7 ppm attributable to ***fac*-2.2** and a doublet at 176.2 ppm and a triplet at 168.8 with J_{PP} = 41.7 Hz attributable to ***mer*-2.2**, five signals were observed clearly. Among them, a triplet at 181.3 ppm (assignable to $\alpha_{P(3)}$ from the molecular symmetry) and a doublet at 173.9 ppm (assignable to $\alpha_{P(1),(2)}$) with J_{PP} = 41.7 Hz are attributable to **α**. The remaining three signals at 184.8 ppm (dd, J_{PP} = 41.7 and 229.3 Hz, assignable to $\beta_{P(3)}$), 174.3 ppm (dd, J_{PP} = 44.3 and 229.3 Hz, assignable to $\beta_{P(1)}$), and 166.2 ppm (t, J_{PP} = 44.3 Hz, assignable to $\beta_{P(2)}$) are attributable to **β**. The product ratio of **α**/**β** estimated from signal intensity (1 : 6) was different from that of *fac*-**2.2**/*mer*-**2.2** (1 : 3.4), indicating that the latter is thermodynamically determined. The ^{29}Si NMR showed two singlets at 6.62 ppm and 6.53 ppm in addition to a strong singlet at 29.8 ppm attributable to the solvent Me_3SiCl. Coordination of nitrogen or oxygen to silicon to form a pentacoordinate bond has been shown to produce a strong shielding effect of the silicon chemical shift.[2 14] Kummer et al. reported the ^{29}Si NMR chemical shift at 11.1 ppm in CD_2Cl_2 for an Si hypervalent compound with Cl and N in apical positions and two Me groups and one CH_2 group in equatorial positions (Chart 2-1).[2 15] The ^{13}C NMR of the Me_3SiCl solution containing ***fac*-2.2** was also measured. Two lumps consisting of several signals were observed at 213.9~214.1 ppm and 218.0~218.2 ppm. These signals are attributable to terminal carbonyl ligands, indicating that Me_3SiCl does not have an interaction with an oxygen atom in terminal carbonyl ligand. Therefore, our observations suggest the formation of hypervalent Si compounds.

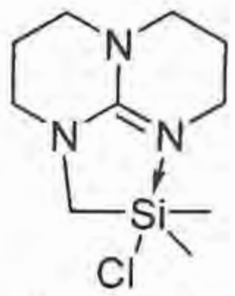

^{29}Si NMR(in CD_2Cl_2) : 11.1 ppm

Chart 2-1. ^{29}Si NMR spectrum of pentacoordinate silicom compound.

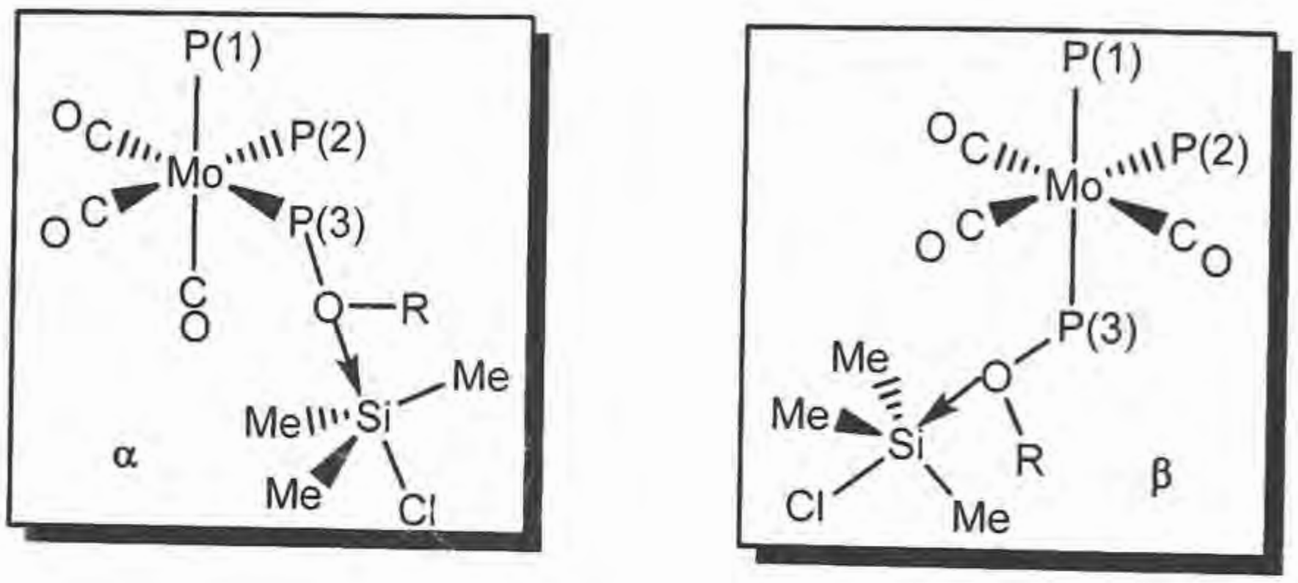

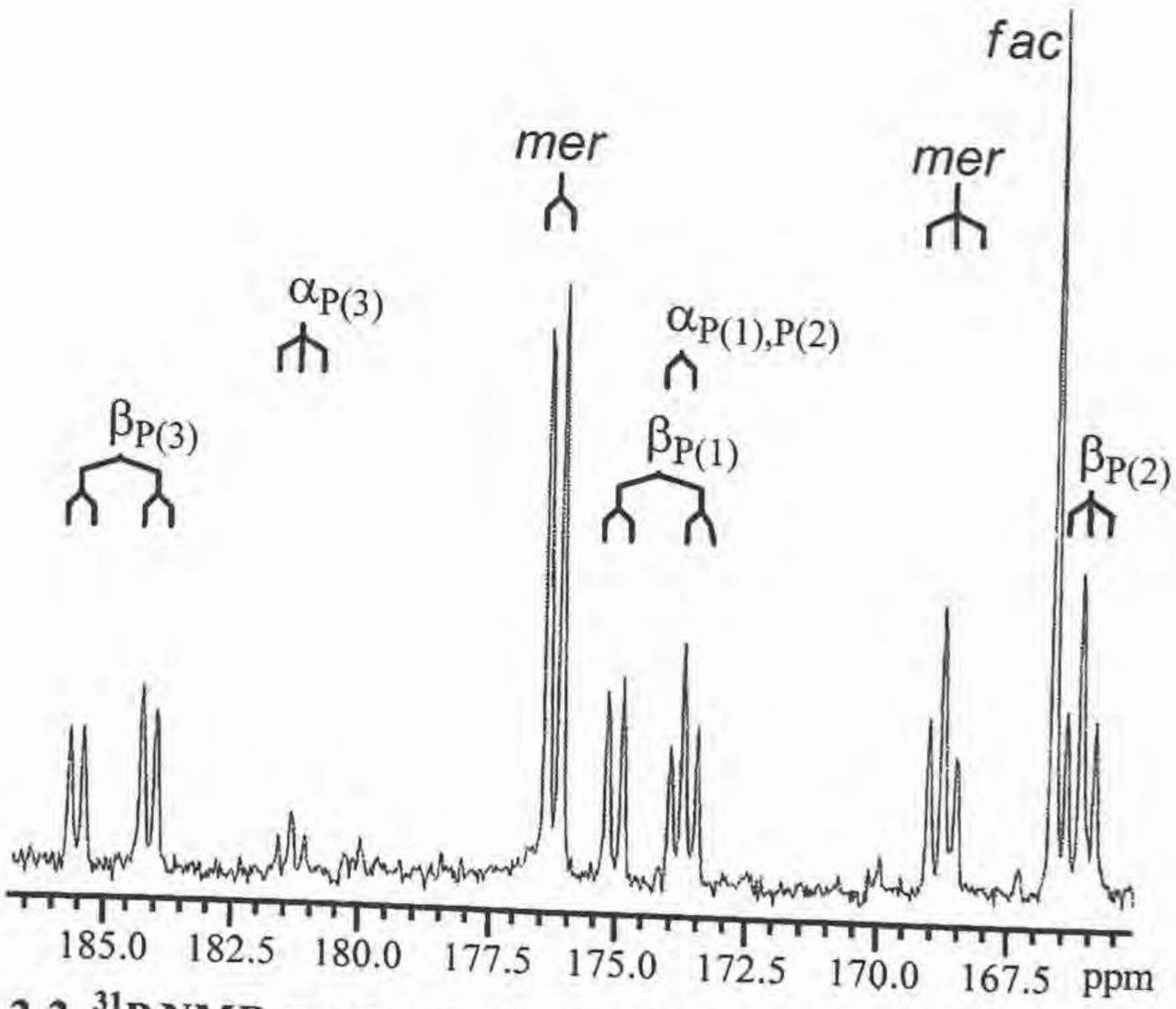

Figure 2-2. ^{31}P NMR spectrum of a Me_3SiCl solution at room temperature in Which *fac*-2.2 is dissolved.

2-2-5 Supporting Results to the Reaction Mechanism

In the previous section, I proposed that an interaction of Si in Me_3SiCl with O in $P(OR)_3$ causes the *fac-mer* isomerization of $Mo(CO)_3(phosphite)_3$. Next, the isomerization of $Mo(CO)_3(phosphine)_3$ (phosphine = PEt_3, $Bu^n{}_3$) having no OR group on a coordinating phosphorus was examined. No *fac-mer* isomerization was confirmed (Scheme 2-10) suggesting that a phosphite oxygen plays a crucial role in *fac-mer* isomerization.

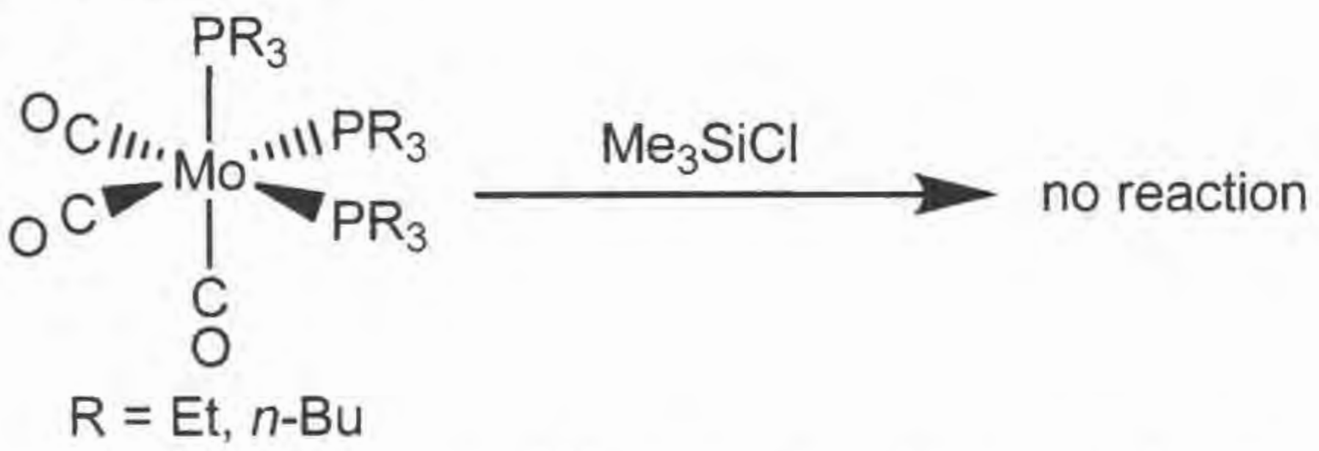

Scheme 2-10. Treatment of $Mo(CO)_3(phosphine)_3$ with Me_3SiCl.

To elucidate whether *fac-mer* isomerization involves a phosphite dissociation process or not, a crossover experiment was performed. Addition of Me_3SiCl to a CH_2Cl_2 solution containing both ***fac*-2.2** and ***fac*-2.3** yielded ***mer*-2.2** and ***mer*-2.3**, but form neither phosphite exchange products such as *fac*- or *mer*-$[Mo(CO)_3\{P(OMe)_3\}_2\{P(OEt)_3\}]$, nor OR exchange products such as *fac*- or *mer*-$[Mo(CO)_3\{P(OMe)_3\}_2\{P(OMe)_2(OEt)\}]$ (Scheme 2-11). These results show intramolecular isomerization, which is consistent with the mechanism shown in Scheme 2-9.

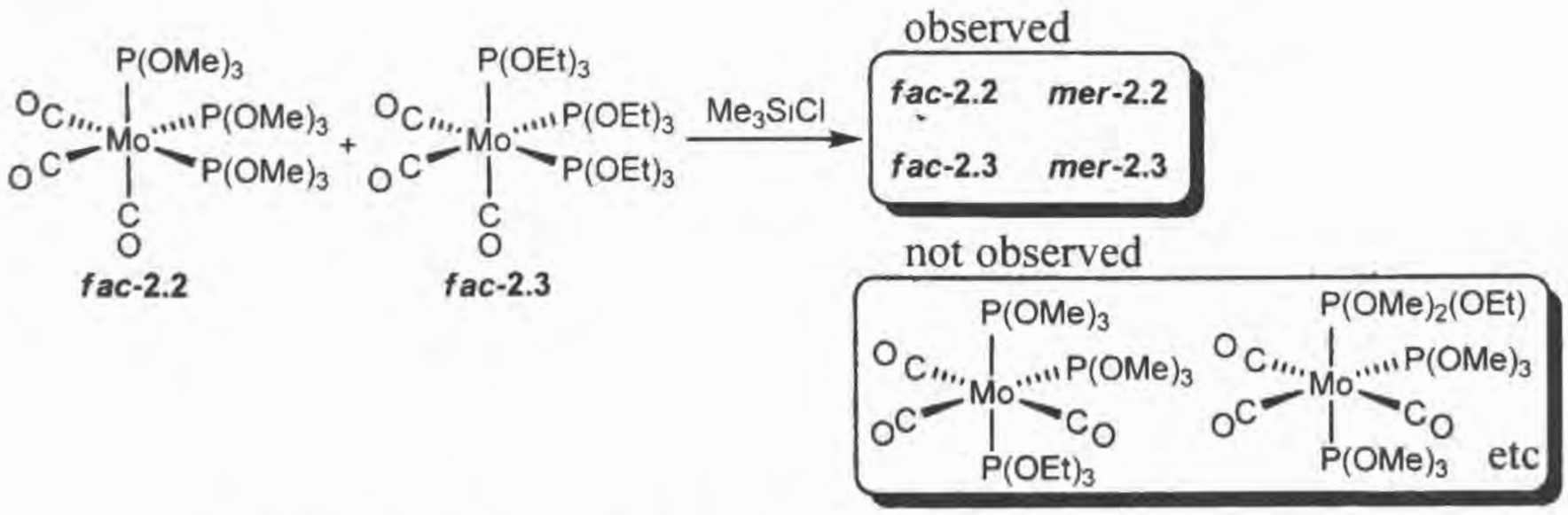

Scheme 2-11. Reaction of *fac*-2.2 and *fac*-2.3 with Me_3SiCl.

2-2-6 Reaction of *fac*-$Mo(CO)_3$(phosphite)$_3$ with group 14 substrates

As it has been shown that Me_3SiCl can promote *fac-mer* isomerization for *fac*-[$Mo(CO)_3$(phosphite)$_3$], activity of other silanes was examined for ***fac*-2.2**. Me_2SiCl_2, $MeSiCl_3$, and $SiCl_4$ promoted the isomerization, but some by-products were also formed. I considered that monochlorophosphite, dichlorophosphite, or trichlorophosphite complexes were generated in the ligand exchange between OR and Cl via hypervalent silicon compounds. Such ligand exchange was already reported.[2 16] For example, *C*-nucleophiles react with acetals in the presence of Me_3SiX with the replacement of the alkoxy group. In the reaction mechanism, the pentacoordinate silicon compound induces the ligand exchange (Scheme 2-12).

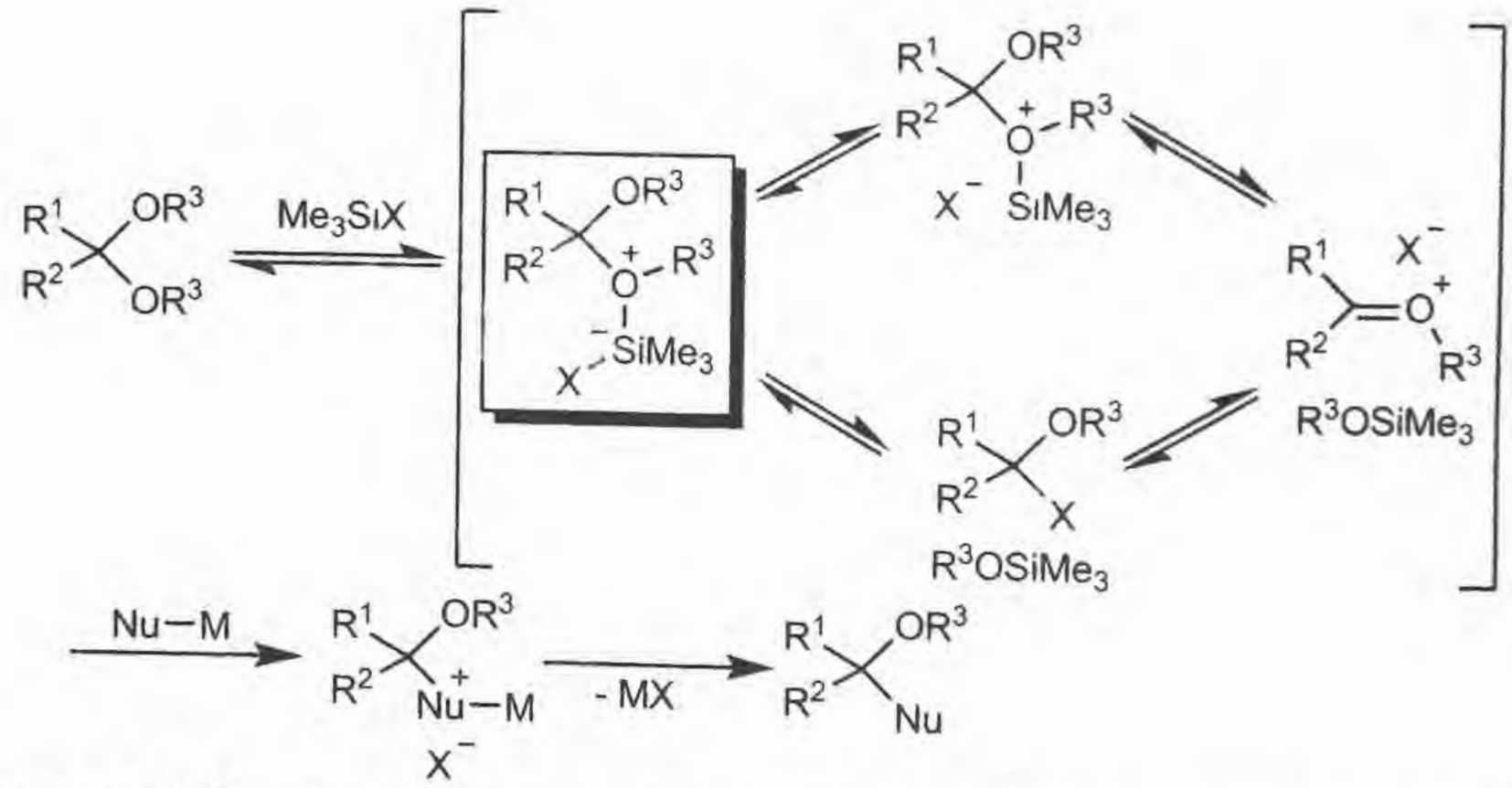

Scheme 2-12. Reaction of an acetal with a nucleophile in the presence of Me_3SiX.

In contrast, $SiMe_4$, with no chloride substituent, did not promote isomerization at all. Therefore, among the Me_nSiCl_{4-n} (n = 0–4) series, Me_3SiCl is the best promoter, which might stem from its superior hypervalent arrangement: two electronegative substituents (Cl and O from phosphite) in apical positions and three electron releasing groups (three Me groups) in equatorial positions.

Table 2-2 shows the activity of R_3EX (E = Si, Ge, Sn). Bromosilane and iodosilane (entries 2, 3) show better activity than that of chlorosilane (entry 1). The

order is parallel to electron density on the central Si reflected by ^{29}Si NMR chemical shift (Me_3SiCl: 35.5 ppm, Me_3SiBr: 26.5 ppm, Me_3SiI: 18.5 ppm). The Ph_3SiCl (entry 4) does not promote isomerization, presumably because of the bulky substituents. Slow isomerization was observed in the reaction with $(EtO)_3SiCl$ (entry 5), which might be attributable to the weak electron releasing ability of an OEt group compared to that of the Me group. A similar *fac-mer* ratio was obtained for entries 1, 2, 3, and 5, meaning that the ratio is determined thermodynamically and is unaffected by the added silane. Chlorogermane and chlorotin (entries 6 and 7) shows worse activity than that of chlorosilane. The order is parallel to the electrophilic order of the 14 group elements.[2 17]

Table 2-2. Isomerization of *fac*-2.2 with halides.[a]

entry	R_3SiX	time (h)	*fac* : *mer*
1	Me_3SiCl	3	1 : 3.4
2	Me_3SiBr	< 0.1	1 : 3.6
3	Me_3SiI	< 0.1	1 : 3.7
4	Ph_3SiCl	25	no reaction
5	$(EtO)_3SiCl$	25	1 : 3.4
6	Me_3GeCl	25	1 : 3.4
7	Me_3SnCl	3 days	1 : 3.4

[a] ***fac*-2.2** was treated with 1 equiv of R_3EX (E = Si, Ge, Sn) in CH_2Cl_2 at room temperature.

2-3 *Isomerization Catalyzed by a Lewis Acids*

2-3-1 *fac-mer* Isomerization of $Mo(CO)_3\{P(OR)_3\}_3$ with a Lewis Acid

I discussed the *fac-mer* isomerization of $Mo(CO)_3\{P(OR)_3\}_3$ by the neutral silicon compound, e.g. Me_3SiCl, in the previous chapters. Similar isomerizations were also examined by a cationic silicon compound, e.g. Me_3SiOTf. Complex ***fac*-2.2** was dissolved in CH_2Cl_2 and an equimolar amount of Me_3SiOTf was added at room temperature and the reaction was monitored by the ^{31}P NMR measurement. Three signals which were attributed to ***fac*-2.2** and ***mer*-2.2** were observed. The isomerization reached at an equibrium after 1.5 h and the the ***fac*-2.2** : ***mer*-2.2** ratio was 1 : 3.4. Next question is whether Me_3SiOTf works as a catalyst or not. The reactions of ***fac*-2.2** with 0.5 and 0.1 equivalent of Me_3SiOTf revealed that the final equilibrium position did not depend on the amount of Me_3SiOTf used although it took a longer time to reach the equilibrium when the amount of Me_3SiOTf was reduced.

Reactions of ***fac*-2.3** and ***fac*-2.4** with Me_3SiOTf were also examined in CH_2Cl_2 at room temperature. In the ^{31}P NMR spectra, new two signals assignable to ***mer*-2.3** were observed in the reaction of ***fac*-2.3**, and new similar signals attributable to ***mer*-2.4** were observed in the reaction of ***fac*-2.4**. The equilibrium *fac-mer* ratios were independent of the amount of Me_3SiOTf used, showing that Me_3SiOTf serves as a catalyst. The results together with those for ***fac*-2.2** are shown in Table 2-3. The equilibrium *fac-mer* ratios are quite dependent on the kind of the phosphite ligand. It should be noted that these values are equal to those for the isomerization promoted by Me_3SiX (X = Cl, Br, I) (Section 2-2-5), and the value for ***fac*-2.2** is similar to that reported by Howell[2 12]. Therefore, it can be said that the values are derived from the thermodynamic stability between the *fac* and *mer* isomers, not from the stability of the intermediates created from a Mo complex and a catalyst (presumably Me_3Si^+, vide infra).

The corresponding isomerization catalyzed by MeOTf as a Lewis acid was examined for ***fac*-2.2** and ***fac*-2.4**. Table 2-4 shows that MeOTf can work as a catalyst in the *fac-mer* isomerization, although it takes a longer time to reach the equiblium.

The isomerization of ***fac*-2.4** by MeOTf demands a longer reaction period than Me_3SiOTf and Me_3SiCl. The results may be rationalized by the lower oxophilicity for Me^+ than for Me_3Si^+.

Table 2-3. Isomerization of $Mo(CO)_3\{P(OR)_3\}_3$ by Me_3SiOTf.[a, b]

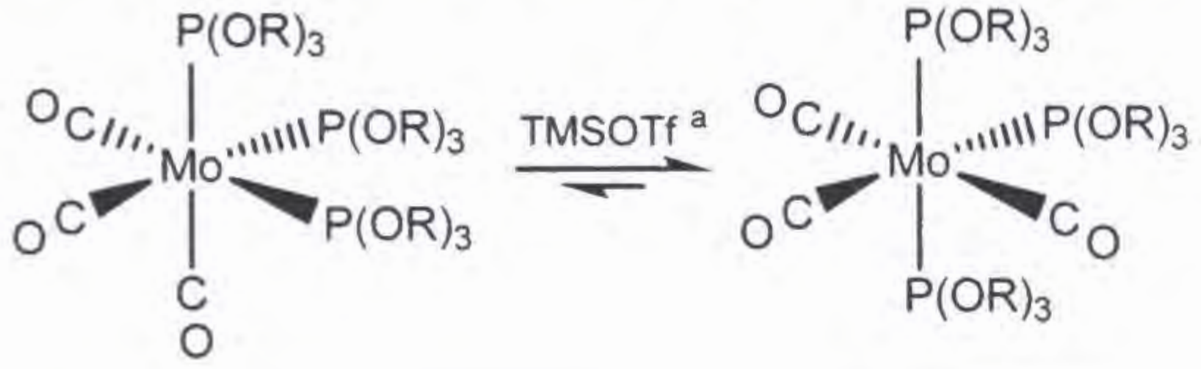

$P(OR)_3$			*fac* : *mer* [c]
$P(OMe)_3$	***fac*-2.2**	***mer*-2.2**	1 : 3.4
$P(OEt)_3$	***fac*-2.3**	***mer*-2.3**	1 : 2.2
$P(OPh)_3$	***fac*-2.4**	***mer*-2.4**	1 : 30

[a] 1.0, 0.5 and 0.1 equvalents based on the *fac* complex were used.
[b] Reaction conditions: room temperature, 0.1 M CH_2Cl_2 solution.
[c] *fac:mer* equilibrium ratio after completion of the isomerization.

Table 2-4. Isomerization of $Mo(CO)_3\{P(OR)_3\}_3$ by R'OTf(R' = Me, Me_3Si).[a, b]

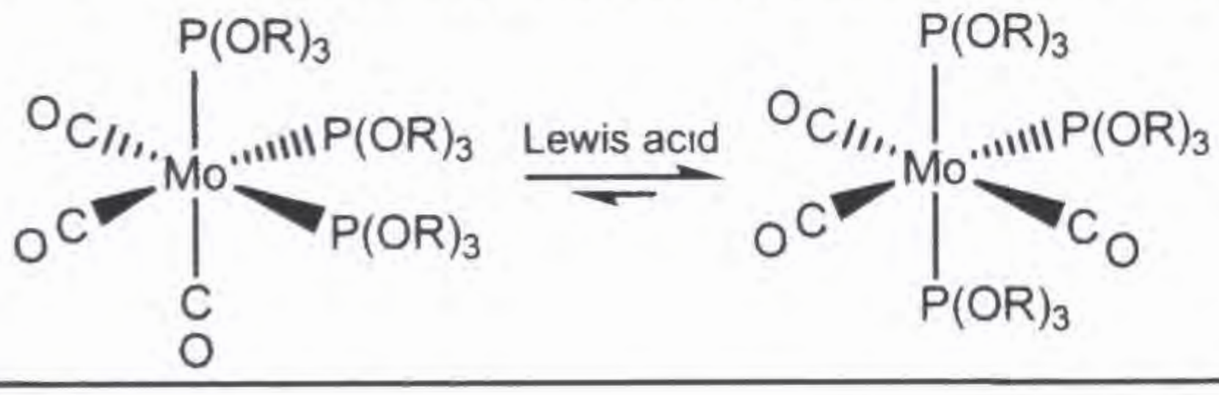

complex	Lewis acid	reaction time	*fac* : *mer*
***fac*-2.2**	0.5 eq. Me_3SiOTf	↑ h	1 : 3.4
***fac*-2.2**	0.5 eq. MeOTf	4 days	1 : 3.4
***fac*-2.4**	1.0 eq. Me_3SiOTf	0.5 h	1 : 30
***fac*-2.4**	1.0 eq. MeOTf	4 days	1 : 0.06[b]

[a] Reaction conditions: room temperature, 0.1 M CH_2Cl_2 solution.
[b] The isomerization is very slow, and the equilibrium is not attained after 4 days.

2-3-2 Structure of *mer*-2.4

Complex ***mer*-2.4** could be isolated from the reaction mixture of ***fac*-2.4** and TMSOTf. After a treatment of ***fac*-2.4** with TMSOTf in CH_2Cl_2, a white-powder which is a mixture of ***fac*-2.4** and ***mer*-2.4** (1 : 30) was washed with hexane/CH_2Cl_2/benzene (100/1/1) solution many times to obtain the pure complex formulated as ***mer*-2.4**·$0.5CH_2Cl_2$·$0.5C_6H_6$ in 53% yield. Although several *mer*-$M(CO)_3L_3$ (M = Cr, Mo, W) type complexes have been reported, this is the first preparation and isolation of *mer*-$M(CO)_3\{P(OPh)_3\}_3$. The structure was confirmed by the X-ray analysis. The ORTEP drawing is depicted in Figure 2-3 and the crystal data are summarized in Table 2-5. This X-ray structure is the first example among *mer*-$M(CO)_3$(tertiary phosphorus compound)$_3$ type complexes. The X-ray structure of ***fac*-2.4** was reported previously[2 18]. The structural comparison between *fac*- and *mer*-$Mo(CO)_3\{P(OPh)_3\}_3$ revealed some interesting points. The bond distance of Mo-C2 for ***mer*-2.4** (2.017 Å) is clearly shorter than those of Mo-C1 (2.041 Å) and Mo-C3 (2.041 Å) (Table 2-6). As C2O2 ligand is *trans* to $P(OPh)_3$, the CO ligand can get more π-back donation from the central metal than C1O1 and C3O3 ligands which are mutually *trans*. The mean Mo-C bond distance for ***fac*-2.4** (1.986 Å) is shorter than that for ***mer*-2.4** (2.033 Å), reasonably understood by greater π-back donation form the Mo to the CO ligands for ***fac*-2.4** because of the *trans* $P(OPh)_3$ ligand. Another interesting point is that the mean Mo-P bond distance for ***fac*-2.4** (2.435 Å) is longer than that for ***mer*-2.4** (2.417 Å). The difference may stem from the steric repulsion between $P(OPh)_3$ ligands in ***fac*-2.4**.

Figure 2-3. ORTEP drawing of *mer*-2.4·0.5CH_2Cl_2·0.5C_6H_6 (50% probability ellipsoids) showing the numbering system.

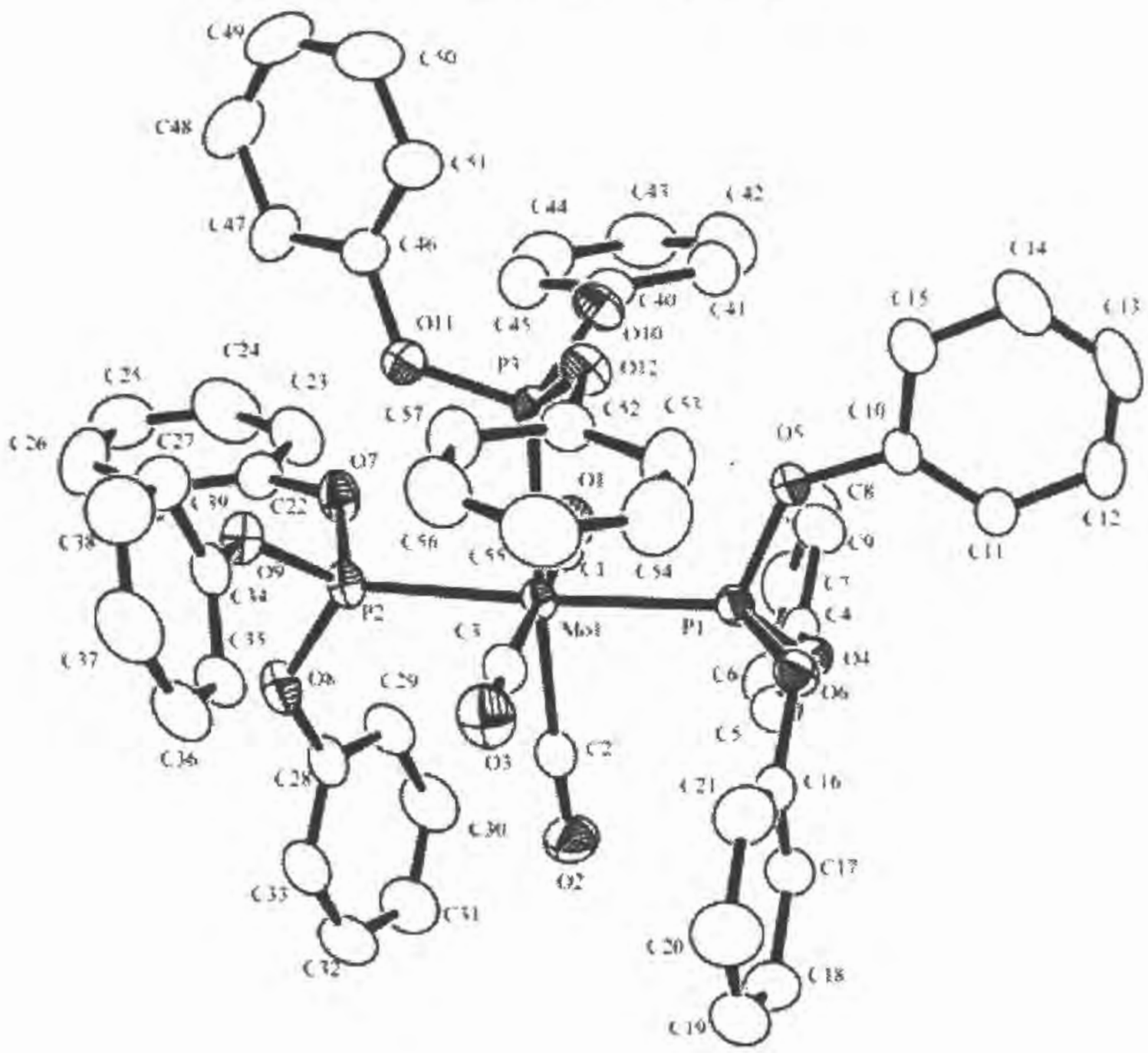

Table 2-5. Crystal data for *mer*-2.4.

Empirical formula	$C_{60\ 50}H_{49}ClMoO_{12}P_3$	V, Å^3	5525.4(4)
Formula weight	1192.30	Z	4
Crystal system	monoclinic	μ, cm^{-1}	4.36
Crystal size(mm^3)	0.45 × 0.35 × 0.15	D_{calcd}, g/cm^3	1.433
Temperature (°C)	-70.0	No. of unique reflections	41908
Space group	$P2_1/n$ (No. 14)	No. of used reflections	12498
a, Å	13.7319(5)	No. of variables	712
b, Å	18.2658(7)	R	0.051
c, Å	22.1401(9)	R_w	0.111
β, deg	95.744(2)	*GOF*	1.06

Table 2-6. Selected bond distance (Å) and angles (deg) for *mer*-2.4.

	Bond Distances		
Mo1-P1	2.4320(4)	Mo1-C1	2.042(1)
Mo1-P2	2.3792(4)	Mo1-C2	2.017(2)
Mo1-P3	2.4390(4)	Mo1-C3	2.041(1)
	Bond Angles		
P1-Mo1-P2	174.25(1)	P2-Mo1-C3	91.50(4)
P1-Mo1-P3	89.56(1)	P3-Mo1-C1	92.30(4)
P1-Mo1-C1	83.08(4)	P3-Mo1-C2	175.91(4)
P1-Mo1-C2	94.53(4)	P3-Mo1-C3	92.38(4)
P1-Mo1-C3	94.23(4)	C1-Mo1-C2	88.43(6)
P2-Mo1-P3	89.76(1)	C1-Mo1-C3	174.58(6)
P2-Mo1-C1	91.24(4)	C2-Mo1-C3	87.09(6)
P2-Mo1-C2	86.21(4)		

2-3-3 Two Types of Reactions of a Phosphite Complex with a Lewis Acid

In Section 2-3-1, I described *fac-mer* isomerization for molybdenum complex bearing phosphite ($P(OMe)_3$) in the reaction with Me_3SiOTf. It has been reported that another type reaction takes place for transition metal complexes bearing diamino-substituted phosphite(s): formation of a cationic phosphenium complex by OR anion abstraction as shown in eq. 2-2, Scheme 2-6, and Scheme 2-8. Transition metal complexes with a phosphenium ligand have attracted considerable attention because a cationic phosphenium ($^{+}PR_2$) is isolobal with a singlet carbene, silylene, and the heavier congeners.[2 19-2 23]

Phosphenium complex formation has been reported for many transition metal complexes bearing a diamino-substituted phosphite; $M(bpy)(CO)_3\{P(\overline{NMeCH_2CH_2N}Me)(OR)\}$ [2 24-2 30], $M(dppe)(CO)_3\{P(NMeCH_2CH_2\overset{+}{N}Me)(OR)\}$[2 25], $M(bpy)(CO)_2\{P(\overline{NMeCH_2CH_2N}Me)(OR)\}_2$[2 26 2 29-2 30], $M(CO)_3\{P(NMeCH_2CH_2\overset{+}{N}Me)(OR)\}_3$[2 13], $M(CO)_4\{P(NMeCH_2CH_2\overset{+}{N}Me)(OR)\}_2$[2 13], $CpM(CO)_2(ER_3)\{P(\overline{NMeCH_2CH_2N}Me)(OR)\}$ (M = Cr, Mo, W)[2 31-2 34], and $CpM(CO)(ER_3)\{P(NMeCH_2CH_2\overset{+}{N}Me)(OR)\}$ (M = Fe, Ru) (ER_3 = CH_3, $SiMe_3$, $GeMe_3$, $SnMe_3$)[2 13, 2 28, 2 35-2 40]. Systematic researches for reactions of $Mo(bpy)(CO)_3\{PXY(OR)\}$ with $BF_3{\cdot}OEt_2$ revealed the effect of the substituents (X, Y) on the stability of cationic phosphenium complexes; the stability increases with increasing the number of amino substituents on the phosphenium phosphorus.[2 27]

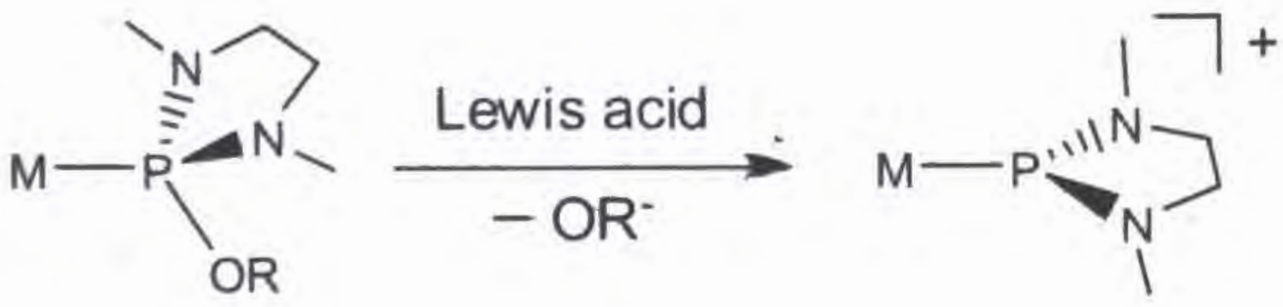

(2-2)

2-3-4 Plausible Isomerization Mechanism of *fac-mer* Isomerization by Me_3SiOTf

Regarding isomerization of $Mo(CO)_3\{P(OR)_3\}_3$ promoted by Me_3SiOTf, two mechanisms are conceivable: mechanisms via a phosphenium complex and via a TMS^+ adduct. The mechanism via a phosphenium complex is shown in Scheme 2-13. As transition-metal complexes bearing a diamino-substituted phosphite have been reported to react with a Lewis acid to give cationic phosphenium complexes by OR^- abstraction as shown in eq 2-2, a similar OR^- abstraction may take place in the reaction of $Mo(CO)_3\{P(OR)_3\}_3$ with TMSOTf to produce a cationic phosphenium complex (***fac'*** in Scheme 2-14). Then, isomerization from ***fac'*** to ***mer'*** is expected to take place. The similar isomerization has been reported previously (Scheme 2-6), where the driving force of the *fac-mer* isomerization is thought to be the gain of more π-back donation for the phosphenium ligand. The reaction of ***mer'*** with Me_3SiOR formed would give *mer*-$Mo(CO)_3\{P(OR)_3\}_3$ with regeneration of TMSOTf. However, this catalytic cycle seems not plausible based on the following observations. (i) A complex having a phosphenium ligand was not detected in the reaction of $Mo(CO)_3\{P(OR)_3\}_3$ with Me_3SiOTf. (ii) After the treatment of ***fac*-2.4** with 1 equiv of Me_3SiOTf in the presence of 1 equiv of Me_3SiOMe in CH_2Cl_2, the ^{31}P NMR spectra of the reaction mixture were measured and ***fac*-2.4** and ***mer*-2.4** were detected but *fac*- and *mer*-$Mo(CO)_3\{P(OPh)_3\}_2\{P(OPh)_2(OMe)\}$ were not detected at all. This indicates that the reaction of ***mer'*** with Me_3SiOR to give ***mer*** in Scheme 2-13 does not proceed.

The other isomerization mechanism is shown in Scheme 2-14. The silicon atom in Me_3Si^+ interacts with one oxygen in $P(OR)_3$ ligands to form ***fac"***, but does not abstract the OR group as an anion. The interaction weakens the coordination of the $P(OR)_3(SiMe_3)$ ligand toward the central metal and makes the ligand bulky, thereby decreasing the isomerization energy barrier to give its *mer* isomer (***mer"***). Dissociation of TMS^+ from ***mer"*** gives *mer*-$Mo(CO)_3\{P(OR)_3\}_3$ with regeneration of Me_3SiOTf. This isomerization mechanism is similar to that by Me_3SiX (X = Cl, Br, I) (Section 2-2-3).

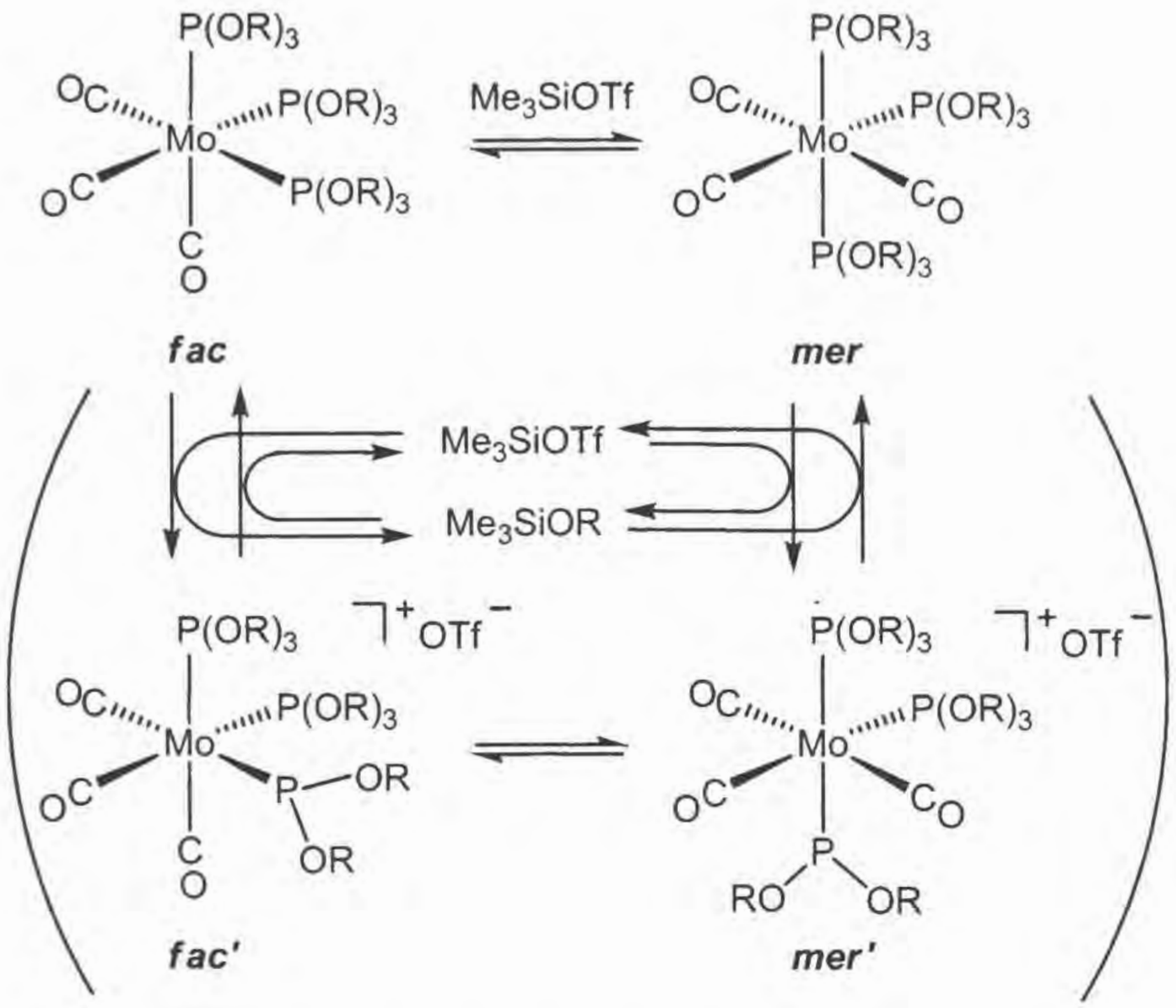

Scheme 2-13. Reaction mechanism via a phosphenium complex .

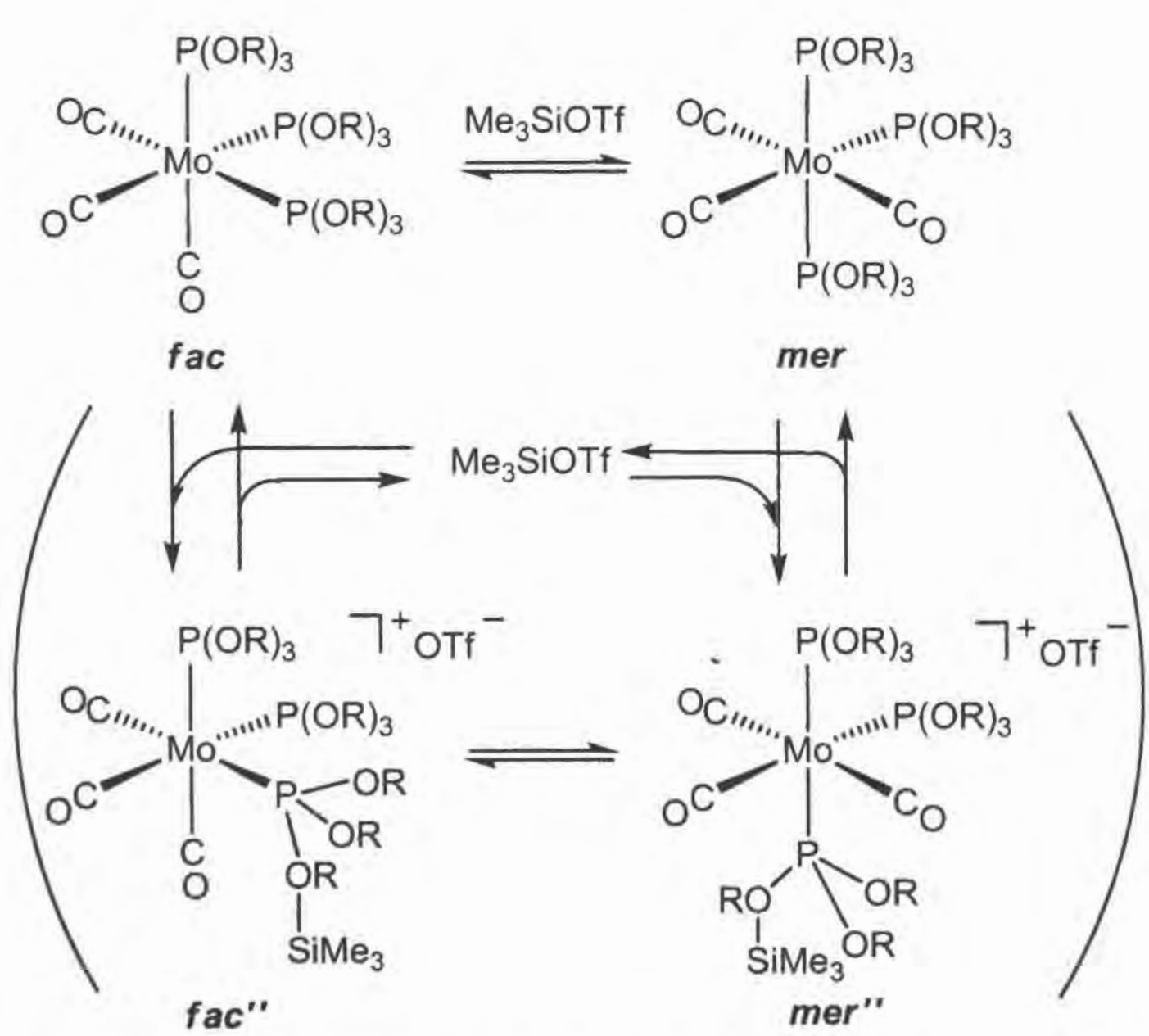

Scheme 2-14. Reaction mechanism via the silyl cation complexes.

There is a possibility that dissociation of one of the phosphites in $Mo(CO)_3\{P(OR)_3\}_3$ induces the isomerization and Me_3SiOTf promotes the dissociation. To check the possibility, a crossover experiment was conducted. Both ***fac*-2.2** and ***fac*-2.3** were dissolved in CH_2Cl_2, Me_3SiOTf was added, and the products were estimated from the ^{31}P NMR spectra of the resulting CH_2Cl_2 solution. Signals assignable to ***mer*-2.2** and ***mer*-2.3**, in addition to ***fac*-2.2** and ***fac*-2.3** were observed, but those due to phosphite exchange products such as *fac*- or *mer*-$Mo(CO)_3\{P(OMe)_3\}_2\{P(OEt)_3\}$ and OR exchange products such as *fac*- or *mer*-$Mo(CO)_3\{P(OMe)_3\}_2\{P(OMe)_2(OEt)\}$ were not detected. These results strongly suggest that neither phosphite dissociation nor OR^- abstraction shown in Scheme 2-13 is involved in the *fac-mer* isomerization. Therefore, we proposed the isomerization mechanism shown in Scheme 2-14, though the intermediates have not been observed.

2-3-5 *cis-trans* Isomerization of $Mo(CO)_4$(phosphite)$_2$ by Me_3SiOTf

In addition to the isomerization of *fac*-$Mo(CO)_3\{P(OR)_3\}_3$ promoted by Me_3SiOTf, the isomerization of *cis*-$Mo(CO)_4\{P(OR)_3\}_2$ was also investigated. The results are shown in Table 2-7. The *cis-trans* isomerization occurred in the presence of Me_3SiOTf and did not in the absence of Me_3SiOTf for ***cis*-2.7**, and ***cis*-2.9**, and Me_3SiOTf worked as a catalyst. The ^{31}P NMR signals of ***trans*-2.7** and ***trans*-2.9** were observed at 173.4 and 155.1 ppm, respectively. In contrast, ***cis*-2.8** did not isomerize to ***trans*-2.8** even in the presence of Me_3SiOTf. For the *cis-trans* isomerization, the reaction pathway similar to that for the *fac-mer* isomerization of $Mo(CO)_3\{P(OR)_3\}_3$ shown in Scheme 2-14 is proposed. Interaction of Me_3Si^+ with an oxygen in the $P(OR)_3$ ligands may initiate the *cis-trans* isomerization. The basicity of the phosphite oxygen in *cis*-$Mo(CO)_4\{P(OR)_3\}_2$ is considered to be less than that in *fac*-$Mo(CO)_3\{P(OR)_3\}_3$ because the former complex has more CO ligands in number being a strong π-accepter ligand. Among ***cis*-2.7**, ***cis*-2.8**, and ***cis*-2.8**, ***cis*-2.8** has least oxygen basicity because of the substituents (Ph vs Me). Therefore, ***cis*-2.8** may not have enough basicity on the oxygen to form an interaction with Me_3Si^+.

Table 2-7. Isomerization of $Mo(CO)_4\{P(OR)_3\}_2$ by Me_3SiOTf in CH_2Cl_2 at room temperature.[a, b]

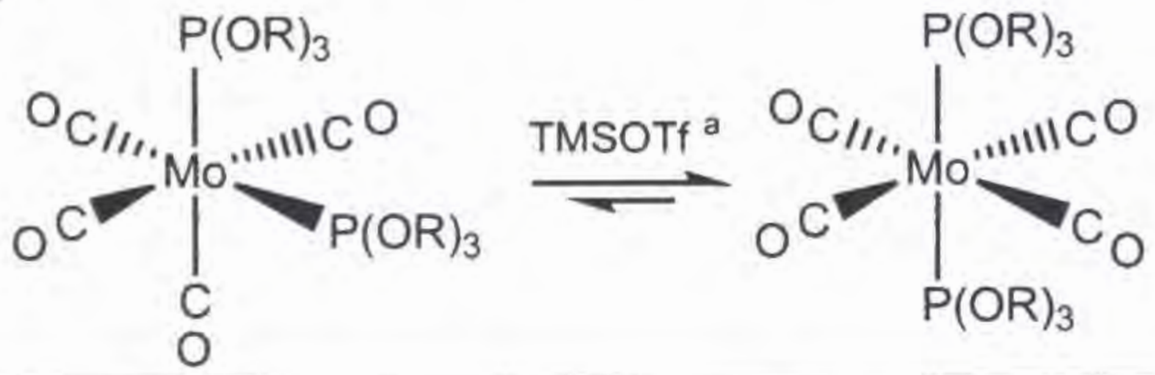

$P(OR)_3$			*cis* : *trans* [c]
$P(OMe)_3$	***cis*-2.7**	***trans*-2.7**	1 : 0.9
$P(OPh)_3$	***cis*-2.8**	***trans*-2.8**	no reaction
$PPh_2(OMe)$	***cis*-2.9**	***trans*-2.9**	1 : 2.3

[a] 1.0, 0.5 and 0.1 equvalents based on the *cis* complex were used.

[b] Reaction conditions: room temperature, 0.1 M CH_2Cl_2 solution

[c] *cis:trans* equilibrium ratio after completion of the isomerization.

2-3-6 Reaction of *fac*-$Mo(CO)_3$(phosphite)$_3$ and *cis*-$Mo(CO)_4$(phosphite)$_2$ with $BF_3 \cdot OEt_2$

Me_3SiOTf and $BF_3 \cdot OEt_2$ are effective Lewis acids to obtain a cationic phosphenium complex by an OR anion abstraction from a diamino-substituted phosphite ligand in a transition metal complex. In contrast, Me_3SiOTf does not abstract an OR anion from a $P(OR)_3$ ligand of *fac*-$Mo(CO)_3\{P(OR)_3\}_3$ and *cis*-$Mo(CO)_4\{P(OR)_3\}_2$, but promotes the *fac-mer* and *cis-trans* isomerization. Therefore, reactions of *fac*-$Mo(CO)_3\{P(OMe)_3\}_3$ (***fac*-2.2**) and *cis*-$Mo(CO)_4\{P(OMe)_3\}_2$ (***cis*-2.7**) with $BF_3 \cdot OEt_2$ were examined and it was found that $BF_3 \cdot OEt_2$ causes some complicated reactions in addition to isomerization.

The ^{31}P NMR spectrum of the reaction mixture of ***fac*-2.2** and an equimolar amount of $BF_3 \cdot OEt_2$ in CH_2Cl_2 showed several unidentified signals in addition to a signals assignable to ***mer*-2.2**. These signals increased in intensity with time but the singlet due to the starting complex (***fac*-2.2**) still remained after several hours.

The reaction of ***cis*-2.7** with an equimolar amount of $BF_3 \cdot OEt_2$ in CH_2Cl_2 at room temperature was followed by the ^{31}P NMR measurement. After 4 h, in addition to a strong singlet due to ***cis*-2.7**, a doublet of doublet at 164.5 ppm (d, J_{PF} = 1157.1, and J_{PP} = 46.9 Hz) and a doublet at 163.4 ppm (d, J_{PP} = 46.9 Hz) were observed. The large coupling constant (1157.1 Hz) suggests the existence of a P-F bond and the small coupling constant (46.9 Hz) indicates that two phosphorus ligands are *cis* to each other. Therefore, the formation of *cis*-$Mo(CO)_4\{P(OMe)_3\}\{P(OMe)_2F\}$ was proposed. The similar OR/F substitution reaction has been reported.[2 16, 2 24, 2 27, 2 29] The ^{31}P NMR spectrum after 24 h, signals due to *cis*-$Mo(CO)_4\{P(OMe)_3\}\{P(OMe)_2F\}$ increased in intensity and a new singlet at 173.4 ppm attributable to ***trans*-2.7** was observed. In addition, several unidentified signals were observed. Therefore, it was found in the reaction of ***cis*-2.7** with $BF_3 \cdot OEt_2$, relatively fast OMe/F substitution reaction and relatively slow *cis* to *trans* isomerization and some unidentified reactions take place.

2-4 Conclusion

In conclusion, this study described, for the first time, a halosilane-catalyzed reaction. Results showed that an interaction of a silane compound with one phosphite oxygen to form a hypervalent silicon structure reduces the *fac-mer* isomerization energy barrier of $Mo(CO)_3(phosphite)_3$. The hypervalent silicon species was detectable spectroscopically. This geometrical isomerizations were also observed in the presence of a catalytic amount of Me_3SiOTf. Crossover experiments suggest that a ligand dissociation is not involved in the isomerization. The catalytic cycle involving an interaction of the silicon atom in Me_3Si^+ with one oxygen in $P(OR)_3$ ligands has been proposed. The first isolation and the X-ray structure analysis were attained for *mer*-$Mo(CO)_3\{P(OPh)_3\}_3$ which was obtained by the Me_3SiOTf-assisted isomerization of *fac*-$Mo(CO)_3\{P(OPh)_3\}_3$. Similar *cis-trans* isomerization of $Mo(CO)_4(phosphite)_2$ proceeded by Me_3SiOTf.

2-5 Experimental Section

General Remarks. All reactions were carried out under an atmosphere of dry nitrogen by using standard Schlenk tube techniques. All solvents were purified by distillation: THF and benzene were distilled from sodium/benzophenone, hexane and *n*-pentane were distilled from sodium metal, CH_3CN and CH_2Cl_2 were distilled from CaH_2. All solvents were stored under nitrogen atmosphere. TMSOTf, MeOTf and BF_3OEt_2 were distilled and were stored under a nitrogen atmosphere. Other reagents employed in this research were used as received. Column chromatography was done quickly in the air.

IR spectra were recorded on a Perkin-Elmer Spectrum One spectrometer. A JEOL JNM-AL400 spectrometer was used to obtain ^{1}H, ^{13}C, ^{29}Si, ^{31}P NMR spectra. ^{1}H, ^{13}C and ^{29}Si NMR data were referenced to Me_4Si. ^{31}P NMR data were referenced to 85 % H_3PO_4.

Preparation of *fac*-$Mo(CO)_3(NCMe)_3$ (*fac*-2.1). ***Fac*-2.1** was prepared according to literature methods.[241] $Mo(CO)_6$ (17.7 g, 6.70 mmol) in CH_3CN (120 mL) was introduced into a 100 mL Schlenk tube equipped with a magnetic stir bar and a reflux condenser connected to an oil bubble. The solution was heated to reflux under dinitrogen for 5 h to result in a dark-yellow solution, at which point the IR spectrum indicated that $Mo(CO)_6$ was completely transformed to ***fac*-2.1**. After filtration to remove insoluble materials, volatile materials were removed under reduced pressure. The resulting precipitate was washed with *n*-pentane and dried in vacuo to give a gray powder of ***fac*-2.1** (16.6 g, 5.48 mmol, 81.7 %).

Preparation of *fac*-$Mo(CO)_3\{P(OMe)_3\}_3$ (*fac*-2.2). ***Fac*-2.2** was synthesized according to the literature methods.[212] $P(OMe)_3$ (0.65 mL, 5.51 mmol) was added to a solution of $Mo(CO)_3(NCMe)_3$ (***fac*-2.1**) (0.55 g, 1.81 mmol) in THF (20 mL) in a Schlenk tube, and the reaction mixture was stirred for 4 h at room temperature. After volatile materials were removed under reduced pressure, the resulting precipitate was

washed with hexane a few times and dried in vacuo to give a white powder of ***fac*-2.2** (0.92 g, 1.67 mmol, 92 %). ^{1}H NMR (δ, in $CDCl_3$): 3.61 (d, 27H, $^{3}J_{PH}$ = 10.8 Hz, OCH_3). $^{13}C\{^{1}H\}$ NMR (δ, in $CDCl_3$): 51.4 (m, OCH_3), 215.9 (m, CO). $^{31}P\{^{1}H\}$ NMR (δ, in $CDCl_3$): 168.0 (s). IR (cm^{-1}, in $CDCl_3$): ν (CO) 1880, 1967.

Preparation of *fac*-$Mo(CO)_3\{P(OEt)_3\}_3$ (*fac*-2.3).[2.42] ***Fac*-2.3** was prepared in a manner similar to that for ***fac*-2.2**. $P(OEt)_3$ (0.67 mL, 3.90 mmol) was added to a solution of $Mo(CO)_3(NCMe)_3$ (***fac*-2.1**) (0.39 g, 1.30 mmol) in THF (20 mL) in a Schlenk tube, and the reaction mixture was stirred for 4 h at room temperature. After volatile materials were removed under reduced pressure, the resulting precipitate was washed with hexane a few times at -78 °C and dried in vacuo to give a white powder of ***fac*-2.3** (0.61 g, 1.2 mmol, 92 %). ^{1}H NMR (δ, in $CDCl_3$): 1.22 (m, 27H, OCH_2CH_3), 3.96 (m, 18H, OCH_2CH_3). $^{13}C\{^{1}H\}$ NMR (δ, in $CDCl_3$): 16.4 (m, OCH_2CH_3), 59.7 (s, OCH_2CH_3), 216.4 (s, CO). $^{31}P\{^{1}H\}$ NMR (δ, in $CDCl_3$): 161.2 (s). IR (cm^{-1}, in $CDCl_3$): ν (CO) 1860, 1963.

Preparation of *fac*-$Mo(CO)_3\{P(OPh)_3\}_3$ (*fac*-2.4).[2.42, 2.43] ***Fac*-2.4** was prepared in a manner similar to that for ***fac*-2.2**. $P(OPh)_3$ (1.36 mL, 5.19 mmol) was added to a solution of $Mo(CO)_3(NCMe)_3$ (***fac*-2.1**) (0.52 g, 1.72 mmol) in THF (20 mL) in a Schlenk tube, and the reaction mixture was stirred for 4 h at room temperature. After volatile materials were removed under reduced pressure, the resulting precipitate was washed with hexane a few times and dried in vacuo to give a white powder of ***fac*-2.4** (1.57 g, 1.41 mmol, 82 %). ^{1}H NMR (δ, in $CDCl_3$): 6.98-7.18 (m, 45H, Ph). $^{13}C\{^{1}H\}$ NMR (δ, in $CDCl_3$): 121.9 (s, *p*-Ph), 124.3 (s, *m*-Ph), 129.4 (s, *o*-Ph), 152.1 (s, *ipso*-Ph), 212.2 (m, CO). $^{31}P\{^{1}H\}$ NMR (δ, in $CDCl_3$): 145.0 (s). IR (cm^{-1}, in $CDCl_3$): ν (CO) 1917, 1992.

Preparation of *fac*-$Mo(CO)_3\{P(\overline{NMeCH_2CH_2NMe})(OMe)\}_3$ (*fac*-2.5). ***Fac*-2.5** was synthesized according to the literature methods.[2.13] $P(\overline{NMeCH_2CH_2NMe})(OMe)$ (0.68 mL, 4.7 mmol) was added to a solution of $Mo(CO)_3(NCMe)_3$ (***fac*-2.1**) (0.44 g, 1.50

mmol) in THF (20 mL) in a Schlenk tube, and the reaction mixture was stirred for 4 h at room temperature. After volatile materials were removed under reduced pressure, the resulting precipitate was washed with hexane a few times and dried in vacuo to give a white powder of ***fac*-2.5** (0.66 g, 1.1 mmol, 71 %). ^{1}H NMR (δ, in $CDCl_3$): 2.80 (m, 18H, NCH_3), 3.14 (m, 6H, NCH_2), 3.17 (m, 9H, OCH_3), 3.27 (m, 6H, NCH_2). $^{13}C\{^{1}H\}$ NMR (δ, in $CDCl_3$): 33.59 (m, NCH_3), 50.20 (m, OCH_3), 52.25 (m, NCH_2), 218.28 (m, CO). $^{31}P\{^{1}H\}$ NMR (δ, in $CDCl_3$): 149.36 (s). IR (cm^{-1}, in $CDCl_3$): ν (CO) 1841,1944.

Isolation of *mer*-$Mo(CO)_3\{P(OPh)_3\}_3$ (*mer*-2.4). A CH_2Cl_2 solution (20 mL) containing ***fac*-2.4** (2.3 g, 2.07 mmol) and TMSOTf (0.38 mL, 2.08 mmol) was stirred for 1.5 h at room temperature. After volatile materials were removed under reduced pressure, the resulting precipitate was washed with hexane (3 mL, 5 times) at -78 °C and dried in vacuo to give a white powder of a mixture of ***fac*-2.4** and ***mer*-2.4** (1 : 30). To obtain pure ***mer*-2.4**, the powder was washed with hexane/CH_2Cl_2 = 100/1 solution (5 mL, 20 times) at room temperature, and the powder was dried in vacuo (1.22 g, 1.10 mmol, 53 %). ^{1}H NMR (δ, in $CDCl_3$): 6.83-7.25 (m, 45H, Ph). $^{13}C\{^{1}H\}$ NMR (δ, in $CDCl_3$): 115.5 (s, Ph), 121.8 (s, Ph), 124.4 (s, Ph), 129.5 (s, Ph), 129.7 (s, Ph), 129.9 (s, Ph), 152.1 (s, Ph), 155.7 (s, Ph), 208.0 (m, CO), 213.0 (m, CO). $^{31}P\{^{1}H\}$ NMR (δ, in $CDCl_3$): 148.6 (t, $^{2}J_{PP}$ = 46.9 Hz, equatorial-P), 155.4 (d, $^{2}J_{PP}$ = 46.9 Hz, apical-P). IR (cm^{-1}, in $CDCl_3$): ν (CO) 1931, 1813.

Preparation of $Mo(CO)_4$(nbd) (nbd = 2,5-norbornadiene) (2.6). Complex **2.6** was prepared according to literature methods.[244] A hexane solution (30 mL) of $Mo(CO)_6$ (4.1 g, 15.4 mmol) and 2,5-norbornadiene (4.7 mL, 46.2 mmol) was introduced into a 100 mL Schlenk tube equipped with a magnetic stir bar and a reflux condenser connected to an oil bubble. The mixture was heated to reflux under dinitrogen for 2 days to result in a dark-brown solution, at which point the IR spectrum indicated $Mo(CO)_6$ was completely transformed to **2.6**. After filtration to remove insoluble materials, volatile materials were removed under reduced pressure. The resulting

precipitate was washed with hexane at -78 °C and dried in vacuo to give a dark-orange powder of **2.6** (3.5 g, 10.6 mmol, 69 %).

Preparation of *cis*-$Mo(CO)_4\{P(OMe)_3\}_2$ (*cis*-2.7).[2.45] $P(OMe)_3$ (0.52 mL, 4.42 mmol) was added to a solution of $Mo(CO)_4$(nbd) (**2.6**) (0.73 g, 2.21 mmol) in CH_2Cl_2 (10 mL) in a Schlenk tube, and the reaction mixture was stirred for 4 h at room temperature. After volatile materials were removed under reduced pressure, the resulting precipitate was washed with hexane a few times at -78 °C and dried in vacuo to give a white powder of ***cis*-2.7** (0.97 g, 2.13 mmol, 96 %). ^{1}H NMR (δ, in $CDCl_3$): 3.62 (d, $^3J_{PH}$ = 5.6 Hz, 9H, OCH_3). $^{13}C\{^1H\}$ NMR (δ, in $CDCl_3$): 51.4 (s, OCH_3), 207.9 (t, $^2J_{PC}$ = 14.1 Hz, *cis*-CO), 212.1 (t, $^2J_{PC}$ = 13.3 Hz, *trans*-CO). $^{31}P\{^1H\}$ NMR (δ, in $CDCl_3$): 165.6 (s). IR (cm^{-1}, in $CDCl_3$): ν (CO) 2036, 1921.

Preparation of *cis*-$Mo(CO)_4\{P(OPh)_3\}_2$ (*cis*-2.8).[2.46] $P(OPh)_3$ (0.83 mL, 4.92 mmol) was added to a solution of $Mo(CO)_4$(nbd) (**2.6**) (0.81 g, 2.42 mmol) in CH_2Cl_2 (10 mL) in a Schlenk tube, and the reaction mixture was stirred for 4 h at room temperature. After volatile materials were removed under reduced pressure, the resulting precipitate was washed with hexane a few times at -78 °C and dried in vacuo to give a white powder of ***cis*-2.8** (1.87 g, 2.26 mmol, 93 %). ^{1}H NMR (δ, in $CDCl_3$): 7.18-7.36 (m, 30H, Ph). $^{13}C\{^1H\}$ NMR (δ, in $CDCl_3$): 121.6 (s, *p*-Ph), 124.9 (s, *m*-Ph), 129.8 (s, *o*-Ph), 151.4 (t, $^2J_{PC}$ = 4.2 Hz, *ipso*-Ph), 205.5 (t, $^2J_{PC}$ = 13.3 Hz, *cis*-CO), 212.1 (t, $^2J_{PC}$ = 18.2 Hz, *trans*-CO). $^{31}P\{^1H\}$ NMR (δ, in $CDCl_3$): 165.6 (s). IR (cm^{-1}, in $CDCl_3$): ν (CO) 2036, 1921.

Preparation of *cis*-$Mo(CO)_4\{PPh_2(OMe)\}_2$ (*cis*-2.9).[2.47] $PPh_2(OMe)$ (0.76 mL, 3.82 mmol) was added to a solution of $Mo(CO)_4$(nbd) (**2.6**) (0.63 g, 1.91 mmol) in CH_2Cl_2 (10 mL) in a Schlenk tube, and the reaction mixture was stirred for 3 h at room temperature. After volatile materials were removed under reduced pressure, the resulting precipitate was washed with hexane a few times at -78 °C and dried in vacuo to give a white powder of ***cis*-2.9** (1.17 g, 1.82 mmol, 96 %). ^{1}H NMR (δ, in $CDCl_3$):

3.27 (d, $^{3}J_{PH}$ = 4.9 Hz, 3H, OCH_3), 7.40-7.53 (m, 10H, Ph). $^{13}C\{^{1}H\}$ NMR (δ, in $CDCl_3$): 53.6 (s, OCH3), 128.1 (s, *p*-Ph), 130.1 (s, *m*-Ph), 131.2 (t, $^{2}J_{PC}$ = 6.6 Hz, *o*-Ph), 139.0 (t, $^{2}J_{PC}$ = 15.8 Hz, *ipso*-Ph), 209.5 (t, $^{2}J_{PC}$ = 10.3 Hz, *cis*-CO), 214.6 (t, $^{2}J_{PC}$ = 9.5 Hz, *trans*-CO). $^{31}P\{^{1}H\}$ NMR (δ, in $CDCl_3$): 144.9 (s). IR (cm^{-1}, in $CDCl_3$): ν (CO) 2026, 1912.

Treatment of complexes with Me_3SiCl, TMSOTf, MeOTf and BF_3OEt_2. *fac*-$Mo(CO)_3$(phosphite)$_3$ and *cis*-$Mo(CO)_4$(phosphite)$_2$ (0.06 mmol) were treated with an appropriate amount of Me_3SiCl, TMSOTf, MeOTf and BF_3OEt_2 in CH_2Cl_2 (0.6 mL). Then, the solutions were subjected to the ^{31}P NMR measurements at room temperature at appropriate intervals.

Detection of Intermediates in the isomerization of *fac*-2.2. ***fac*-2.2** (100 mg, 0.18 mmol) was dissolved in Me_3SiCl (0.6 mL) and the solution was subjected to the ^{31}P and ^{29}Si NMR measurements at room temperature.

X-ray Crystal Structure Determination of *mer*-2.4. Crystals of ***mer*-2.4** suitable for an X-ray diffraction study were obtained through crystallization from CH_2Cl_2/hexane/benzene for a few days. The single crystal was mounted in a glass capillary. Data for ***mer*-2.4** were collected at -70 °C to a maximum 2θ value of 55.0 ° on Rigaku/MSC Mercury CCD area-detector diffractometer equipped with monochromated Mo Kα radiation (λ =0.71070 Å). Cell constants and an orientation matrix for data collection corresponded to a primitive monoclinic cell with dimensions of a = 11.9900(3) Å, b = 20.7000(4) Å, c = 24.1000(1) Å, α = 67.630(4) °, β = 77.640(6) °, γ = 87.590(6) °, Z = 4 and V = 53980(3) Å^3. P-1 (No. 2) was selected as the space group, which led to successful refinements. All calculations for ***mer*-2.4** were performed with the teXan crystallographic software package of Molecular Structure Corporation. H atoms were refined using a riding model, with C-H = 0.95 Å, and fixed individual displacement parameters [U_{iso} (H) = U_{eq} (C)]. The crystal was formulated as ***mer*-2.4**·$0.5CH_2Cl_2 \cdot 0.5C_6H_6$. The CH_2Cl_2 molecule was disordered in two positions with 50:50

probability in the unit cell.

2-6 References

2.1 Larson, G. L. In *The Chemistry of Organic Silicon Compounds*; Patai, S., Rappoport, Z., Eds.; Wiley: London **1989**; p763.

2.2 Miura, K.; Hosomi, A. In *Main Group Metals in Organic Synthesis* Yamamoto, H., Oshima, K., Eds.;Wiley-VCH: Weinheim, Germany **2004**; p 409.

2.3 Mukaiyama, T. In *Organic Reactions*; Wiley, New York **2000**.

2.4 Gennari, C. In *Comprehensive Organic Synthesis*; Trost, B. M., Fleming, I., Eds.; Pergamon Press, Oxford **1991**, *2*, Chap. 2.4, p 629.

2.5 Hosomi, A. *Acc. Chem. Res*. **1988**, *21*, 200.

2.6 Fleming, I. In *Comprehensive Organic Synthesis*; Trost, B. M., Fleming, I., Eds.; Pergamon Press, Oxford **1991**, *2*, Chap. 2.2, p 563.

2.7 (a) Hiyama, T. In *Metal-Catalyzed Cross Coupling Reactions*; Wiley, Weinheim **1998**, Chap. 10, p 421. (b) Hatanaka, Y.; Hiyama, T. *Synlett* **1991**, 845.

2.8 Sugiura, M.; Hagio, H.; Hirabayashi, R.; Kobayashi, S. *J. Am. Chem. Soc*. **2001**, *123*, 12510.

2.9 Bond, A. M.; Colton, R.; Feldberg, S. W.; Mahon, P. J.; Whyte, T. *Organometallics* **1991**, *10*, 3320.

2.10 Nakazawa, H.; Yamaguchi, Y.; Miyoshi, K. *J. Organomet. Chem*. **1994**, *465*, 193.

2.11 Rousche, J. –C.; Dobson, G. R. *Inorg. Chim. Acta* **1978**, *28*, L139.

2.12 Howell, J. A. S.; Yates, P. C.; Ashford, . F.; Dixon, D. T.; Warren, R. *J. Chem. Soc. Dalton Trans*. **1996**, *20*, 3959.

2.13 Nakazawa, H.; Miyoshi, Y.; Katayama, T.; Mizuta, T.; Miyoshi, K.; Tsuchida, N.; Ono, A.; Takano, K. *Organometallics* **2006**, *25*, 5913.

2.14 Williams, E. A. In *The Chemistry of Organic Silicon Compounds*; Patai, S., Rappoport, Z., Eds.; John Wiley & Sons Ltd. **1989**; p 511.

2.15 Kummer, D.; Halim, S. H. A.; Kuhs, W.; Mattern, G. *J. Organomet. Chem.* **1993**, *446*, 51.

2.16 Dilma, A. D.; Ioffe, S. L. *Chem. Rev.* **2003**, *103*, 733.

2.17 Giju, K. T.; Proft, F. D.; Geerlings, P. *J. Phys. Chem. A* **2005**, *109*, 2925.

2.18 Dobson, G. R.; Rettenmaier, A. J. *Inorg. Chim. Acta* **1972**, *6*, 433.

2.19 Cowley, A. H.; Kemp, R. A. *Chem. Rev.* **1985**, *85*, 367.

2.20 (a) Sanchez, M.; Mazieres, M. R.; Lamande, L.; Wolf, R. *Multiple Bonds and Low Coordination in Phosphorus Chemistry,* Regitz, M., Scherer, O. J., Eds., Thieme, New York **1990**; Chapter D1. (b) Schmidpeter, A. *Multiple Bonds and Low Coordination in Phosphorus Chemistry*, Regitz, M., Scherer, O. J., Eds., Thieme, New York **1990**; Chapter D2.

2.21 Gudat, D. *Coord. Chem. Rev.* **1997**, *163*, 71.

2.22 Nakazawa, H. *J. Organomet. Chem.* **2000**, *611*, 349.

2.23 Nakazawa, H. *Avd. Organomet. Chem.* **2004**, *50*, 107.

2.24 Nakazawa, H.; Ohta, M.; Miyoshi, K.; Yoneda, H. *Organometallics* **1989**, *8*, 638.

2.25 Nakazawa, H.; Yamaguchi, Y.; Miyoshi, K. *J. Organomet. Chem.* **1994**, *465*, 193.

2.26 Nakazawa, H.; Yamaguchi, Y.; Mizuta, T.; Miyoshi, K. *Organometallics* **1995**, *14*, 4137.

2.27 Yamaguchi, Y.; Nakazawa, H.; Itoh, T.; Miyoshi, K. *Bull. Chem. Soc. Jpn.* **1996**, *69*, 983.

2.28 Nakazawa, H.; Yamaguchi, Y.; Miyoshi, K. *Phosphorus Sulfur Silicon* **1996**, *109*, 129.

2.29 Nakazawa, H.; Yamaguchi, Y.; Miyoshi, K.; Nagasawa, A. *Organometallics* **1996**, *15*, 2517.

2.30 Takano, K.; Tsumura, H.; Nakazawa, H.; Murakata, M.; Hirano, T. *Organometallics* **2000**, *19*, 3323.

2.31 Nakazawa, H.; Kishishita, M.; Yoshinaga, S.; Yamaguchi, Y.; Mizuta, T.; Miyoshi, K. *J. Organomet. Chem.* **1997**, *529*, 423.

2.32 Nakazawa, H.; Kishishita, M.; Miyoshi, K. *Phosphorus Sulfur Silicon* **1999**, *144*, 45.

2.33 Nakazawa, H.; Kishishita, M.; Ishiyama, T.; Mizuta, T.; Miyoshi, K. *J. Organomet. Chem.* **2001**, *617-618*, 453.

2.34 Nakazawa, H.; Yamashita, Y.; Miyoshi, K. *Phosphorus Sulfur Silicon* **2002**, *177*, 1533.

2.35 Nakazawa, H.; Yamaguchi, Y.; Mizuta, T., Ichimura, S.; Miyoshi, K. *Organometallics* **1995**, *14*, 4635

2.36 Nakazawa, H.; Yamaguchi, Y., Miyoshi, K *Organometallics* **1996**, *15*, 1337

2.37 Nakazawa, H.; Yamaguchi, Y., Kawamura, K., Miyoshi, K *Organometallics* **1997**, *16*, 4626.

2.38 Kawamura, K.; Nakazawa, H., Miyoshi, K *Organometallics* **1999**, *18*, 1517.

2.39 Kawamura, K.; Nakazawa, H., Miyoshi, K *Organometallics* **1999**, *18*, 4785

2.40 Nakazawa, H., Kishishita, M., Nakamoto, T., Makanura, N., Ishiyama, T.; Miyoshi, K. *Chem. Lett* **2000**, 230

2.41 Li, C.-I.; Yeh, W.-Y., Peng, S.-M., Lee, G.-H *J Organomet Chem.* **2001**, *620*, 106-112.

2.42 Poilblanc, P. R.; Bigorgne, M *Bull Soc Chim France* **1962**, 1301

2.43 Alyea, E. C.; Ferguson, G., Song, S.-Q *Acta Cryst* **1995**, *C51*, 2238

2.44 Chow, T. J., Wu, M.-Y., Liu, L.-K *J Organomet Chem* **1985**, *281*, C33-C37.

2.45 Ogilvie, F. B; Jenkins, J. M., Verkade, J. G *J Am Chem Soc* **1970**, *92*, 1916.

2.46 Dobson, G. R., Rettenmaier, A. J *Inorg Chim Acta* **1972**, *6*, 507

2.47 Gary, M. G.; Krahanzel, C. S *J Organomet Chem* **1983**, *241*, 201

Chapter 3.

N-CN Bond Cleavage of Cyanamide by a Transition Metal Complex Bearing a Silyl Ligand

3-1 Introduction

3-1-1 Character of Cyanamides (R_2NCN)

In the last two decades, considerable efforts have been devoted to cleavage of carbon-hydrogen,[31] carbon-carbon,[32] carbon-nitrogen[33] and carbon-oxygen.[34] Direct cleavage of these bonds provides several advantages in organic syntheses, including atom efficiency, low environmental load, and the potential for unusual chemoselectivity. Here I focus attention on the N-CN bond cleavage of cyanamide (R_2N-CN) by a transition metal complex.

H_2N-CN, the simplest cyanamide, consists of an amino group and a cyano group and is synthesized from chlorocyane and ammonia at first time in 1838 (von Braun reaction).[35] Nowadays, most cyanamides including H_2N-CN have been prepared from calcium cyanamide (CaNCN), which has been obtained from calucium carbide (CaC) and dinitrogen (N_2).[36]

H_2N-CN and HN=C=NH (carbodiimide) are referred to as tautomers. This phenomenon indicates that N-CN bond has a double bond character (eq. 3-1).

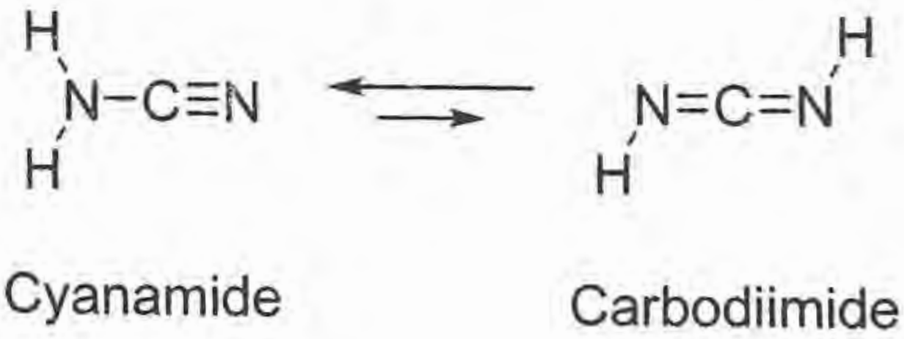

Cyanamide Carbodiimide (3-1)

Other cyanamides have similar double bond character in the N-CN bond. Cunningham et al. reported that the N-CN bond length in Me(p-C_6H_4Cl)N-CN is 1.331 Å, which lies just between those of a normal N-C single bond (1.47 Å) and an N=C double bond (1.27 Å) (Figure 3-1).[37]

As mentioned above, the N-CN bond in cyanamide is strong and difficult to cleavage. The von Braun reaction is the only reaction known to date to cleave the R_2N-CN bond.[38] However, it requires harsh reaction conditions (strong acid or base

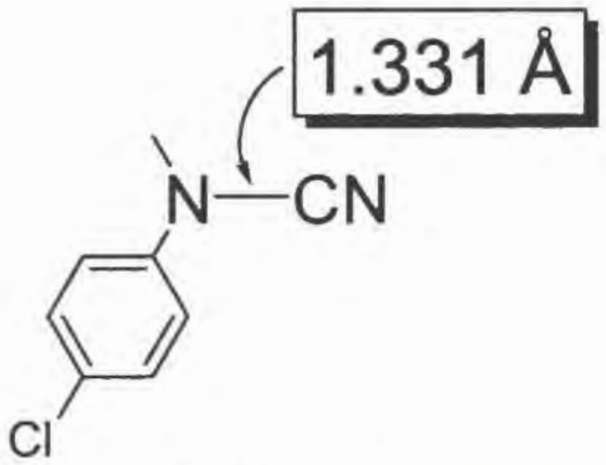

General Bond Distance	
N−C	1.47 Å
N=C	1.27 Å
N≡C	1.16 Å

Figure 3-1. N-CN bond length of Me(*p*-C_6H_4Cl)N-CN.

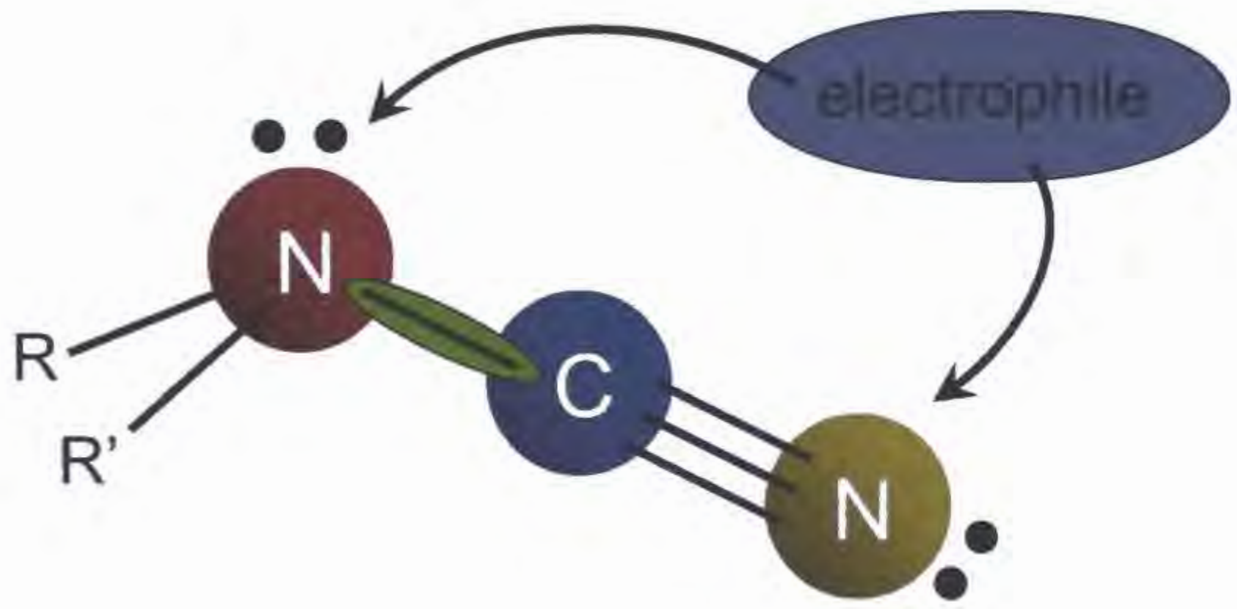

Figure 3-2. Cyanamide molecular model.

conditions).

Another general character of cyanamide is that the molecule has two nitrogen atoms, which are both electrophilic sites (Figure 3-2). For example, a Lewis acid BH_3 attacks the N atom of the amine fragment selectively in the reaction of Me_2NCN with BH_3. The fact demonstrates that the N atom of the amine fragment has higher nucleophilicity than that of the cyano group. Thereby the selective reaction for the cyano group is difficult.

3-1-2 C-CN bond Cleavage of Organonitriles with an Iron Complex

Nakazawa et al. recently reported reactions of C-CN bond cleavage of organonitriles promoted by a silyl-iron complex.[3 2(d)] The essence of the reaction mechanism for Me-CN bond cleavage is depicted in eq. 3-2. Acetonitrile coordinates to a 16e silyl-iron complex $Cp(CO)Fe(SiEt_3)$ produced from $Cp(CO)_2Fe(SiEt_3)$ (**3.1**) in a photoreaction to give an η^1-MeCN complex, which is converted into an η^2-MeCN complex. Then, silyl migration from Fe to the nitrile nitrogen atom occurs to form η^2-iminoacyl complex. The transition state of this step has a pentacoordinate silicon structure. The theoretical calculation revealed that the activation energy is only 4.8 kcal/mol. Following C-C bond cleavage on the coordination sphere gives a methylsilylisocyanide complex. The η^2-coodination of acetonitrile through the C≡N π-bond induces silyl migration, which then causes C-CN bond cleavage. The reaction sequences stimulate me to examine the possibility of R_2N-CN bond cleavage by a silyl-iron complex because the replacement of the R group in RCN by an NR_2 group yields cyanamide. Herein, I describe the first R_2N-CN bond cleavage reaction by a transition-metal complex, isolation of an intermediate, and establishment of a catalytic cycle involving R_2N-CN bond cleavage.

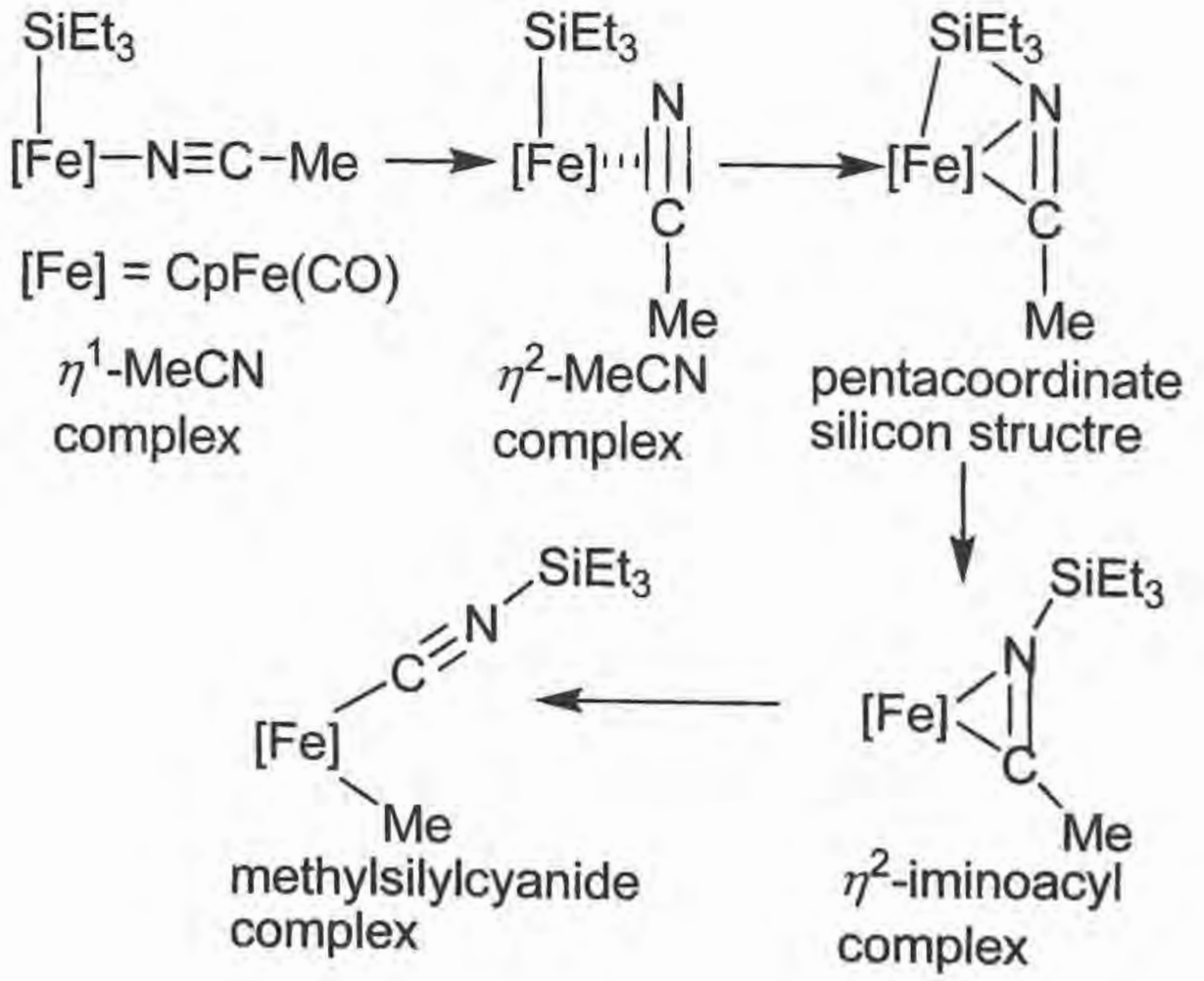

(3-2)

3-2 N-CN Bond Cleavage with a Silyl-Iron Complex

3-2-1 N-CN Bond Cleavage of Masked Cyanamides

The amino nitrogen atom in R_2NCN has higher nucleophilicity than the cyano nitrogen atom. Coordination of cyanamide to the 16e Fe species, $Cp(CO)Fe(SiEt_3)$, through the amino nitrogen, may reduce the activity of the iron complex toward R_2N-CN bond cleavage (Figure 3-3). Derivation of cyanamide into the borane adduct at the amino nitrogen, $R_2N(BX_3)CN$ (X = H, F)[39], might engender more effective R_2N-CN bond cleavage because of masking of the lone pair electrons on the amino nitrogen.

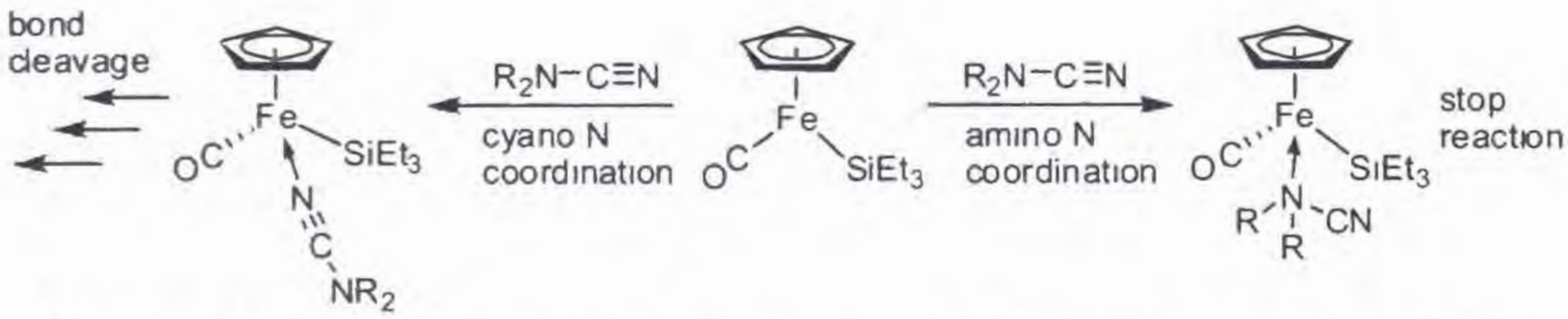

Figure 3-3. Expected paths in the treatment of 16e Fe complex with Me_2NCN.

A THF solution containing $Cp(CO)_2Fe(SiEt_3)$ (**3.1**) and R_2NCN bearing a Lewis acid was irradiated with a 400 W medium pressure mercury arc lamp at room temperature for 24 h and Et_3SiCN formed was determined by gas chromatography. The results are listed in Table 3-1. A small amount of Et_3SiCN was produced in the reaction of BH_3 adduct of Me_2NCN, indicating the N-CN bonds was cleaved (entry 1). Similar results were obtained for BH_3 adducts of other cyanamides (entries 2 to 4). It should be noted that better N-CN bond cleavage without BH_3 (vide infra). No N-CN bond cleavage was attained for cyanamide was observed for the BF_3 and $AlCl_3$ adducuts (entries 5 and 6).

Table 3-1. Photoreaction of 3.1 with cyanamides bearing with Lewis acid.

$Cp(CO)_2(SiEt_3)$ **(3.1)** + substrate $\xrightarrow[\text{in THF}]{h\nu \text{ for } 24H}$ Et_3SiCN

entry	substrate	GC Yield of Et_3SiCN	entry	substrate	GC Yield of Et_3SiCN
1	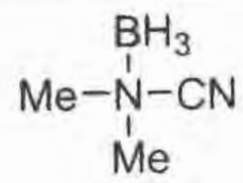	14 %	4	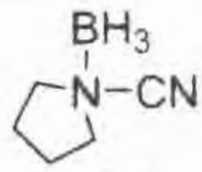	19 %
2	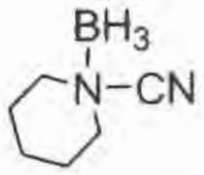	18 %	5	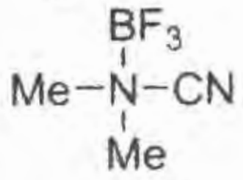	0 %
3	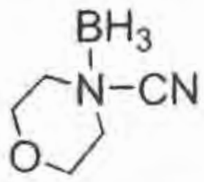	8 %	6	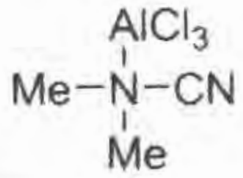	0 %

3-2-2 N-CN Bond Cleavage of Non-Masked Cyanamides

The reaction of **3.1** with cyanamides without a Lewis acid was examined. The results are presented in Table 3-2. Although the yields of Et_3SiCN are less than 50%, these N-CN bonds are cleaved. The reaction of H_2NCN is noteworthy (entry 6). The H_2N-CN bond has a double bond character because H_2N-CN (cyanamide) is a tautomer of HN=C=NH (carbodiimide) (Chapter 3-1-1). Therefore, H_2N-CN bond is stronger than other R_2N-CN. The first H_2N-CN bond cleavage is attainable in our reaction conditions, although the efficiency remains insufficient.

Table 3-2. Photoreaction of cyanamides with 3.1.

$Cp(CO)_2(SiEt_3)$ **(3.1)** + substrate $\xrightarrow[\text{in THF, hν, 24 h}]{}$ Et_3SiCN

entry	substrate	GC Yield of Et_3SiCN	entry	substrate	GC Yield of Et_3SiCN[a]
1	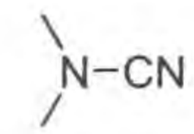	51 %	4	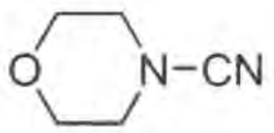	32 %
2	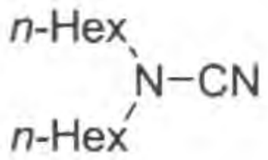	30 %	5	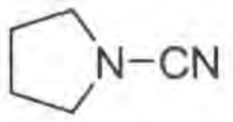	26 %
3	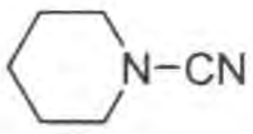	41 %	6	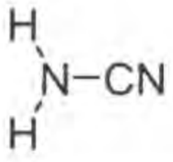	20 %[b]

[a]Yield of Et_3SiCN obtained by GC. [b]In 1,2-dichloroethane.

3-2-3 Optimization of Solvent and Reaction Time in the N-CN Bond Cleavage of Me_2NCN

Optimization of a reaction solvent and time in the reaction of Me_2NCN with a silyl-iron complex **3.1** under photo-irradiation was performed. The attempted solvents were listed in Table 3-3. Halogen-containing solvents (entries 1 and 2) and toluene (entry 3) showed relatively good results. N-coordinative solvents except NEt_3, however, showed worse results (entries 4, 6-8). Other solvents showed unfavorable results except DMF (entries 9-13). Consequently, 1,2-dichloroethane, toluene and DMF seem to be good solvents.

Table 3-3. Photoreaction of Me_2NCN with 3.1 in various solvents.[a]

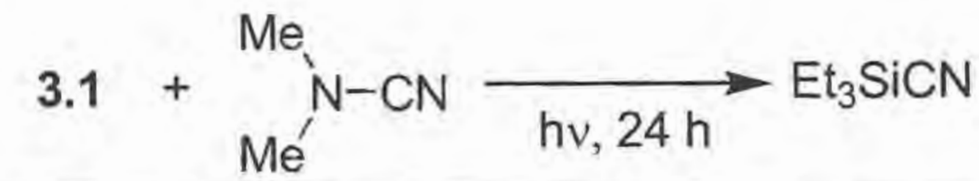

entry	Solvents	GC Yield of Et_3SiCN	entry	Solvents	GC Yield of Et_3SiCN
1	chloroform	43 %	8	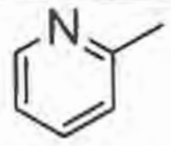	32 %
2	1,2-dichloroethane	52 %	9	DMSO	10 %
3	toluene	50 %	10	DMF	50 %
4	THF	27 %	11	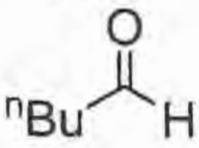	8 %
5	NEt_3	43 %	12	EtOH	8 %
6	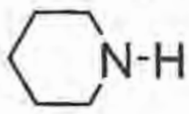	10 %	13	H_2O / NEt_3 = 1 / 9	0 %
7	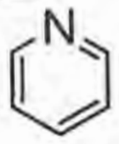	26 %			

[a] Complex **3.1** was treated with 1 equiv of Me_2NCN at room temperature under photo-irradiation for 24 h.

Figure 3-4 showes the time course chart of the yield of Et_3SiCN in the reaction of $Cp(CO)_2Fe(SiEt_3)$ with Me_2NCN under photo-irradiation. The chart indicates that the stoichiometric cleavage was completed around 11 hours.

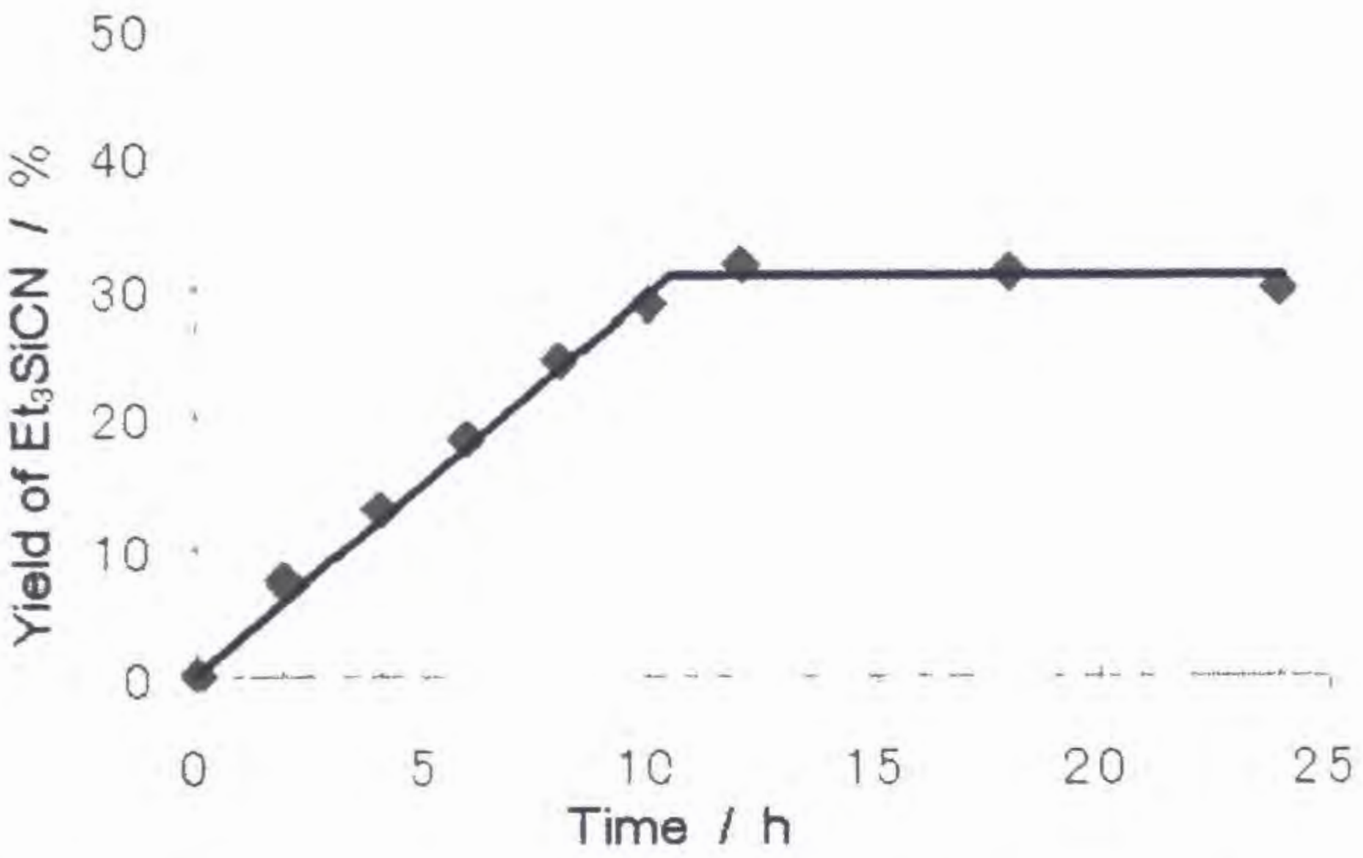

Figure 3-4. Time course of the yield of Et_3SiCN in the reaction of 3.1 with Me_2NCN under photo-irradiation (entry 4 in Table 4-4).

3-2-4 Synthesis, Isolation, and Characterization of N-Silylated η^2-Amidino Iron Complex

Reaction sequences resembling those in eq. 3-2 are expected for the reaction of **3.1** with cyanamide (eq. 3-3). We attempted to isolate N-silylated η^2-amidino iron

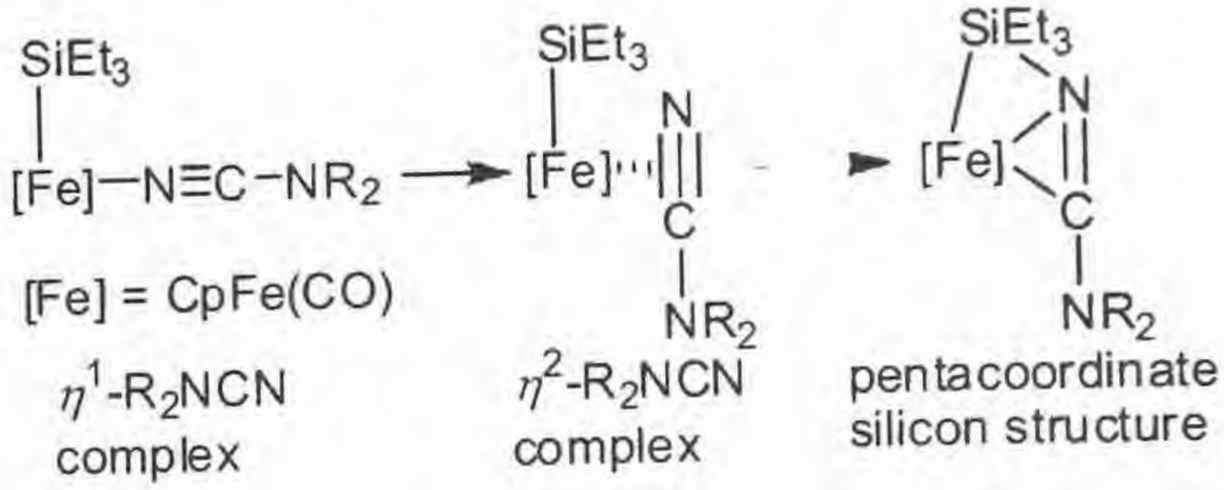

(3-3)

complex as one intermediate, but it was unsuccessful in the reaction of **3.1** with Me_2NCN. However, reactions with Me_2NCN of $(C_5R_5)Fe(CO)(py)(SiR'R''_2)$ (py = pyridine), considered as a synton of a 16e complex $(C_5R_5)Fe(CO)(SiR'R''_2)$, led to isolation of N-silylated η^2-amidino iron complexes (Scheme 3-1). Heating a solution containing **3.3** and Me_2NCN in benzene at 50°C for 10 h yielded **3.4** quantitatively according to the NMR measurements, but the isolation as a solid was failed. In contrast, a reaction of **3.5** with Me_2NCN yielded **3.6**, which can be isolated as dark-red powders in 85% yield. The unprecedented η^2-amidino complex was confirmed using X-ray analysis (Figure 3-5, Tables 3-4, 3-5). The iron takes a distorted three-legged piano-stool structure with an η^2-amidino fragment. The bond distance of N1-C2 (1.327 Å) is shorter than that of a typical N-C single bond (*e.g.*, C3-N1 = 1.455 Å, C4-N1 = 1.458 Å), and is rather similar to that of an N=C double bond (*e.g.*, N2-C2 = 1.303 Å). The sum of angles around N1 is 359.9°. These structural characters are

consistent with sp^2 hybridization of N1. The C3-N1-C2-N2 fragment is nearly planar with a torsion angle of 2.6(4)°. Both ^1H and ^{13}C NMR spectra show that the structure in a solid state is maintained in solution. Two NCH_3 resonances were observed at room temperature in ^1H and ^{13}C NMR (2.37 ppm (s) and 3.05 ppm (s) in ^1H NMR, 39.6 ppm (s) and 42.4 ppm (s) in ^{13}C NMR), reflecting that the C2-N1 bond does not rotate freely at room temperature.

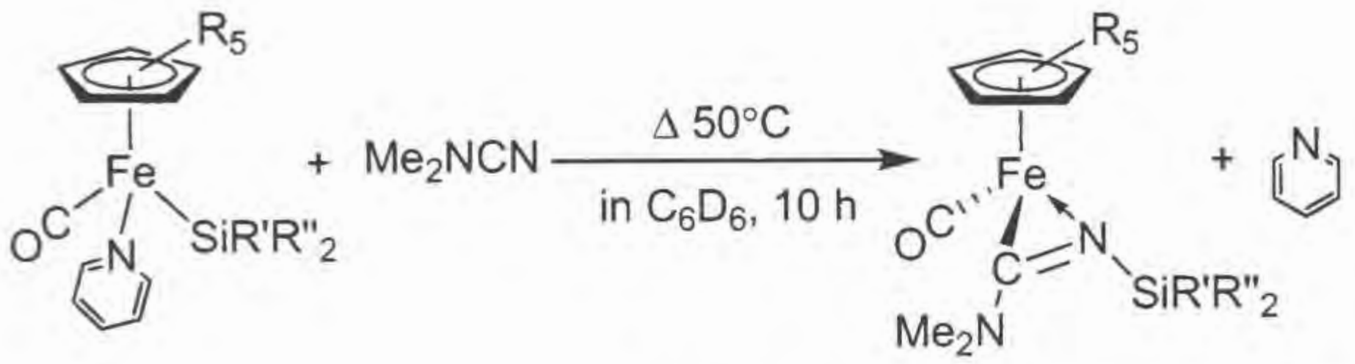

N-silylated η^2-amidino iron complex

R = H; R',R" = Et **3.3**
R = Me; R' = Ph; R" = Me **3.5**

R = H; R',R" = Et **3.4**
R = Me; R' = Ph; R" = Me **3.6**

Scheme 3-1. Synthesis of N-silylated η^2-amidino iron complexes.

Figure 3-5.ORTEP drawing of 3.6 showing the number system.

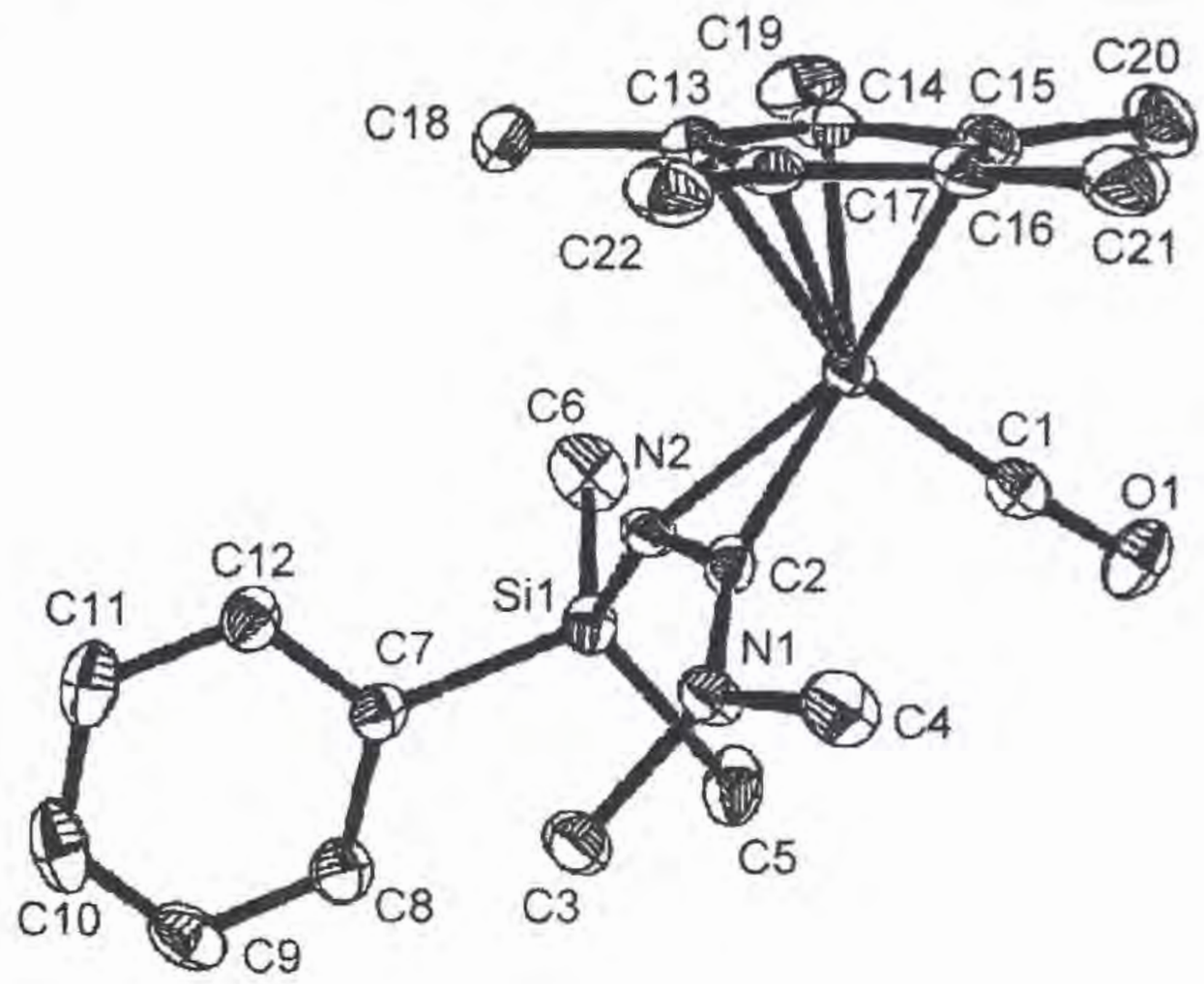

Table 3-4. Crystal data for 3.6.

Empirical formula	$C_{22}H_{32}FeN_2OS_1$	V, Å^3	2251.0(4)
Formula weight	424.44	Z	4
Crystal system	monoclinic	μ, cm^{-1}	7.358
Crystal size(mm^3)	0.18 × 0.10 × 0.06	D_{calcd}, g/cm^3	1.252
Temperature (°C)	-70.0	No. of unique reflections	16617
Space group	$P2_1/n$ (No. 14)	No. of used reflections	5062
a, Å	12.2300(12)	No. of variables	373
b, Å	9.0822(8)	R	0.0680
c, Å	20.872(2)	R_W	0.1077
β, *deg*	103.847(5)	*GOF*	1.116

Table 3-5. Selected bond distance (Å) and angles (deg) for 3.6.

Bond Distances			
Fe1-N2	2.043(2)	Fe1-C1	1.732(2)
Fe1-C2	1.859(2)	Si1-N2	1.7181(18)
Si1-C5	1.866(3)	Si1-C6	1.847(3)
Si1-C7	1.880(2)	O1-C1	1.167(3)
N1-C2	1.327(3)	N1-C3	1.455(3)
N1-C4	1.458(3)	N2-C2	1.303(2)
Bond Angles			
N2-Fe1-C1	100.34(10)	N2-Fe1-C2	38.65(8)
C1-Fe1-C2	94.65(12)	N2-Si1-C5	110.25(12)
N2-Si1-C6	107.96(13)	N2-Si1-C7	107.79(10)
C5-Si1-C6	110.58(17)	C5-Si1-C7	110.05(14)
C6-Si1-C7	110.15(15)	C2-N1-C3	123.4(2)
C2-N1-C4	119.5(2)	C3-N1-C4	117.0(2)
Fe1-N2-Si1	134.04(12)	Fe1-N2-C2	63.04(13)
Si1-N2-C2	141.24(19)	Fe1-C1-O1	175.0(2)
Fe1-C2-N1	149.40(17)	Fe1-C2-N2	78.31(15)
N1-C2-N2	132.3(2)		

Complexes **3.4** and **3.6** were subjected to a thermal reaction. Although **3.6** produced a small amount of $PhMe_2SiCN$ on heating in toluene at 110°C for 24 h, **3.4** gave Et_3SiCN in 62% yield on heating in toluene at 70°C for 24 h (Scheme-3-2). The results show clearly that an N-silylated η^2-amidino complex is an intermediate in the N-CN bond cleavage of cyanamide.

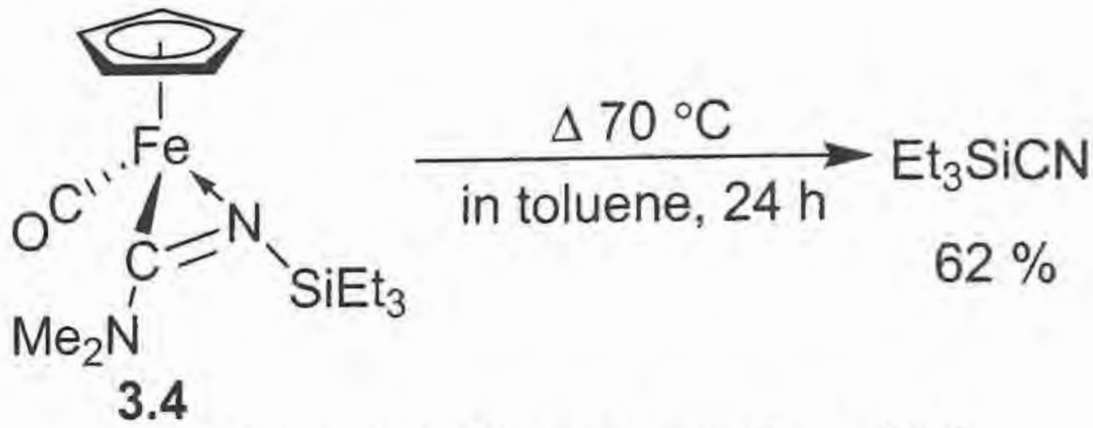

Scheme 3-2. Thermal reaction of 3.4.

3-3 Catalytic N-CN Bond Cleavage

Next, I attempted to extend the stoichiometric R_2N-CN bond cleavage to a catalytic reaction. I envision a catalytic cycle for Fe and Mo complexes shown in Scheme 3-3 based on that of R-CN bond cleagave.[3 10-3 11] A 16e silyl complex **A** reacts with Me_2NCN to give an N-silylated η^2-amidino complex **B**, followed by N-CN bond cleavage to give **C** and dissociation of silyl isocyanide to give a 16e amido complex **D**. It may react with Et_3SiH to produce **E**, then reductive elimination of Me_2NH reproduces **A** to complete the catalytic cycle. Complex **A** is expected to be obtained from $Cp[M](CO)_2Me$ ([M] = Fe, Mo(CO)) via CO dissociation and Et_3Si-H oxidative addition, and successive CH_4 reductive elimination.

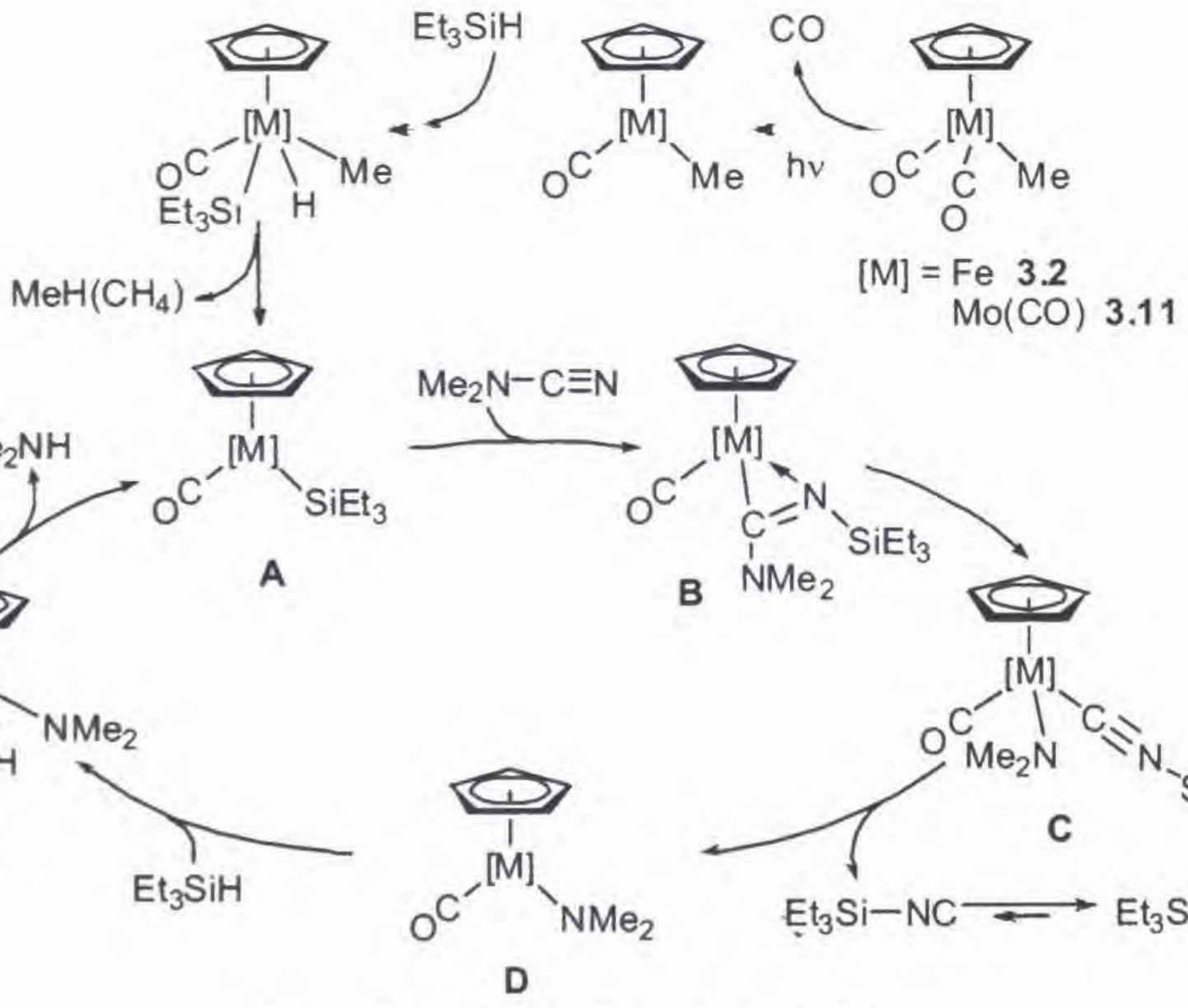

Scheme 3-3. Proposed catalytic cycle.

$(C_5H_5)Fe(CO)_2Me$, $(C_5H_5)Mo(CO)_3Me$ and their devivations were selected as catalyst precursors for the reaction of Me_2NCN with Et_3SiH. Table 3-6 shows the results of reactions of Me_2NCN with Et_3SiH in the presence of an equimolar amount of

a transition-metal methyl complex. An iron complex and a molybdenum complex with a C_5H_5 ligand (**3.2** and **3.11**) showed better reactivity than complexes with a modified Cp ligand.

Table 3-6. Yield of Et_3SiCN in the cleavage with methyl complexes.

Me complex + Et_3SiH + Me_2NCN $\xrightarrow[\text{in toluene}]{h\nu}$ Et_3SiCN

	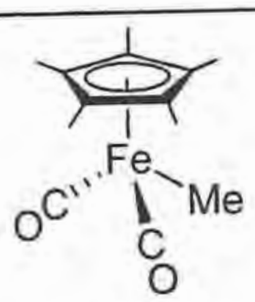 **3.8**	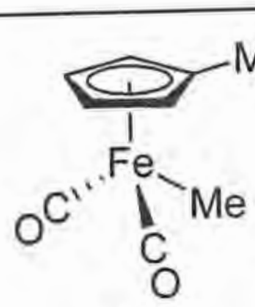 **3.9**	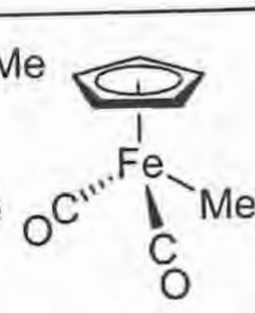 **3.2**	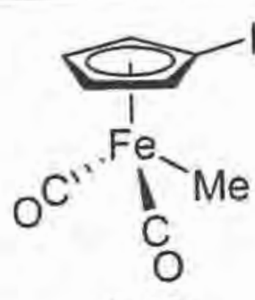 **3.10**	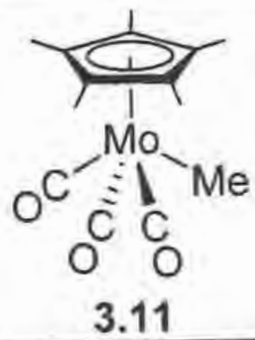 **3.11**	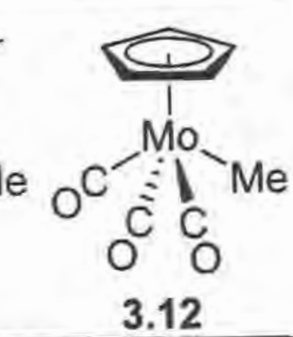 **3.12**
reaction time	Yield of Et_3SiCN					
12 h	20 %	10 %	51 %	17 %	38 %	44 %
24 h	22 %	28 %	52 %	19 %	41 %	49 %

Next, the catalytic activity of **3.2** and **3.12** was examined. The results are shown in Table 3-7. Entry 1 shows that the Fe complex does not work as a catalyst, whereas the Mo complex does under photo-irradiation conditions (entry 2). The Mo complex shows catalytic activity even under thermal conditions (entries 4-6).

Table 3-7. Catalytic cleavage under photolysis or heating.

Me_2NCN + Et_3SiH $\xrightarrow[\text{in toluene}]{\text{cat. 3.2 or 3.12}}$ Et_3SiCN

entry	cat.	[M]:[N]:[Si][a]	condition	temp/°C	time/h	TON[b]
1	**3.2**	1 : 10 : 10	hv	25	24	0.4
2	**3.12**	1 : 10 : 10	hv	25	24	1.4
3	**3.2**	1 : 1 : 1	Δ	80	12	0
4	**3.12**	1 : 1 : 1	Δ	100	12	0.52
5[c]	**3.12**	1:10:1000	Δ	100	48	7.9
6[c]	**3.12**	1:1000:5000	Δ	100	120	32.3

[a]Molar ratio of a transition metal complex, Me_2NCN, and Et_3SiH. [b]Calculated from the isolated Et_3SiCN. The values are based on the concentration of a transition metal complex. [c]In free solvent.

3-4 Unsaturated Bond Cleavage by an Iron Complex

3-4-1 C=S Bond Cleavage of Me_2NCHS

In Section 3-3-5, I described the synthesis of N-silylated η^2-amidino complex which corresponds to an intermediate in the N-CN bond cleavage sequences of cyanamide. The pyridine complex **3.3** was treated in toluene with N,N-dimethylthioformamide, Me_2NCHS containing a C=S unsaturated bond in toluene for 3 hours at 50 °C to generate quantitatively a Fischer-type carbene complex **3.13** (Scheme 3-4). Complex **3.14** was also obtained as a dark-red powder in 90 % yield in the reaction of the pyridine complex **3.7** with Me_2NCHS.

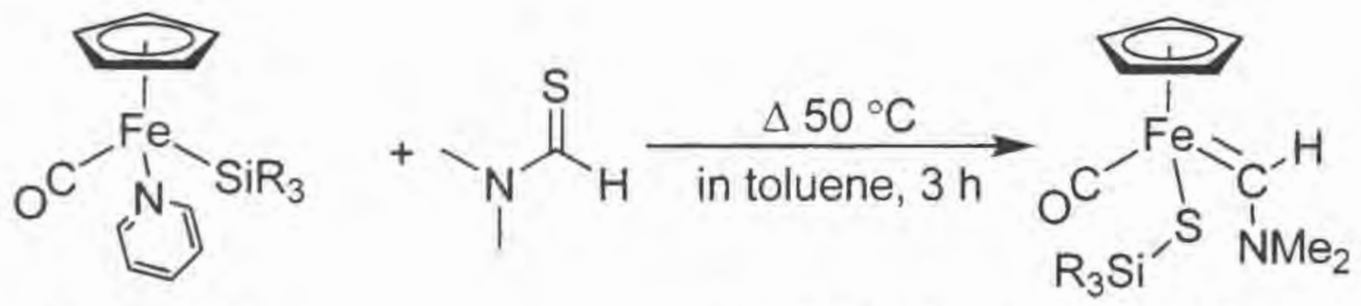

R = Et **3.3** — R = Et **3.13** 100 % (^{1}H NMR Yield)[a]

R = Ph **3.7** — R = Ph **3.14** 90 % (Isolated Yield)

[a] Complex **3.13** was not isolated as a solid.

Scheme 3-4. Reaction of iron complex bearing pyridine with Me_2NCHS.

The structure of **3.14** was confirmed by X–ray crystal structure analysis (Figure 3-7, Tables 3-8, 3-9). Complex **3.14** adopts a three-legged piano-stool geometry: the iron center possesses one Cp, one carbonyl, one thiosiloxy and one amino-substituted carbene fragment. The bond distance of Fe1-C3 (1.8891 Å) is shorter than that of a typical Fe=C bond in a Fischer-type carbene (e.g., Dillen et al. reported 1.974 Å in a iron complex) (Figure 3-6).[3 12] The bond length between the nitrogen atom N1 and the

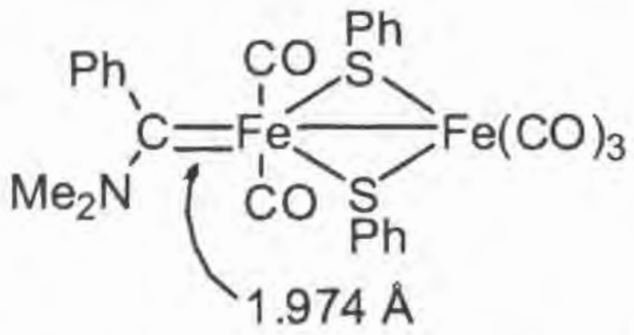

Figure 3-6. Fe=C bond length in a Fischer-type carbene complex.

Figure 3-7.ORTEP drawing of 3.14 showing the number system.

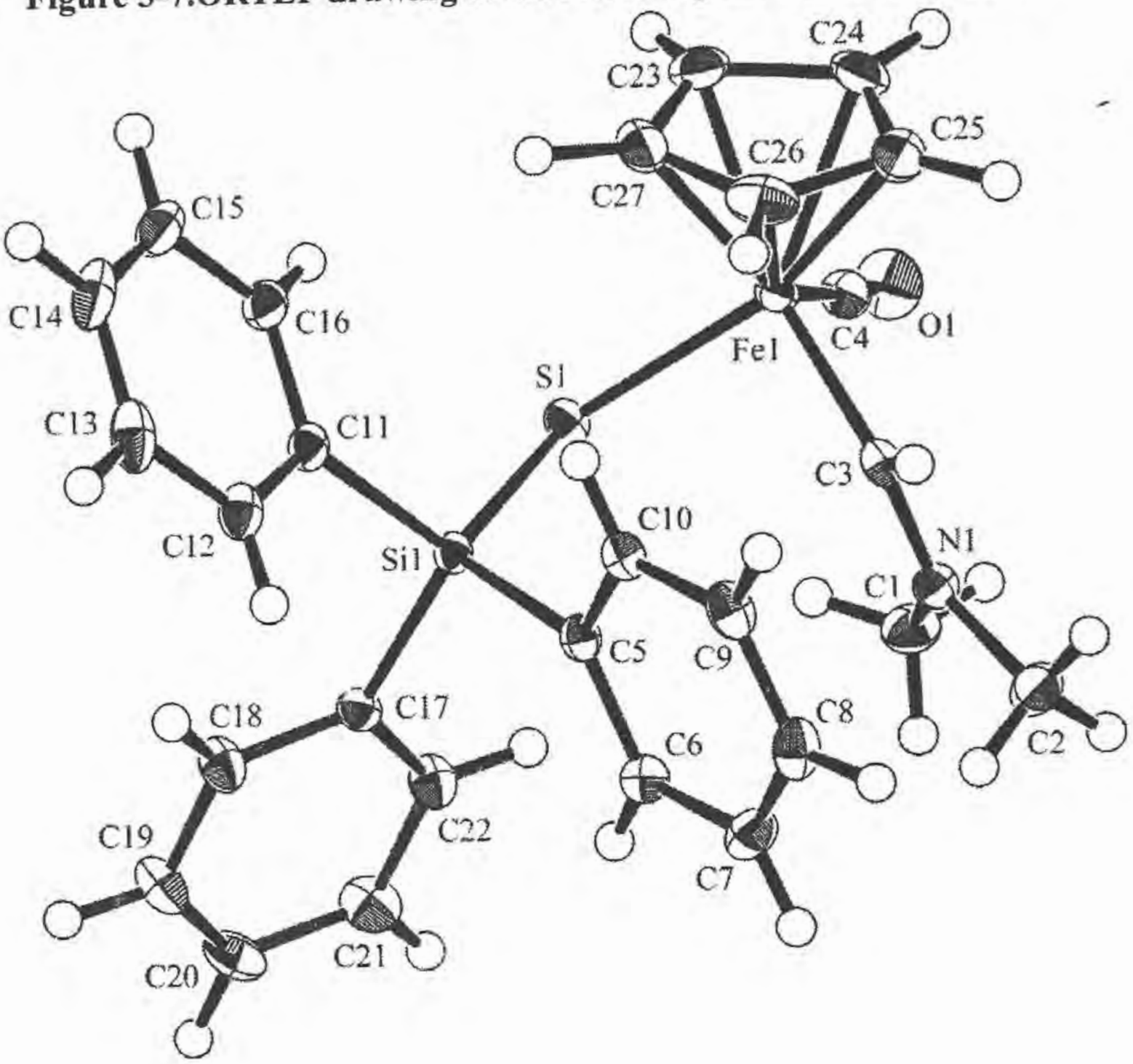

Table 3-8. Crystal data for 3.14.

Empirical formula	$C_{27}H_{27}FeNOSSi$	V, Å^3	2410.0(5)
Formula weight	497.51	Z	4
Crystal system	monoclinic	μ, cm^{-1}	7.813
Crystal size(mm^3)	0.45 × 0.30 × 0.30	D_{calcd}, g/cm^3	1.371
Temperature (°C)	-70.0	No. of unique reflections	23293
Space group	$P2_1/n$ (No. 14)	No. of used reflections	5411
a, Å	16.037(2)	No. of variables	373
b, Å	9.3525(11)	R	0.0328
c, Å	16.402(3)	R_W	0.1051
β, *deg*	101.572(3)	*GOF*	1.007

Table 3-9. Selected bond distance (Å) and angles (deg) for 3.14.

Bond Distances			
Fe1-S1	2.3371(3)	Fe1-C3	1.8891(15)
Fe1-C4	1.7434(17)	S1-Si1	2.1016(5)
N1-C1	1.466(2)	O1-C4	1.153(2)
N1-C3	1.306(2)	N1-C2	1.473(2)
Bond Angles			
S1-Fe1-C3	96.42(5)	S1-Fe1-C4	87.39(5)
C3-Fe1-C4	97.34(7)	Fe1-S1-Si1	115.482(19)
S1-Si1-C5	112.96(4)	S1-Si1-C11	113.45(5)
S1-Si1-C17	107.24(5)	C5-Si1-C11	106.44(7)
C5-Si1-C17	107.72(7)	C11-Si1-C17	108.86(7)
C1-1-C2	113.75(13)	C1-N1-C3	123.56(13)
C2-N1-C3	122.54(14)	Fe1-C3-N1	135.96(12)
Fe1-C4-O1	174.95(16)		

carbene carbon atom C3 is also shorter than that of a typical N-C single bond (1.47 Å). This tendency is very similar to that for the N-silylated η^2-amidino complex **3.6**. The sum of angles around N1 is 359.85 °. These characters are consistent with sp^2 hybridization of N1.

Proposed reaction mechanism is shown in Scheme 3-5. A pyridine in the precursor is released to give $CpFe(CO)(SiR_3)$. The C=S bond coordinates to the 16-electron species in an η^2-fashion, followed by silyl migration to the sulfer atom to give **a** and successive C-S bond cleavage in the coordination sphere, thereby yielding a Fischer-type carbene iron complex. Comparison of eq. 3-3 with Scheme 3-5 is interesting. The N-silylated η^2-amidino complex exhabits N-CN bond cleavage, whereas **a** exhibits C-S bond cleavage instead of C-N bond cleavage. The reaction corresponds to the convertion of C=S double bond into C=Fe double bond.

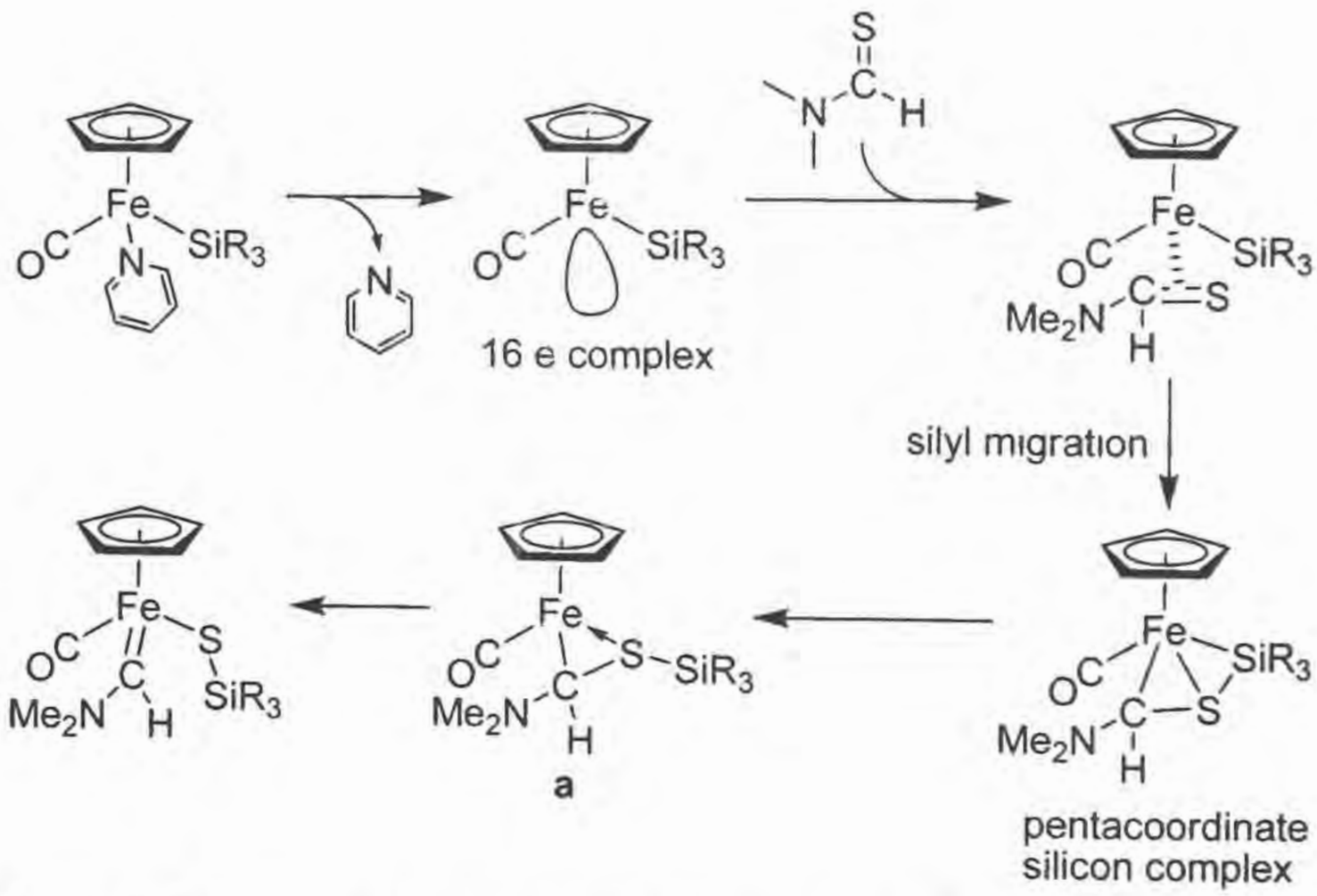

Scheme 3-5. Proposed reaction mechanism in the cleavage of C=S bond.

3-4-2 C=S Bond Cleavage of MeN=C=S

The treatment of **3.3** in toluene with methyl isothiocyanate MeNCS containing a C=N unsaturated bond in addition to a C=S bond for 2.5 hours at 50 °C generated an isocyanide complex **3.15** quantitatively (Scheme 3-6). Complex **3.16** could be also obtained as a dark-red powder in 80 % yield in the reaction of the pyridine complex **3.7** with MeNCS.

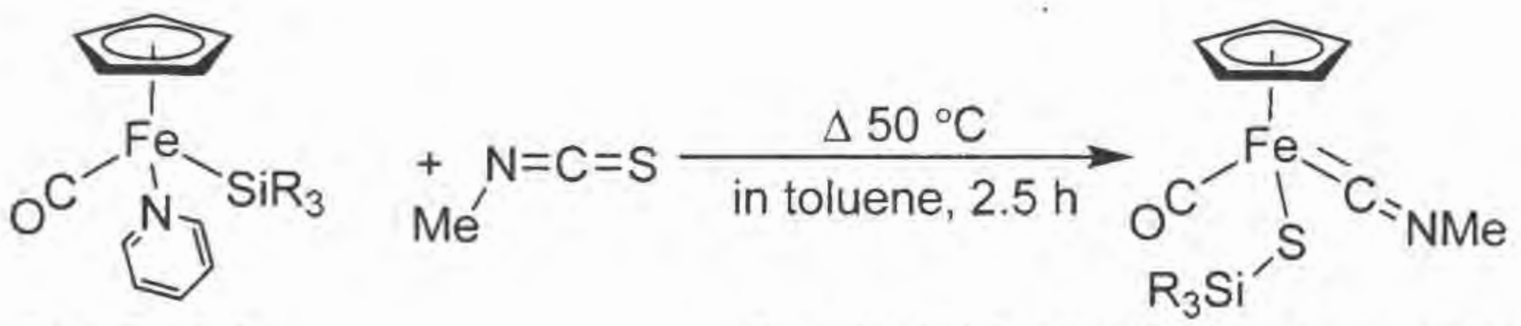

R = Et **3.3**
R = Ph **3.7**

R = Et **3.15** 100 % (^{1}H NMR Yield)[a]
R = Ph **3.16** 80 % (Isolated Yield)

[a] Complex **3.15** was not isolated as a solid.

Scheme 3-6. Reaction of the pyridine complex with MeNCS.

The structure of the isocyanide complex **3.16** was confirmed by X-ray analysis (Figure 3-9, Tables 3-10, 3-11). The iron takes a distored three-legged piano-stool structure with a Cp, a carbonyl, a thiosiloxy and an isocyanide ligand. The bond distances of Fe1-C2 (1.843 Å) and N1-C2 (1.152 Å) are similar to those of other isocyanide complexes (e.g., Adams et al. reported 1.805 Å assignable to Fe=C bond and 1.158 Å assignable to C=N bond)[3 13] (Figure 3-8). The bond angles of Fe1-C2-N1 and C1-N1-C2 are 176.5 ° and 177.6 ° respectively. The angle of Fe-S-Si in a literature complex is 129.01 °.[3 14]

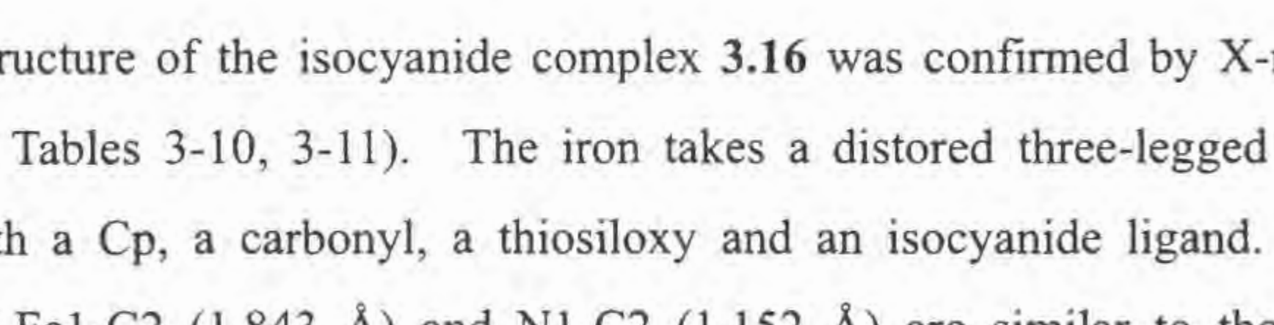

Figure 4-8. Bond distances and bond angle.

Figure 3-9.ORTEP drawing of 3.16 showing the number system.

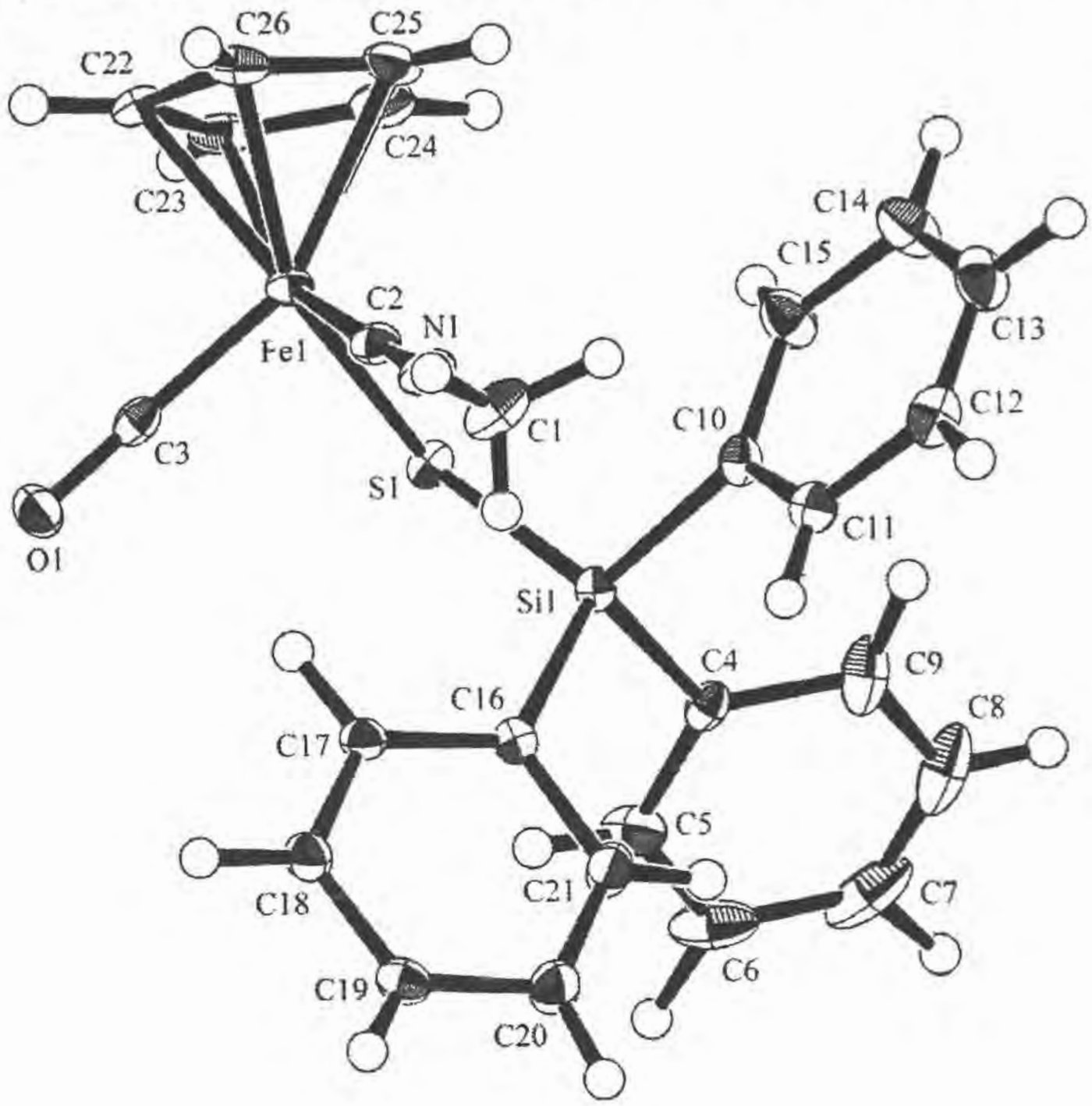

Table 3-10. Crystal data for 3.16.

Empirical formula	$C_{26}H_{23}FeNOSSi$	*γ, deg*	74.018(16)
Formula weight	481.47	*V*, Å^3	1127.7(5)
Crystal system	triclinic	Z	2
Crystal size(mm^3)	0.40 × 0.40 × 0.40	μ, cm^{-1}	8.323
Temperature (˚C)	-70.0	D_{calcd}, g/cm^3	1.418
Space group	P-1 (No. 2)	No. of unique reflections	11012
a, Å	8.639(2)	No. of used reflections	5007
b, Å	8.698(2)	No. of variables	372
c, Å	16.057(4)	*R*	0.0491
α, deg	84.537(19)	R_W	0.1753
β, deg	76.620(16)	*GOF*	1.003

Table 3-11. Selected bond distance (Å) and angles (deg) for 3.16.

Bond Distances			
Fe1-S1	2.3344(7)	Fe1-C2	1.843(2)
Fe1-C3	1.759(2)	S1-Si1	2.0936(7)
Si1-C4	1.881(2)	Si1-C10	1.884(3)
Si1-C16	1.891(2)	O1-C3	1.155(3)
N1-C1	1.432(3)	N1-C2	1.152(3)
Bond Angles			
S1-Fe1-C2	94.84(8)	S1-Fe1-C3	88.49(8)
C2-Fe1-C3	95.04(11)	Fe1-S1-Si1	114.39(3)
S1-Si1-C4	105.59(8)	S1-Si1-C10	113.37(7)
S1-Si1-C16	115.68(7)	C4-Si1-C10	107.08(12)
C4-Si1-C16	104.10(11)	C10-Si1-C16	110.12(11)
C1-N1-C2	177.6(2)	Fe1-C2-N1	176.5(2)
Fe1-C3-O1	179.4(2)		

The reaction exhibited C=S double bond cleavage in isothiosyanate, which has not been reported to date. The reaction is expected to proceed in the similar mechanism shown in Scheme 3-5, but silyl migration from Fe to S in isothiocyanate.

3-5 Conclusion

The R_2N-CN bond is known to be strong and not broken readily. Only under harsh conditions the bond is cleaved (von Braun reaction). I could exhibit the first example of R_2N-CN bond cleavage under mild conditions by using a transition metal catalyst. In the reaction, silyl migration from a transition metal to a nitrogen atom of η^2-coordinated cyanamide is a trigger of the successive N-CN bond activation. The migration may be owing to the property of silicon to take readily a hypervalent structure. N-silylated η^2-amidino iron complex corresponding to the complex right after the silyl migration could be isolated and characterized by X-ray analysis.

3-6 Experimental Section

General Remarks. All reactions were carried out under an atmosphere of dry nitrogen by using standard Schlenk tube techniques. All solvents were purified by distillation: ether and toluene were distilled from sodium/benzophenone, pentane and hexane were distilled from sodium metal, and CH_2Cl_2 was distilled from CaH_2. All solvents were stored under nitrogen atmosphere. Most chemicals were commercially available except di-*n*-hexylcyanamide, N-cyanopiperidine, N-cyanomorpholine, and N-cyanopyrrolidine. Column chromatography was done quickly with non-anhydrous pentane in the air. Photo-irradiation was performed with a 400 W medium-pressure mercury arc lamp at room temperature under nitrogen atmosphere.

IR spectra were recorded on a Perkin-Elmer Spectrum One spectrometer. A JEOL JNM-AL400 spectrometer was used to obtain ^{1}H, ^{13}C, ^{29}Si NMR spectra. All NMR data were referenced to Me_4Si.

Preparation of cyanamides. Di-*n*-hexylcyanamide, N-cyanopiperidine, N-cyanomorpholine, and N-cyanopyrrolidine were synthesized according to the literature methods.[3 15] Secondary amine (10.0 mmol) was added to 20 mL of anhydrous ether at room temperature with stirring and the mixture was cooled to 0 °C. To the solution was added dropwise over 30 min 20 mL of anhydrous ether containing cyanogen bromide (5.0 mmol, 0.530 g). Then, the reaction mixture was allowed to warm to room temperature, and was stirred for 2 h. Precipitates of ammonium chloride formed were removed by filtration, and the filtrate was concentrated under reduced pressure to a small volume, which was distilled to give the desired cyanamide. The spectroscopic data (^{1}H and ^{13}C NMR and IR data) were identical with those in the literatures.

Photoreaction of cyanamides with $Cp(CO)_2Fe(SiEt_3)$ (3.1). In a typical reaction, a solution of dimethylcyanamide (0.0787 mmol, 6.57μL) and $Cp(CO)_2Fe(SiEt_3)$ (**3.1**) (0.0787 mmol, 23.0 mg) in toluene (0.31 mL, 0.25 M solution) was photo-irradiated.

After removal of volatile materials at 3000 Pa, the residue was dissolved in a small amount of pentane and loaded on a silicagel column, and eluted with pentane to isolate triethylsilyl cyanide.

Preparation of $Cp^*(CO)(py)Fe(SiMe_2Ph)$ (py = pyridine) (3.5). Complex **3.5** was prepared in a manner similar to that for $Cp(CO)(py)Fe(SiEt_3)$.[3 10] A solution of $Cp^*(CO)_2Fe(SiMe_2Ph)$ (2.21 mmol, 844 mg) and pyridine (11.0 mmol, 0.893 mL) in toluene (10 mL) was subjected to photo-irradiation for several hours. Removal of volatile materials under reduced pressure led to the formation of a dark-red solid, which was washed three times with hexane at -78 °C. Pure crystals of **3.5** were obtained by recrystallization with hexane at -20 °C (1.66 mmol, 721 mg, 75 %). ^1H NMR (δ, in C_6D_6): 0.72 (s, 3H, $SiCH_3$), 0.63 (s, 3H, $SiCH_3$), 1.42 (s, 15H, C_5Me_5), 5.96 (s, 1H, *p*-NC_5H_5), 6.46 (s, 2H, *m*-NC_5H_5), 7.23-7.80 (m, 5H, Ph), 8.31 (s, 2H, *o*-NC_5H_5). $^{13}C\{^1H\}$ NMR (δ, in C_6D_6): 2.7 (s, $SiCH_3$), 3.6 (s, $SiCH_3$), 10.0 (s, C_5Me_5), 90.4 (s, C_5Me_5), 123.2 (s, *p*-NC_5H_5), 126.7 (s, Ph), 127.1 (s, Ph), 133.2 (s, *m*-NC_5H_5), 134.1 (s, Ph), 150.5 (s, *o*-NC_5H_5), 156.6 (s, Ph), 223.4 (s, *C*O). ^{29}Si NMR (δ, in C_6D_6): 34.5 (s). IR (cm^{-1}, in C_6D_6): ν (CO): 1874.

Preparation of $Cp(CO)(py)Fe(SiPh_3)$ (py = pyridine) (3.7). Complex **3.7** was prepared in a manner similar to that for $Cp(CO)(py)Fe(SiEt_3)$.[3 10] A solution containing $Cp(CO)_2Fe(SiPh_3)$ (0.740 mmol, 323 mg) and pyridine (13.1 mmol, 1.06 mL) in toluene (2.5 mL) was subjected to photo-irradiation for 1 day. CO was degassed from the solution in the first 1 hour, 3 hours and 12 hours. Removal of volatile materials under reduced pressure led to the formation of a dark-red solid, which was washed three times with ether at -78 °C. Pure crystals of **3.7** were obtained by recrystallization with ether at -20 °C (0.518 mmol, 252 mg, 70 %). ^1H NMR (δ, in $CDCl_3$): 4.37 (s, 5H, C_5H_5), 6.64 (s, 2H, *m*-NC_5H_5), 7.20-7.28 (m, 15H, Ph), 7.63 (s, 1H, *p*-NC_5H_5), 8.43 (s, 2H, *o*-NC_5H_5). $^{13}C\{^1H\}$ NMR (δ, in $CDCl_3$): 82.7 (s, C_5H_5), 123.1 (s, *p*-NC_5H_5), 126.9 (s, Ph), 127.9 (s, Ph), 134.4 (s, *m*-NC_5H_5), 135.4 (s, Ph), 144.3 (s,

o-NC_5H_5), 158.0 (s, Ph), 222.6 (s, *C*O). ^{29}Si NMR (δ, in $CDCl_3$): 39.5 (s). IR (cm^{-1}, in CH_2Cl_2): ν (CO): 1896. Anal. Calc. for $C_{29}H_{25}FeNOSi$: C, 71.46; H, 5.17; N, 2.87. Found: C, 71.72; H, 5.22; N, 2.87.

Syntheses of N-silylated η^2-amidino complexes $Cp(CO)Fe\{\kappa^2(C,N)\text{-}C(NMe_2)=N(SiEt_3)\}$ (3.4) and $Cp^*(CO)Fe\{\kappa^2(C,N)\text{-}C(NMe_2)=N(SiMe_2Ph)\}$ (3.6). Complex **3.3** (1.37 mmol, 592 mg) was treated with Me_2NCN (1.37 mmol, 0.114 mL) in toluene at 50 °C for 10 h. Removal of volatile materials under reduced pressure led to the formation of the corresponding N-silylated η^2-amidino complex **3.4** as a dark-red oil in 100 % ^{1}H NMR yield. In a similar way, the N-silylated η^2-amidino complex **3.6** was obtained as orange powders which were purified by washing with pentane at -78 °C (1.16 mmol, 492 mg, 85 %). **3.4**; ^{1}H NMR (δ, in C_6D_6): 0.64 (q, 6H, $SiCH_2CH_3$, $^3J_{HH}$ = 75.9 Hz), 0.95 (t, 9H, $SiCH_2CH_3$, $^3J_{HH}$ = 75.9 Hz), 2.49 (s, 3H, NCH_3), 3.20 (s, 3H, NCH_3), 4.36 (s, 5H, Cp). $^{13}C\{^1H\}$ NMR (δ, in C_6D_6): 7.1 (s, $SiCH_2CH_3$), 7.7 (s, $SiCH_2CH_3$), 39.1 (s, NCH_3), 42.8 (s, NCH_3), 79.5 (s, Cp), 194.8 (s, NCN), 219.5 (s, CO). ^{29}Si NMR (δ, in C_6D_6): 7.1 (s). IR (cm^{-1}, in toluene): ν (CO): 1902. **3.6**; ^{1}H NMR (δ, in C_6D_6): 0.32 (s, 3H, $SiCH_3$), 0.47 (s, 3H, $SiCH_3$) 1.72 (s, 15H, C_5Me_5), 2.37 (s, 3H, NCH_3), 3.05 (s, 3H, NCH_3) 7.22-7.60 (m, 5H, Ph) $^{13}C\{^1H\}$ NMR (δ, in C_6D_6): 0.9 (s, $SiCH_3$), 3.1 (s, $SiCH_3$), 10.9 (s, C_5Me_5), 39.6 (NCH_3), 42.4 (s, NCH_3), 89.9 (s, C_5Me_5), 128.6 (s, Ph), 129.2 (s, Ph), 133.8 (s, Ph), 141.1 (s, Ph), 204.0 (s, NCN), 220.6 (s, CO). ^{29}Si NMR (δ, in C_6D_6): 35.4 (s). IR (cm^{-1}, in toluene): ν (CO): 1884.

Photoreaction of dimethylcyanamide with triethylsilane in the presence of methyl complex. A solution containing methyl complex **3.2**, **3.8**, **3.9**, **3.10**, **3.11** or **3.12** (0.0150 mmol), dimethylcyanamide (0.150 mmol, 12.5 μL) and triethylsilane (0.150 mmol, 24.0 μL) in toluene (3.0 mL) was photo-irradiated. After removal of volatile materials at 3000 Pa, the residue was dissolved in a small amount of pentane and was charged on a silicagel column to isolate triethylsilyl cyanide.

Thermal reaction of dimethylcyanamide with triethylsilane in the presence of methyl complex. In stoichiometric reactions, a solution containing methyl complex **3.2** or **3.12** (0.0150 mmol), dimethylcyanamide (0.0150 mmol, 12.5 μL) and triethylsilane (0.0150 mmol, 24.0 μL) in toluene (3.0 mL) was heated at 80 °C or 100 °C under nitrogen atmosphere. Then, triethylsilylcyanide formed was isolated in the similar manner described above. The catalytic activities of **3.2** and **3.12** were also examined.

Syntheses of carben complexes $Cp(CO)Fe(=CHNMe_2)(SSiR_3)$ (R = Et, 3.13; R = Ph, 3.14). Complex **3.7** (0.343 mmol, 167 mg) was treated with Me_2NCHS (0.370 mmol, 31.1 μL) in toluene (6 mL) at 50 °C for 3 h. Removal of volatile materials under reduced pressure led to the formation of the corresponding carbene complex **3.14** as dark-red powders which were purified by washing with ether at -60 °C (0.300 mmol, 149 mg, 88 %). In a similar way, the carbene complex **3.13** was obtained as a dark-red oil in 100 % ^{1}H NMR yield. **3.13**; ^{1}H NMR (δ, in C_6D_6): 0.92 (m, 6H, $SiCH_2CH_3$), 1.24 (m, 9H, $SiCH_2CH_3$), 2.42 (s, 3H, NCH_3), 3.20 (s, 3H, NCH_3) 4.49 (s, 5H, C_5H_5), 11.99 (s, 1H, Fe=CH). $^{13}C\{^1H\}$ NMR (δ, in C_6D_6): 8.74 (s, $SiCH_2CH_3$), 9.59 (s, $SiCH_2CH_3$), 44.4 (s, NCH_3), 53.6 (s, NCH_3), 86.0 (s, C_5H_5), 223.77 (s, CO), 256.0 (s, Fe=C). ^{29}Si NMR (δ, in C_6D_6): 22.6 (s). IR (cm^{-1}, in toluene): ν (CO): 1932. **3.14**; ^{1}H NMR (δ, in C_6D_6): 2.17 (s, 3H, NCH_3), 3.05 (s, 3H, NCH_3) 4.19 (s, 5H, C_5H_5), 7.21-8.03 (m, 15H, Ph), 11.74 (s, 1H, Fe=CH). $^{13}C\{^1H\}$ NMR (δ, in C_6D_6): 44.4 (s, NCH_3), 53.4 (s, NCH_3), 85.7 (s, C_5H_5), 127.62 (s, Ph), 128.8 (s, Ph), 136.5 (s, Ph), 140.8 (s, Ph), 222.9 (s, CO), 255.8 (s, Fe=C). ^{29}Si NMR (δ, in C_6D_6): 1.8 (s). IR (cm^{-1}, in toluene): ν (CO): 1937. Anal. Calc. for $C_{27}H_{27}FeNOSSi$: C, 65.18; H, 5.47; N, 2.82. Found: C, 65.04; H, 5.41; N, 2.75.

Synthesis of carben complexes $Cp(CO)Fe(C=NMe)(SSiR_3)$ (R = Et, 3.15; R = Ph, 3.16). Complex **3.7** (0.401 mmol, 196 mg) was treated with MeNCS (0.428 mmol, 29.3 μL) in toluene (5 mL) at 50 °C for 2.5 h. Removal of volatile materials under

reduced pressure led to the formation of the corresponding carbene complex **3.16** as dark-red powders which were purified by washing with ether at -60 °C (0.311 mmol, 150 mg, 78 %). In a similar way, the carbene complex **3.15** was obtained as a dark-red oil in 100 % ^{1}H NMR yield. **3.15**; ^{1}H NMR (δ, in C_6D_6): 0.98 (m, 6H, $SiCH_2CH_3$), 1.29 (m, 9H, $SiCH_2CH_3$), 2.16 (s, 3H, NCH_3), 4.32 (s, 5H, C_5H_5). $^{13}C\{^1H\}$ NMR (δ, in C_6D_6): 8.75 (s, $SiCH_2CH_3$), 9.61 (s, $SiCH_2CH_3$), 29.78 (s, NCH_3), 83.3 (s, C_5H_5), 162.6 (s, FeCN), 219.9 (s, CO). ^{29}Si NMR (δ, in C_6D_6): 16.1 (s). IR (cm^{-1}, in toluene): ν (CO): 1962, ν (C=N): 2172. **3.16**; ^{1}H NMR (δ, in C_6D_6): 1.86 (s, 3H, NCH_3), 4.03 (s, 5H, C_5H_5), 7.19-8.07 (m, 15H, Ph). $^{13}C\{^1H\}$ NMR (δ, in C_6D_6): 29.74 (s, NCH_3), 83.4 (s, C_5H_5), 127.7 (s, Ph), 128.8 (s, Ph), 136.3 (s, Ph), 140.4 (s, Ph), 161.3 (s, FeCN), 218.4 (s, CO). ^{29}Si NMR (δ, in C_6D_6): 1.9 (s). IR (cm^{-1}, in toluene): ν (CO): 1973, ν (C=N): 2180. Anal. Calc. for $C_{26}H_{23}FeNSSi$: C, 64.86; H, 4.82; N, 2.91. Found: C, 64.82; H, 4.77; N, 2.83.

X-ray Crystal structure determination of 3.6. Dark-red crystals of **3.6** suitable for an X-ray diffraction study were obtained through crystallization from pentane. The single crystal was mounted in a glass capillary. Data for **3.6** were collected at -70 °C on Rigaku/MSC Mercury CCD area-detector diffractometer equipped with monochromated MoKα radiation (λ =0.71070 Å). Calculations for **3.6** were performed with the teXane crystallographic software package of Molecular Structure Corporation. Crystal Data: $C_{22}H_{32}FeN_2OSi$, M = 424.44, orange plate, 0.18 × 0.10 × 0.06 mm, monoclinic, space group $P2_1/c$ (No. 14), a = 12.2300(12) Å, b = 9.0822(8) Å, c = 20.872(2) Å, β = 103.847(5)°, V = 2251.0(4) Å^3, Z = 4, μ(MoKα) = 7.358 cm^{-1}, D_{calc} = 1.252 g/cm^3, 16617 reflections collected, 5062 ($I > 3\sigma I$) unique reflections were used in all calculations, number of variables = 373, R = 0.0680, R_w = 0.1077, and goodness of fit = 1.116.

X-ray Crystal structure determination of 3.14 Dark-red crystals of **3.14** suitable for an X-ray diffraction study were obtained through crystallization from CH_2Cl_2/hexane. The single crystal was mounted in a glass capillary. Data for **3.14** were collected at 20

°C on Rigaku/MSC Mercury CCD area-detector diffractometer equipped with monochromated MoKα radiation (λ =0.71070 Å). Calculations for **3.14** were performed with the teXane crystallographic software package of Molecular Structure Corporation. Crystal Data: $C_{27}H_{27}FeNOSSi$, M = 497.51, red block, 0.45 × 0.30 × 0.30 mm, monoclinic, space group $P2_1/c$ (No. 14), a = 16.037(2) Å, b = 9.3525(11) Å, c = 16.402(3) Å, β = 101.572(3)°, V = 2410.0(5) Å^3, Z = 4, μ(MoKα) = 7.813 cm^{-1}, D_{calc} = 1.371 g/cm^3, 16617 reflections collected, 5411 ($I > 3\sigma I$) unique reflections were used in all calculations, number of variables = 373, R = 0.0328, R_w = 0.1051, and goodness of fit = 1.007.

X-ray Crystal structure determination of 3.16. Dark-red crystals of **3.16** suitable for an X-ray diffraction study were obtained through crystallization from CH_2Cl_2/hexane. The single crystal was mounted in a glass capillary. Data for **3.16** were collected at 20 °C on Rigaku/MSC Mercury CCD area-detector diffractometer equipped with monochromated MoKα radiation (λ =0.71070 Å). Calculations for **3.16** were performed with the teXane crystallographic software package of Molecular Structure Corporation. Crystal Data: $C_{26}H_{23}FeNOSSi$, M = 481.47, red block, 0.40 × 0.40 × 0.34 mm, triclinic, space group P-1 (No. 2), a = 8.639(2) Å, b = 8.698(2) Å, c = 16.057(4) Å, α = 84.537(10) °, β = 101.572(3)°, γ = 74.018(16) °, V = 1127.7(5) Å^3, Z = 2, μ(MoKα) = 8.323 cm^{-1}, D_{calc} = 1.418 g/cm^3, 11012 reflections collected, 5007 ($I > 3\sigma I$) unique reflections were used in all calculations, number of variables = 372, R = 0.0491, R_w = 0.1753, and goodness of fit = 1.003.

3-7 References

3.1 See for example: (a) Ritleng, V.; Sirlin, C.; Pfeffer, M. *Chem. Rev.* **2002**, *102*, 1731. (b) Dyker, G. *Angew. Chem., Int. Ed.* **1999**, *38*, 1698. (c) Naota, T.; Takaya, H.; Murabashi, S. I. *Chem. Rev.* **1998**, *98*, 2599. (d) Zhang, Y.; Li, C.-J.; *Angew. Chem., Int. Ed.* **2006**, *45*, 1949. (e) Ma, K.; Piers, W. E.; Parvez, M. *J. Am. Chem. Soc.* **2006**, *128*, 3303. (f) Kakiuchi, F.; Kan, S.; Igi, K.; Chatani, N.; Murai, S. *J. Am. Chem. Soc.* **2003**, *125*, 1698. (g) Goosen, L. J. *Angew. Chem., Int. Ed.* **2002**, 41, 3775. (h) Arndtsen, B. A.; Bergman, R. G.; Mobley, T. A.; Peterson, T. H. *Acc. Chem. Res.* **1995**, *28*, 154. (i) Crabtree, R. H. *J. Organomet. Chem.* **2004**, *689*, 4083.

3.2 See for example: (a) Jun, C.-H. *Chem. Soc. Rev.* **2004**, *33*, 610. (b) Rybtchinski, B; Milstein, D. *Angew. Chem., Int. Ed.* **1999**, *38*, 870. (c) Storsberg, J.; Yao, M.-L.; Öcal, N.; De Meijere, A.; Adam, A. E. W.; Kaufmann, D. E. *Chem. Commun.* **2005**, 5665. (d) Nakazawa, H.; Kawasaki, T.; Miyoshi, K.; Suresh, C. H.; Koga, N. *Organometallics* **2004**, *23*, 117. (e) Chianese, A. R.; Zeglis, B. M.; Crabtree, R. H. *Chem. Commun.* **2004**, 2176. (f) Terao, Y.; Wakui, H.; Satoh, T.; Miura, M.; Nomura, M. *J. Am. Chem. Soc.* **2001**, *123*, 10407.

3.3 (a) Lei, Y.; Wrobleski, A. D.; Golden, J. E.; Powell, D. R.; Aubé, J. *J. Am. Chem. Soc.* **2005**, *127*, 4552. (b) Fran, L.; Yang, L.; Guo, C.; Foxman, B. M.; Ozerov, O. V. *Organometallics* **2004**, *23*, 4778. (c) Yao, M.-L.; Adiwidjaja, G.; Kanfmann, D. E. *Angew. Chem., Int. Ed.* **2002**, *41*, 3375. (d) Niklas, N.; Heinemann, F. W.; Hampel, F.; Alsfasser, R. *Angew. Chem., Int. Ed.* **2002**, *41*, 3386.

3.4 See for example: (a) Maercker, A. *Angew. Chem., Int. Ed.* **1987**, *26,* 972. (b) Kabalka, G. W; Yao, M.-L.; Borella, S.; Goins, L. K. *Organometallics* **2007**, *26*, 4112. (c) Szu, P.-h.; He, X.; Zhao, L.; Liu, H.-w. *Angew. Chem., Int. Ed.* **2005**, *44*, 6742. (d) Casado, F.; Pisano, L.; Farriol, M.; Gallardo, I.; Marquet, J.; Melloni, G. *J. Org. Chem.* **2000**, *65*, 322.

3.5 Bineau, A. *Ann. Chim. Phys.* **1838**, *s2 v67*, 225.

3.6 Frank, A.; Caro, N. *Ger. Patent* **1895**, 88363.

3.7 Cunningham, I. D.; Light, M. E.; Hursthouse, M. B. *Acat Cryst. Sect. C, Cryst. Struct. Commun*. **1999**, *55*, 1833.

3.8 E. B. Vliet, *Organic Syntheses, Coll. Vol.* **1941**, *1*, 201.

3.9 Syntheses of boran adduct of cyanamide and confirmation of the adduct at the amino nitrogen have been reported: Henneike, H. F.; Drago, R. S. *Inorg. Chem.* **1968**, *7*, 1908-1915.

3.10 Nakazawa, H.; Itazaki, M.; Kamata, K.; Ueda, K. *Chem. Asian. J.* **2007**, *2*, 882-888.

3.11 Nakazawa, H.; Kamata, K.; Itazaki, M. *Chem. Commun*. **2005**, 4004.

3.12 Dillen, J. L. M.; van Dyk, M. M.; Lotz, S. *J. Chem. Soc., Dalton Trans.* **1989**, 2199.

3.13 Adams, R. D.; Cotton, F. A.; Troup, J. M. *Inorg. Chem*. **1974**, *13*, 257.

3.14 Kuckman, T. I.; Dornhaus, F.; Bolte, M.; Lerner, H.-W.; Holthausen, M. C.; Wagner, M. *Eur. J. Inorg. Chem*. **2007**, 1989.

3.15 Overman, L. E.; Tsuboi, S.; Roos, J. P.; Taylor, C. F. *J. Am. Chem. Soc*. **1980**, *102*, 747.

Acknowledgement

The thesis for a doctorate is completed by summarizing the research results which were carried out from 2004 to 2009 in Coordination Chemistry Laboratory, Department of Chemistry, Graduate School of Science, Osaka City University. At first, I would like to express my deep gratitude to Professor Hiroshi Nakazawa. Because of his direction and help, I completed this dissertation and lived a happy life in the laboratory. Secound I would like to thank Dr. Masumi Itazaki whose comments contributed to my work.

I owe a very important debt to Professor Akio Ichimura and Professor Hiroshi Tsukube at Osaka City University for their kind advice and reviewing this thesis.

I am deeply indebted to all members of Professor Nakazawa's laboratory, particularly Mr. Koji Kamata, Mr. Masaharu Ohba, Mr. Ryohei Nakamura, Ms. Seijo Ou, Ms. Rie Ujihara, Ms. Kumiko Nito, Mr. Tsukuru Oya , Ms. Michiho Kasa and Mr. Yuta Nakai for the enjoyable discussions and experimental assistance. My special thanks are due to Mr. Akina Nigi, Mr. Jun Okamoto, Mr. Ken-Ichiro Okuma, Mr. Kensuke Ueda, Mr. Kunihisa Noichi, Mr. Masahiro Kamitani, Ms. Makiko Minakata, Mr. Wataru Nakamura, Ms. Yuka Sigesato, Mr. Yasuhiro Hashimoto, Dr. Naumov Roman, and all other colleagues in Coordination Chemistry Laboratory for their enormous collaborations, kind help, and friendship.

I also gratefully appreciate the financial support of Nakato Scholarship Foundation and Japan Securities Scholarship Foundation that made it possible to complete my thesis.

Finally, I would like to express my heartfelt acknowledgment to my parents, Nobuaki and Junko Fukumoto, and my sister, Rie Fukumoto, for their patient assistance, kind help and continuous encouragement. I also wish to thank my friends, especially Ms. Akiyo Miyajima, for their heartfelt encouragement.

Kozo Fukumoto

Kozo Fukumoto
Department of Chemistry,
Graduate School of Science,
Osaka City University
March 2009

References for the Thesis

(1) Silane-Catalyzed Reaction: *fac-mer* Isomerization of [$Mo(CO)_3$(phosphite)$_3$]
Kozo Fukumoto, Hiroshi Nakazawa
Organometallics **2007**, *26*, 6505-6507.

(2) Geometrical isomerization of *fac/mer*-$Mo(CO)_3$(phosphite)$_3$ and *cis/trans*-$Mo(CO)_4$(phosphite)$_2$ catalyzed by $Me_3SiOSO_2CF_3$
Kozo Fukumoto, Hiroshi Nakazawa
Journal of Organometallic Chemistry **2008**, *693*, 1968-1974.

(3) N-CN Bond Cleavage of Cyanamides by a Transition-metal Complex
Kozo Fukumoto, Tsukuru Oya, Masumi Itazaki, Hiroshi Nakazawa
Journal of American Chemical Society **2009**, *131*, 38-39.

ORGANOMETALLICS

Volume 26, Number 26, December 17, 2007

Communications

Silane-Catalyzed Reaction: *fac*−*mer* Isomerization of $[Mo(CO)_3(phosphite)_3]$

Kozo Fukumoto and Hiroshi Nakazawa*

Department of Chemistry, Graduate School of Science, Osaka City University, Sumiyoshi-ku, Osaka 558-8585, Japan

Received September 3, 2007

Summary: Me_3SiX (X = Cl, Br, I) and related silane compounds catalyze fac−mer isomerization of $[Mo(CO)_3\{P(OR)_3\}_3]$ at room temperature. A hypervalent silicon structure has been shown to play a crucial role in the catalytic reaction.

Because of their unique, efficient, and selective reactivity, in addition to their ready availability and low toxicity, organosilicon compounds have been widely used, especially for organic syntheses.[1,2] Extensive studies over the past three decades have examined silicon compounds and have created many useful reactions, most of which involve conversion of a silicon compound into another silicon compound. In addition, several silicon-based catalysts have been developed. R_3SiOTf, $R_3SiB(OTf)_4$, $R_3SiB(OTf)_3Cl$, $R_3SiN(SO_2F)_2$, and $R_3SiN(Tf)_2$.[2] These catalysts can be described as containing R_3Si^+ and are considered Lewis acids. In contrast, no report describes silane (a neutral four-coordinate silicon compound) serving as a catalyst instead of a reagent. It has been speculated that a silane is not a catalyst any more than an alkane is. This is the first report of a silane-catalyzed reaction. Me_3SiX (X = Cl, Br, I) and related silane compounds catalyze *fac*−*mer* isomerization of $[Mo(CO)_3\{P(OR)_3\}_3]$ at room temperature.

Regarding $M(CO)_3L_3$ (M = Cr, Mo, W; L = phosphine, phosphite), principally two geometrical isomers exist: facial (*fac*) and meridional (*mer*) forms. The *fac* isomer is considered more stable electronically, as this isomer achieves stronger M to CO back-donation, but the *mer* isomer is favored from a steric point of view. The $M(CO)_3L_3$ complexes prepared to date from their transition-metal precursors and L have exclusively *fac* geometry. The *mer* isomers were obtained using isomerization of the *fac* isomers. Bond et al. reported *fac*−*mer* isomerization via a one-electron oxidation to produce the 17e cation species for $M(CO)_3(\eta^3\text{-}Ph_2PCH_2CH_2P(Ph)CH_2CH_2PPh_2)$.[3] We reported the related isomerization for *fac*-$[M(CO)_3(bpy)\{P(NMeCH_2)_2(OMe)\}]$ (bpy = 2,2′-bipyridine, $P(NMeCH_2)_2(OMe)$ = $P(NMeCH_2CH_2NMe)(OMe)$). The reaction of the *fac* isomer with $BF_3\cdot OEt_2$ gives the cationic phosphenium complex *fac*-$[Mo(bpy)(CO)_3\{P(NMeCH_2)_2\}]^+$, which then isomerizes to the *mer* form. It does so because the phosphenium ligand shows strong π acidity, leading to an electron-deficient metal center (not complete one-electron oxidation, but partial oxidation).[4] Thermal *fac*−*mer* isomerization has been reported by Rousche et al. for *fac*-$[Mo(CO)_3(\eta^2\text{-dppe})\{P(O^iPr)_3\}]$[5] and by Howell et al. for *fac*-$[M(CO)_3\{P(OR)_3\}_3]$.[6]

We examined the reaction of *fac*-$[Mo(CO)_3\{P(OMe)_3\}_3]$ (***fac*-1**) with 1 equiv of Me_3SiCl in CH_2Cl_2 at room temperature. The reaction was monitored by measuring the $^{31}P\{^1H\}$ NMR

* To whom correspondence should be addressed. E-mail: nakazawa@sci.osaka-cu.ac.jp.

(1) Larson, G. L. In *The Chemistry of Organic Silicon Compounds*; Patai, S., Rappoport, Z., Eds.; Wiley: London, 1989; p 763.

(2) Miura, K.; Hosomi, A. In *Main Group Metals in Organic Synthesis*; Yamamoto, H., Oshima, K., Eds.; Wiley-VCH: Weinheim, Germany, 2004; p 409.

(3) Bond, A. M.; Colton, R.; Feldberg, S. W.; Mahon, P. J.; Whyte, T. *Organometallics* **1991**, *10*, 3320.

(4) Nakazawa, H.; Yamaguchi, Y.; Miyoshi, K. *J. Organomet. Chem.* **1994**, *465*, 193.

(5) Rousche, J.-C.; Dobson, G. R. *Inorg. Chim. Acta* **1978**, *28*, L139.

(6) Howell, J. A. S.; Yates, P. C.; Ashford, N. F.; Dixon, D. T.; Warren, R. *J. Chem. Soc., Dalton Trans.* **1996**, *20*, 3959.

10.1021/om7008827 CCC: $37.00

Publication on Web 11/10/2007

Table 1. Isomerization by Me_3SiCl in CH_2Cl_2 at Room Temperature

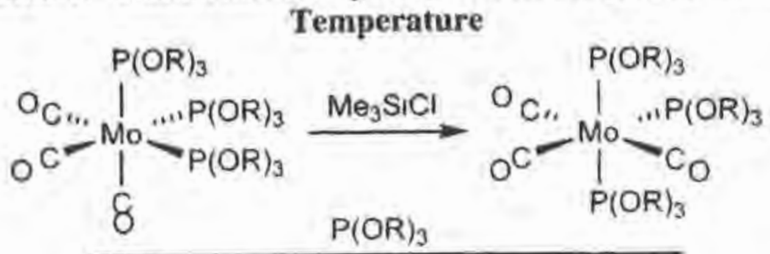

	$P(OR)_3$	
***fac*-1**	$P(OMe)_3$	***mer*-1**
***fac*-2**	$P(OEt)_3$	***mer*-2**
***fac*-3**	$P(OPh)_3$	***mer*-3**
***fac*-4**	$P(NMeCH_2)_2(OMe)$	***mer*-4**

entry	complex	amt of Me_3SiCl (equiv)	time (h)	*fac mer*
1	***fac*-1**	1 0	3	1 3 4
2	***fac*-1**	0 5	5	1 3 4
3	***fac*-1**	0 1	8	1 3 4
4	***fac*-2**	1 0	2	1 2 2
5	***fac*-3**	1 0	72	1 1 3[a]
6	***fac*-4**	1 0	12	1 0 5

[a] The isomerization is very slow, and the equilibrium is not attained after 72 h The final ratio obtained by using Me_3SiOTf is 1 30 (unpublished results)

spectrum. A triplet at 167.1 ppm (J_{PP} = 44.3 Hz) and a doublet at 175.3 ppm (J_{PP} = 41.7 Hz) attributable to ***mer*-1** appeared at the expense of an intensity of a singlet at 164.8 ppm because of ***fac*-1**. After 3 h, equilibrium between ***fac*-1** and ***mer*-1** was established with the ratio of 1.3 4 [7] Next, the reactions with 0.5 and 0.1 equiv of Me_3SiCl were examined Table 1 (entries 1–3) shows that the final equilibrium position was found not to depend on the amount of Me_3SiCl used, although it takes a longer time to reach the equilibrium when the amount of Me_3SiCl is reduced. The equilibrium ratio resembles that obtained in thermolysis by Howell et al. (1 3). These results show that Me_3SiCl acts as a catalyst for *fac*−*mer* isomerization.

In our experiments dry CH_2Cl_2 distilled from CaH_2 was used. However, there is a possibility that adventitious HCl from Me_3SiCl hydrolysis could be responsible for the observed isomerization. Thus, the ^{29}Si NMR of Me_3SiCl in CH_2Cl_2 was measured. No signal other than a singlet attributable to Me_3SiCl was observed, indicating no silicon compound derived from Me_3SiCl hydrolysis exists (less than 5%, if any). We observed that the isomerization of ***fac*-1** is completed within 8 h in the presence of 10 mol % of Me_3SiCl. If 10% of the Me_3SiCl produces adventitious HCl, then the amount of HCl would be 1 mol % based on ***fac*-1** under the above conditions. The CH_2Cl_2 solution of ***fac*-1** containing 1 mol % of HCl was prepared and monitored by the ^{31}P NMR measurement, and no isomerization was observed after 10 h. These results clearly indicate that the *fac*−*mer* isomerization is catalyzed by Me_3SiCl but not by HCl.

The corresponding isomerization catalyzed by Me_3SiCl was observed for the triethyl phosphite complex ***fac*-2**, the triphenyl phosphite complex ***fac*-3**, and the diamino-substituted phosphite complex ***fac*-4**. In all cases, the ^{31}P NMR spectra of the reaction mixture suggested the formation of the corresponding *mer* isomers.[8] The isomerization of ***fac*-3** to ***mer*-3** was much slower (more than 72 h) than that of ***fac*-1** to ***mer*-1** (3 h), which might be attributed to a steric cause. The reaction of ***fac*-4** is noteworthy. We found that the reaction of ***fac*-4** with Me_3SiOTf abstracts one OMe as an anion from the phosphorus to give a cationic phosphenium complex, *fac*-$[Mo(CO)_3\{P(NMeCH_2)_2(OMe)\}_2\{P(NMeCH_2)_2\}]^+$.[9] In contrast, on the basis of ^{31}P NMR monitoring, the reaction of ***fac*-4** with Me_3SiCl generated no cationic phosphenium complex, which suggests that the pathway of the isomerization promoted by Me_3SiCl differs from that involving a cationic phosphenium complex produced by Me_3SiOTf.

Scheme 1. Proposed *fac*−*mer* Isomerization Mechanism Catalyzed by Me_3SiCl

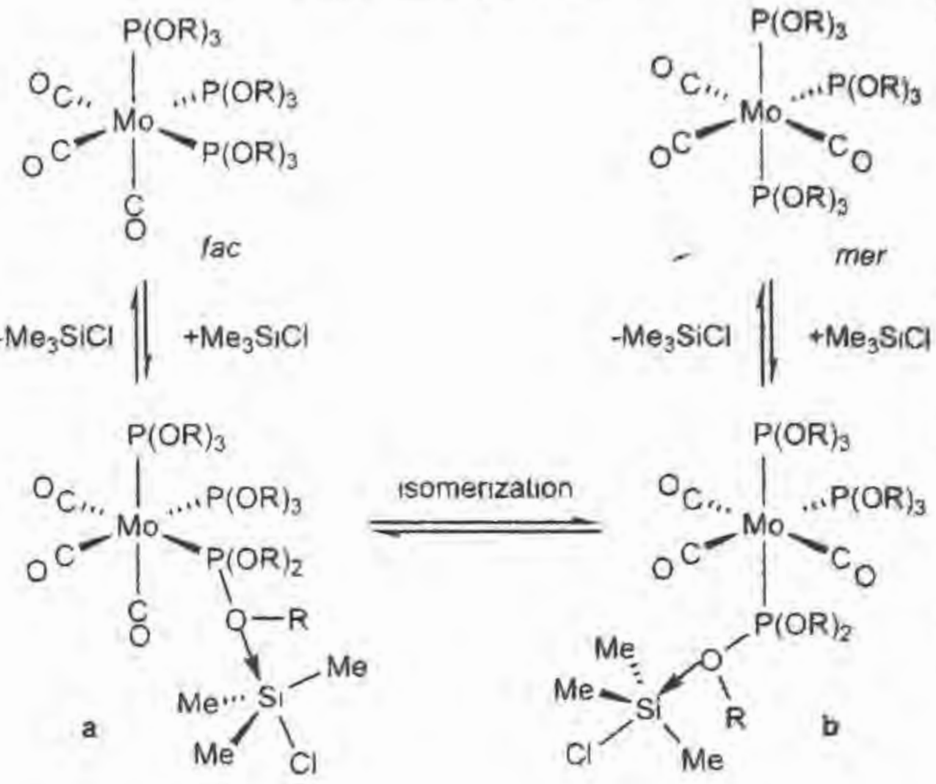

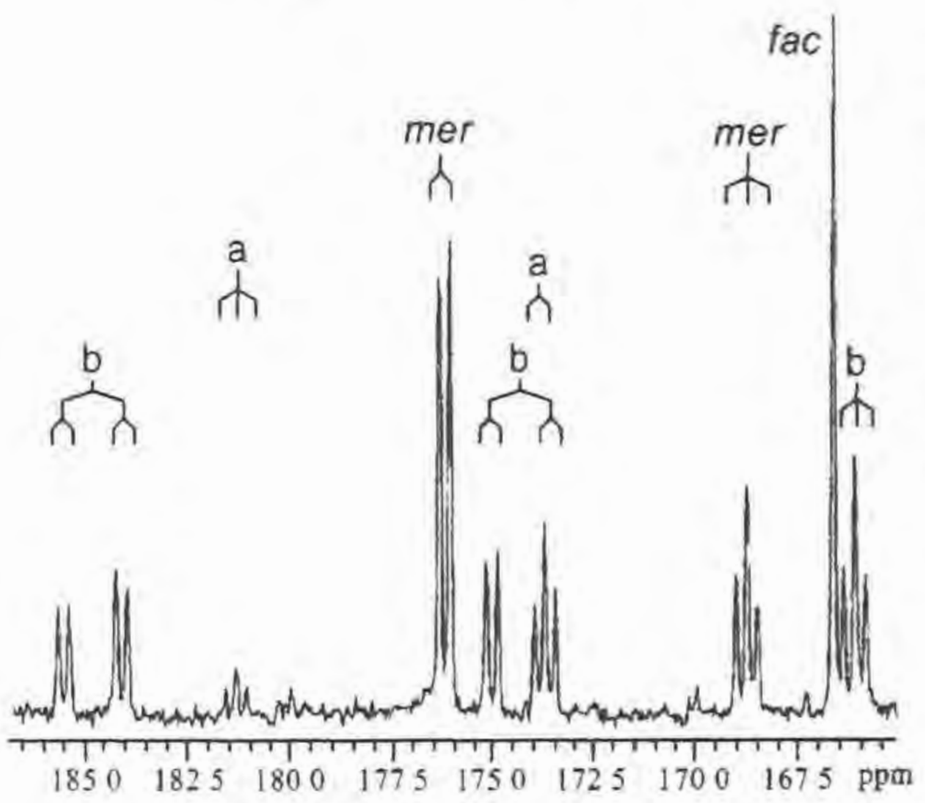

Figure 1. ^{31}P NMR spectrum of a Me_3SiCl solution at room temperature in which ***fac*-1** is dissolved

Scheme 1 presents a plausible mechanism for the *fac*−*mer* isomerization promoted by Me_3SiCl. The silicon atom in Me_3SiCl interacts with one oxygen in $P(OR)_3$ ligands to form a Si hypervalent structure (**a**). The interaction weakens the coordination of $P(OR)_3 \cdot Me_3SiCl$ toward the central metal and makes the ligand bulky, thereby decreasing the isomerization energy barrier to give its *mer* isomer (**b**). The following dissociation of the Me_3SiCl gives the *mer* isomer, reproducing free Me_3SiCl.

The ^{31}P and ^{29}Si NMR measurements of a CH_2Cl_2 solution containing ***fac*-1** and Me_3SiCl showed no signals assignable to either **a** or **b** in Scheme 1. To obtain some evidence of **a** and **b**, we dissolved ***fac*-1** in Me_3SiCl and measured the ^{31}P and ^{29}Si NMR spectra of the solution. The ^{31}P NMR is shown in Figure 1. In addition to a singlet at 166.7 ppm attributable to ***fac*-1** and a doublet at 176.2 ppm and a triplet at 168.8 with J_{PP} =

(7) In the absence of Me_3SiCl no *fac*−*mer* isomerization occurred at room temperature in CH_2Cl_2

(8) $^{31}P\{^1H\}$ NMR (161 7 MHz, CH_2Cl_2, 25 °C, reference 85% H_3PO_4, δ, ppm) ***fac*-1**, 164 8 (s), ***mer*-1**, 167 1 (t, J_{PP} = 44 3 Hz, *cis*-PP), 175 3 (d, J_{PP} = 41 7 Hz, *trans*-PP), ***fac*-2**, 145 4 (s), ***mer*-2**, 148 8 (t, J_{PP} = 52.1 Hz, *cis*-PP). 155 7 (d, J_{PP} = 52 1 Hz, *trans*-PP), ***fac*-3**, 146 1 (s), ***mer*-3**, 143 9 (d, J_{PP} = 46 9 Hz, *cis*-PP), 180 9 (t, J_{PP} = 46 9 Hz, *trans*-PP)

(9) Nakazawa, H , Miyoshi, Y , Katayama, T , Mizuta, T.; Miyoshi, K., Tsuchida, N., Ono; A., Takano, K *Organometallics* **2006**, *25*, 5913.

41.7 Hz attributable to ***mer*-1**, five signals were observed clearly. Among them, a triplet at 181.3 ppm and a doublet at 173 9 ppm with J_{PP} = 41.7 Hz can be assigned to **a**. The triplet is assignable to P(OMe)$_3$·Me$_3$SiCl because of the molecular symmetry. The remaining three signals at 184 8 ppm (dd, J_{PP} = 41.7 and 229.3 Hz), 174.3 ppm (dd, J_{PP} = 44 3 and 229.3 Hz), and 166.2 ppm (t, J_{PP} = 44 3 Hz) can be reasonably assigned respectively to P(OMe)$_3$·Me$_3$SiCl and trans and cis P(OMe)$_3$ in P(OMe)$_3$·Me$_3$SiCl in **b** The ^{29}Si NMR showed two singlets at 6.62 and 6.53 ppm in addition to a strong singlet at 29.8 ppm attributable to the solvent Me$_3$SiCl. Coordination of nitrogen or oxygen to silicon to form a pentacoordinate bond has been shown to produce a strong shielding effect of the silicon chemical shift.[10] Kummer et al reported the ^{29}Si NMR chemical shift at 11 1 ppm in CD_2Cl_2 for an Si hypervalent compound with Cl and N in apical positions and two Me groups and one CH_2 group in equatorial positions [11] The ^{13}C NMR of the Me$_3$SiCl solution containing ***fac*-1** was also measured Two lumps consisting of several signals were observed at 213 9−214 1 and 218 0−218.2 ppm. These signals are attributable to terminal carbonyl ligands, indicating that Me$_3$SiCl does not have an interaction with an oxygen atom in the terminal carbonyl ligand Therefore, our observations suggest the formation of hypervalent Si compounds

No *fac*−*mer* isomerization was confirmed in reactions between Me$_3$SiCl and *fac*-[Mo(CO)$_3$(phosphine)$_3$] (phosphine = PEt$_3$, Bu$^n_3$) having no OR group on a coordinating phosphorus, suggesting that a phosphite oxygen plays a crucial role in *fac*−*mer* isomerization.

To elucidate whether *fac*−*mer* isomerization involves a phosphite dissociation process or not, a crossover experiment was performed Addition of Me$_3$SiCl to a CH_2Cl_2 solution containing both ***fac*-1** and ***fac*-2** yielded ***mer*-1** and ***mer*-2** but formed neither phosphite exchange products such as *fac*- and *mer*-[Mo(CO)$_3${P(OMe)$_3$}$_2${P(OEt)$_3$}] nor OR exchange products such as *fac*- and *mer*-[Mo(CO)$_3${P(OMe)$_3$}$_2${P(OMe)$_2$(OEt)}]. These results show intramolecular isomerization, which is consistent with the mechanism shown in Scheme 1

The results showed that Me$_3$SiCl can promote *fac*−*mer* isomerization for *fac*-[Mo(CO)$_3$(phosphite)$_3$], the activity of other silanes was examined for ***fac*-1** Me$_2$SiCl$_2$, MeSiCl$_3$, and SiCl$_4$ promoted the isomerization, but some byproducts were also formed In contrast, SiMe$_4$, with no chloride substituent, did not promote isomerization at all Therefore, among the Me$_n$SiCl$_{4-n}$ (n = 0–4) series, Me$_3$SiCl is the best promoter, which might stem from its superior hypervalent arrangement two electronegative substituents (Cl and O from phosphite) in apical positions and three electron -releasing groups (three Me groups) in equatorial positions Table 2 shows the R$_3$SiX activity Bromosilane and iodosilane (entries 2 and 3) show activity better than that of chlorosilane Ph$_3$SiCl (entry 4) does not promote isomerization, presumably because of the bulky substituents Slow isomerization was observed in the reaction with (EtO)$_3$SiCl (entry 5), which might be attributable to the weak electron-releasing ability of an OEt group compared to that of the Me group A similar *fac*−*mer* ratio was obtained for entries 1−3 and 5, meaning that the ratio is determined thermodynamically and is unaffected by the added silane

Table 2. Isomerization of *fac*-1 Promoted by R$_3$SiX[a]

entry	R$_3$SiX	time (h)	*fac mer*
1	Me$_3$SiCl	3	1 3 4
2	Me$_3$SiBr	<0 1	1 3 6
3	Me$_3$SiI	<0 1	1 3 7
4	Ph$_3$SiCl	25	no reacn
5	(EtO)$_3$SiCl	25	1 3 4

[a] ***fac*-1** was treated with 1 equiv of R$_3$SiX in CH_2Cl_2 at room temperature

In conclusion, this paper describes, for the first time, a halosilane-catalyzed reaction The results showed that an interaction of silane with one phosphite oxygen to form a hypervalent silicon structure reduces the *fac*−*mer* isomerization energy barrier of [Mo(CO)$_3$(phosphite)$_3$]. The hypervalent silicon species was detectable spectroscopically This finding is believed to be a starting point for exploring the potential catalytic activity of halosilanes.

Acknowledgment. This work was supported by a Grant-in-Aid for Science Research on Priority Area (No 18033044, Chemistry of Coordination Space, and No. 19027047, Synergistic Effect of Elements) from the Ministry of Education, Culture, Sports, Science and Technology

Supporting Information Available: Detailed experimental procedures and the characterization of products This material is available free of charge via the Internet at http://pubs acs org

OM7008827

(10) Williams, E A In *The Chemistry of Organic Silicon Compounds*, Patai, S , Rappoport, Z , Eds , Wiley London, 1989, p 511

(11) Kummer, D , Halim, S H A , Kuhs, W , Mattern, G *J Organomet Chem.* **1993**, *446*, 51

Available online at www sciencedirect.com
ScienceDirect
Journal of Organometallic Chemistry 693 (2008) 1968–1974
Journal of Organometallic Chemistry
www elsevier com/locate/jorganchem

Geometrical isomerization of *fac/mer*-$Mo(CO)_3(phosphite)_3$ and *cis/trans*-$Mo(CO)_4(phosphite)_2$ catalyzed by $Me_3SiOSO_2CF_3$

Kozo Fukumoto, Hiroshi Nakazawa *

Department of Chemistry, Graduate School of Science, Osaka City University, Sumiyoshi-ku, Osaka 558-8585, Japan

Received 16 January 2008, received in revised form 18 February 2008, accepted 21 February 2008
Available online 4 March 2008

Abstract

Geometrical isomerization of *fac*-$Mo(CO)_3L_3$ ($L = P(OPh)_3$, $P(OMe)_3$, $P(OEt)_3$) to the *mer* form and that of *cis*-$Mo(CO)_4L_2$ ($L = P(OPh)_3$, $P(OMe)_3$, $PPh_2(OMe)$) to the *trans* form were observed in CH_2Cl_2 at room temperature in the presence of a catalytic amount of $Me_3SiOSO_2CF_3$ (TMSOTf). Crossover experiments suggest that a ligand dissociation is not involved in the isomerization. A catalytic cycle involving an interaction of the silicon atom in Me_3Si^+ with one oxygen in $P(OR)_3$ ligands has been proposed. The first isolation and the X-ray structure analysis were attained for *mer*-$Mo(CO)_3\{P(OPh)_3\}_3$ through the TSMOTf-assisted isomerization of *fac*-$Mo(CO)_3\{P(OPh)_3\}_3$.

Keywords: Geometrical isomerization, Catalysis; Mo complex, Phosphite

1. Introduction

Transition metal complexes with a phosphenium ligand ($^+PR_2$) have attracted considerable attention because a cationic phosphenium is isolobal with a singlet carbene, silylene, and the heavier congeners [1–5]. One of the best methods for preparation of cationic phosphenium complexes of transition metals is OR anion abstraction by a Lewis acid such as $BF_3 \cdot OEt_2$ or TMSOTf ($Me_3SiOSO_2CF_3$) from coordinating diamino-substituted phosphite $P(NMeCH_2)_2(OR)$ as shown in Eq. (1) [4,5]. This method is applicable for many types of transition metal complexes; $M(bpy)(CO)_3\{P(NMeCH_2)_2(OR)\}$ [6–12], $M(dppe)(CO)_3\{P(NMeCH_2)_2(OR)\}$ [7], $M(bpy)(CO)_2\{P(NMeCH_2)_2(OR)\}_2$ [8,11,12], $M(CO)_3\{P(NMeCH_2)_2(OR)\}_3$ [13], $M(CO)_4\{P(NMeCH_2)_2(OR)\}_2$ [13], $CpM(CO)_2(ER_3)\{P(NMeCH_2)_2(OR)\}$ (M = Cr, Mo, W) [14–17], and $CpM(CO)(ER_3)\{P(NMeCH_2)_2(OR)\}$ (M = Fe, Ru) ($ER_3 = CH_3$, $SiMe_3$, $GeMe_3$, $SnMe_3$) [10,18–23]. Systematic researches for reactions of $Mo(bpy)(CO)_3\{PXY(OR)\}$ with $BF_3 \cdot OEt_2$ revealed the effect of the substituents (X, Y) on the stability of cationic phosphenium complexes; the stability increases with increasing the number of amino substituents on the phosphenium phosphorus [9]. TMSOTf has been demonstrated to be an appropriate Lewis acid for *fac*-$Mo(CO)_3\{P(NMeCH_2)_2(OR)\}_3$ and *cis*-$Mo(CO)_4\{P(NMeCH_2)_2(OR)\}_2$ [13].

During the course of investigation of suitability of a Lewis acid to yield a cationic phosphenium complex by OR anion abstraction, we obtained unexpected results in the reaction with TMSOTf of *fac*-$Mo(CO)_3\{P(OR)_3\}_3$ and *cis*-$Mo(CO)_4\{P(OR)_3\}_2$ having no amino-substituent on the coordinating phosphites; TMSOTf does not abstract an

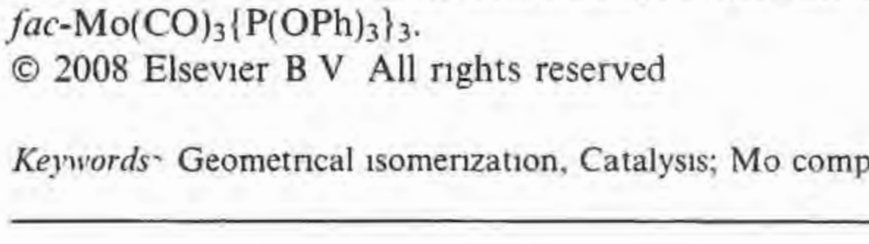

(1)

* Corresponding author
E-mail address: nakazawa@osaka-cu ac jp (H Nakazawa)

0022-328X/$ - see front matter © 2008 Elsevier B V. All rights reserved
doi 10 1016/j.jorganchem 2008 02 024

OR anion to give a cationic phosphenium complex, but promotes the geometrical isomerization of the complexes (*fac–mer* and *cis–trans* isomerization), and it works as a catalyst.

The $Mo(CO)_3L_3$ complexes (M = Cr, Mo, W; L = phosphine, phosphite) have been synthesized in the facial form from $M(CO)_3L'_3$ (L' = weekly coordinating 2e-donor ligand) and L. The *mer* isomers were obtained by using isomerization of the corresponding *fac* isomers. Bond et al. reported that a one electron-oxidation promotes *fac–mer* isomerization for $M(CO)_3\{Ph_2PCH_2CH_2P(Ph)CH_2CH_2PPh_2\text{-}\kappa^3P\}$ [24]. We reported that the reaction of *fac*-$M(CO)_3(bpy)\{P(NMeCH_2)_2(OMe)\}$ with $BF_3 \cdot OEt_2$ yields a cationic phosphenium complex, *fac*-$[M(CO)_3(bpy)\{P(NMeCH_2)_2\}]^+$, which then isomerizes to the *mer* form [7–9]. The strong π-acidity of a phosphenium ligand causes an electron deficient metal center which may induce the *fac–mer* isomerization. Thermal *fac–mer* isomerization has been reported by Rousche et al. for *fac*-$Mo(CO)_3(\eta^2\text{-dppe})\{P(O^iPr)_3\}$ [25] and by Howell et al. for *fac*-$M(CO)_3\{P(OR)_3\}_3$ [26]. We recently found that Me_3SiX (X = Cl, Br, I) promotes the *fac–mer* isomerization for *fac*-$Mo(CO)_3\{P(OR)_3\}_3$ [27].

2. Results and discussion

2.1. Preparation of *fac*-$Mo(CO)_3\{P(OR)_3\}_3$ and *cis*-$Mo(CO)_4\{P(OR)_3\}_2$

The *fac*-$Mo(CO)_3\{P(OR)_3\}_3$ complexes were obtained in good yield by modifying the literature methods [28]. $Mo(CO)_3(NCMe)_3$ was treated with $P(OR)_3$ in 1:3 molar ratio in THF at room temperature (Eq. (2)). A preparative method for *cis*-$Mo(CO)_4\{P(OR)_3\}_2$ was briefly described in the literature, where $Mo(CO)_4(NMe_2(CH_2)_3NMe_2)$ was used as an Mo source [29]. We modified the starting complex. $Mo(CO)_4(nbd)$ (nbd = norbornadiene) and $P(OR)_3$ were treated in 1:2 molar ratio in CH_2Cl_2 at room temperature to give *cis*-$Mo(CO)_4\{P(OR)_3\}_2$ in excellent yield (Eq. (3)).

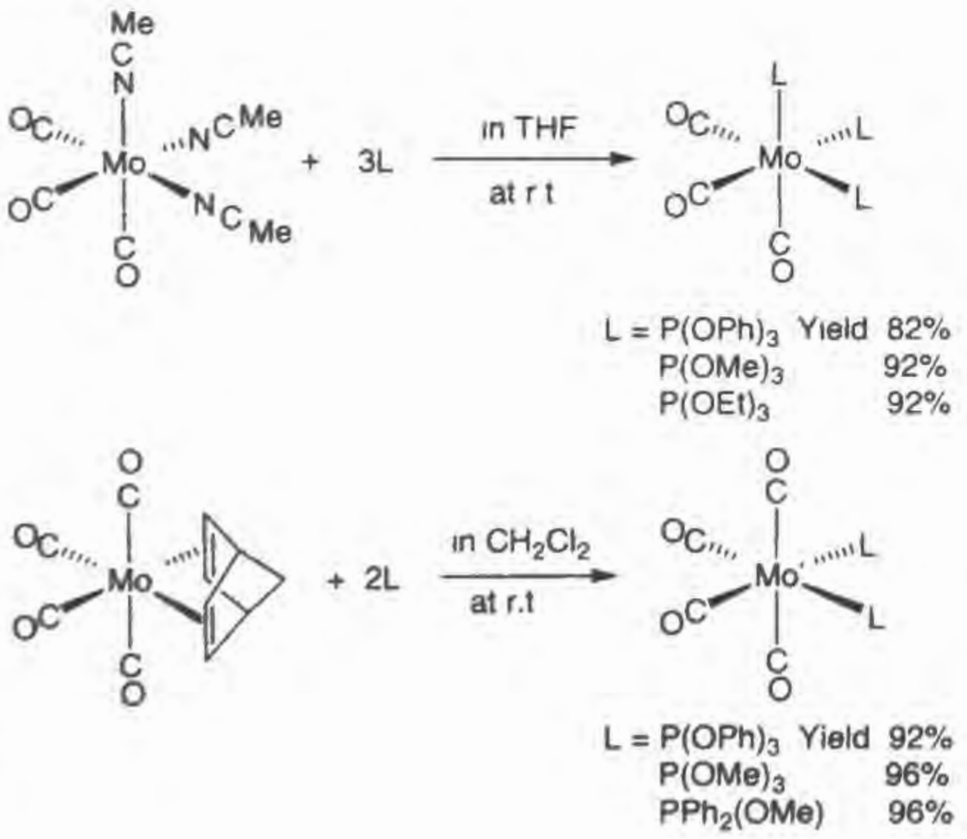

(2)

(3)

2.2. Reaction of *fac*-$Mo(CO)_3L_3$ with TMSOTf

The *fac*-$Mo(CO)_3\{P(OPh)_3\}_3$ (***fac*-1**) was dissolved in CH_2Cl_2 and an equimolar amount of TMSOTf was added at room temperature and the reaction was monitored by the ^{31}P NMR measurement. A triplet at 148.2 ppm (t, $^2J_{PP} = 47.0$ Hz) and a doublet at 155.2 ppm (d, $^2J_{PP} = 47.0$ Hz) were newly observed at the expense of a singlet at 144.4 ppm attributed to ***fac*-1**. The new signals were reasonably assigned to ***mer*-1** based on their coupling pattern and the coupling constant. The isomerization reached at an equilibrium after 1.5 h and the ***fac*-1**:***mer*-1** ratio was 1:30.

We confirmed that ***fac*-1** did not isomerize to ***mer*-1** in CH_2Cl_2 in the absence of TMSOTf at room temperature and even at the reflux temperature, showing that TMSOTf promotes its isomerization. Next question is whether TMSOTf works as a catalyst or not. The reactions of ***fac*-1** with 0.5 and 0.1 equivalent of TMSOTf revealed that the final equilibrium position did not depend on the amount of TMSOTf used although it took a longer time to reach the equilibrium when the amount of TMSOTf was reduced.

The ***mer*-1** could be isolated from the reaction mixture of ***fac*-1** and TMSOTf. After a treatment of ***fac*-1** with TMSOTf in CH_2Cl_2, a white powder which is a mixture of ***fac*-1** and ***mer*-1** (1:30) was washed with hexane/CH_2Cl_2/benzene (100/1/1) solution many times to obtain the pure complex formulated as ***mer*-1** $\cdot 0.5CH_2Cl_2 \cdot 0.5C_6H_6$ in 53% yield. Although several *mer*-$M(CO)_3L_3$ (M = Cr, Mo, W) type complexes have been reported, this is the first preparation and isolation of *mer*-$M(CO)_3\{P(OPh)_3\}_3$. The structure was confirmed by the X-ray analysis. The ORTEP drawing is depicted in Fig. 1 and the crystal data are summarized in Table 1. This X-ray structure is the first example among *mer*-$M(CO)_3$(tertiary phosphorus compound)$_3$ type complexes. The X-ray structure of ***fac*-1** was reported previously [29]. The structural comparison between *fac*- and *mer*-$Mo(CO)_3\{P(OPh)_3\}_3$ revealed some interesting points. The bond distance of Mo–C2 for ***mer*-1** (2.018 Å) is clearly shorter than those of Mo–C1 (2.041 Å) and Mo–C3 (2.041 Å). As C2O2 ligand is *trans* to $P(OPh)_3$, the CO ligand can get more π-back donation from the central metal than C1O1 and C3O3 ligands which are mutually *trans*. The mean Mo–C bond distance for ***fac*-1** (1.986 Å) is shorter than that for ***mer*-1** (2.033 Å), reasonably understood by greater π-back donation from the Mo to the CO ligands for ***fac*-1** because of the *trans* $P(OPh)_3$ ligand. Another interesting point is that the mean Mo–P bond distance for ***fac*-1** (2.435 Å) is longer than that for ***mer*-1** (2.417 Å). The difference may stem from the steric repulsion between $P(OPh)_3$ ligands in ***fac*-1**.

The ***mer*-1** did not isomerize to ***fac*-1** in CH_2Cl_2 at room temperature, but it did by the addition of an equimolar amount or even a catalytic amount of TMSOTf. After several hours, the ***fac*-1**:***mer*-1** ratio was 1:30. The results mentioned above show that the equilibrium ratio is determined

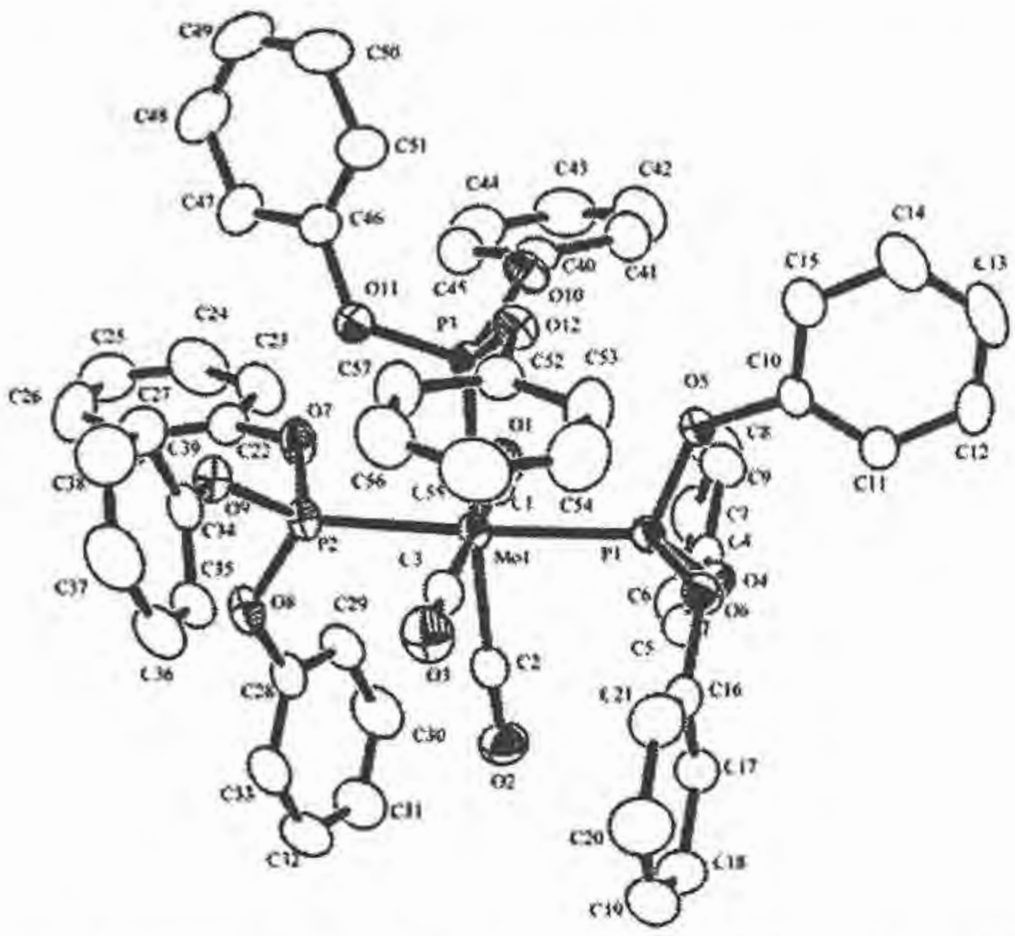

Fig. 1. ORTEP drawing of *mer*-**1**·0.5CH_2Cl_2·0.5C_6H_6 (50% probability ellipsoids) showing the numbering system. All hydrogen atoms and the solvated CH_2Cl_2 and C_6H_6 molecules are omitted for clarity. Selected bond distances (Å) and bond angles (°): Mo1–P1, 2.3796(7); Mo1–P2, 2.4319(7); Mo1–P3, 2.4390(7); Mo1–C1, 2.041(3); Mo1–C2, 2.018(3); Mo1–C3, 2.041(3); P1–Mo1–P2, 174.24(2); P1–Mo1–P3, 89.76(2); P2–Mo1–P3, 89.57(2); P1–Mo1–C1, 91.21(8); P1–Mo–C2, 86.15(8); P1–Mo–C3, 91.51(8).

Table 1
Crystal data for *mer*-**1**·0.5CH_2Cl_2·0.5C_6H_6

Empirical formula	$C_{60.50}H_{49}ClMoO_{12}P_3$
Formula weight	1192.30
Crystal system	Monoclinic
Crystal size (mm^3)	0.45 × 0.35 × 0.15
Temperature (°C)	−70.0
Space group	$P2_1/n$ (No. 14)
a (Å)	13.7319(5)
b (Å)	18.2658(7)
c (Å)	22.1401(9)
β (°)	95.744(2)
V (Å^3)	5525.4(4)
Z	4
μ (cm^{-1})	4.36
D_{calc} (g/cm^3)	1.433
Number of unique reflections	41908
Number of used reflections	12498
Number of variables	712
R	0.051
R_W	0.111
Goodness-of-Fit	1.06

thermodynamically and TMSOTf serves as a catalyst for the *fac–mer* isomerization.

Reactions of *fac*-$Mo(CO)_3\{P(OMe)_3\}_3$ (***fac*-2**) and *fac*-$Mo(CO)_3\{P(OEt)_3\}_3$ (***fac*-3**) with TMSOTf were also examined in CH_2Cl_2 at room temperature. In the ^{31}P NMR spectra, a triplet at 166.9 ppm (t, $^2J_{PP} = 41.7$ Hz) and a doublet at 175.1 ppm (d, $^2J_{PP} = 41.7$ Hz) assignable to ***mer*-2** were observed in the reaction of ***fac*-2**, and a triplet at 162.7 ppm (t, $^2J_{PP} = 41.7$ Hz) and a doublet at 170.5 ppm (d, $^2J_{PP} = 41.7$ Hz) attributable to ***mer*-3** were observed in the reaction of ***fac*-3**. The equilibrium *fac–mer* ratios were independent of the amount of TMSOTf used, showing that TMSOTf serves as a catalyst. The results together with those for ***fac*-1** are shown in Table 2. The equilibrium *fac–mer* ratios are quite dependent on the kind of the phosphite ligand. It should be noted that these values are equal to those for the isomerization promoted by Me_3SiX (X = Cl, Br, I) [27], and the value for ***fac*-2** is similar to that reported by Howell [26]. Therefore, it can be said that the values are derived from the thermodynamic stability between the *fac* and *mer* isomers, not from the stability of the intermediates created from an Mo complex and a catalyst (presumably TMS^+, vide infra).

2.3. Isomerization mechanism

Regarding isomerization of $Mo(CO)_3\{P(OR)_3\}_3$ promoted by TMSOTf, two mechanisms are conceivable: mechanisms via a phosphenium complex and via a TMS^+ adduct.

A mechanism via a phosphenium complex is shown in Scheme 1. As transition-metal complexes bearing a diamino-substituted phosphite have been reported to react with a Lewis acid to give cationic phosphenium complexes by OR^- abstraction as shown in Eq. (1), a similar OR^- abstraction may take place in the reaction of $Mo(CO)_3\{P(OR)_3\}_3$ with TMSOTf to produce a cationic phosphenium complex (***fac'*** in Scheme 1). Then, isomerization from ***fac'*** to ***mer'*** is expected to take place. The similar isomerization has been reported previously (Eq. (4)), where the driving force of the *fac–mer* isomerization is thought to be the gain of more π-back donation for the phosphenium ligand. The reaction of ***mer'*** with TMSOR formed would give *mer*-$Mo(CO)_3\{P(OR)_3\}_3$ with regeneration of TMSOTf. However, this catalytic cycle seems not plausible based on the following observations. (i) A complex having a phosphenium ligand was not detected in the reaction of $Mo(CO)_3\{P(OR)_3\}_3$ with TMSOTf. (ii) After the treatment

Table 2
Isomerization of $Mo(CO)_3\{P(OR)_3\}_3$ by TMSOTf in CH_2Cl_2 at room temperature

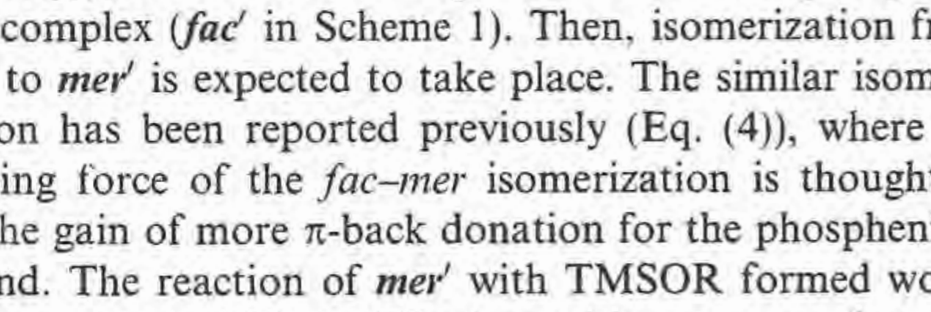

$P(OR)_3$			*fac*:*mer*[b]
$P(OPh)_3$	***fac*-1**	***mer*-1**	1:30
$P(OMe)_3$	***fac*-2**	***mer*-2**	1:3.4
$P(OEt)_3$	***fac*-3**	***mer*-3**	1:2.2

[a] 1.0, 0.5 and 0.1 equvalents based on the *fac* complex were used.
[b] *fac*:*mer* equilibrium ratio after completion of the isomerization.

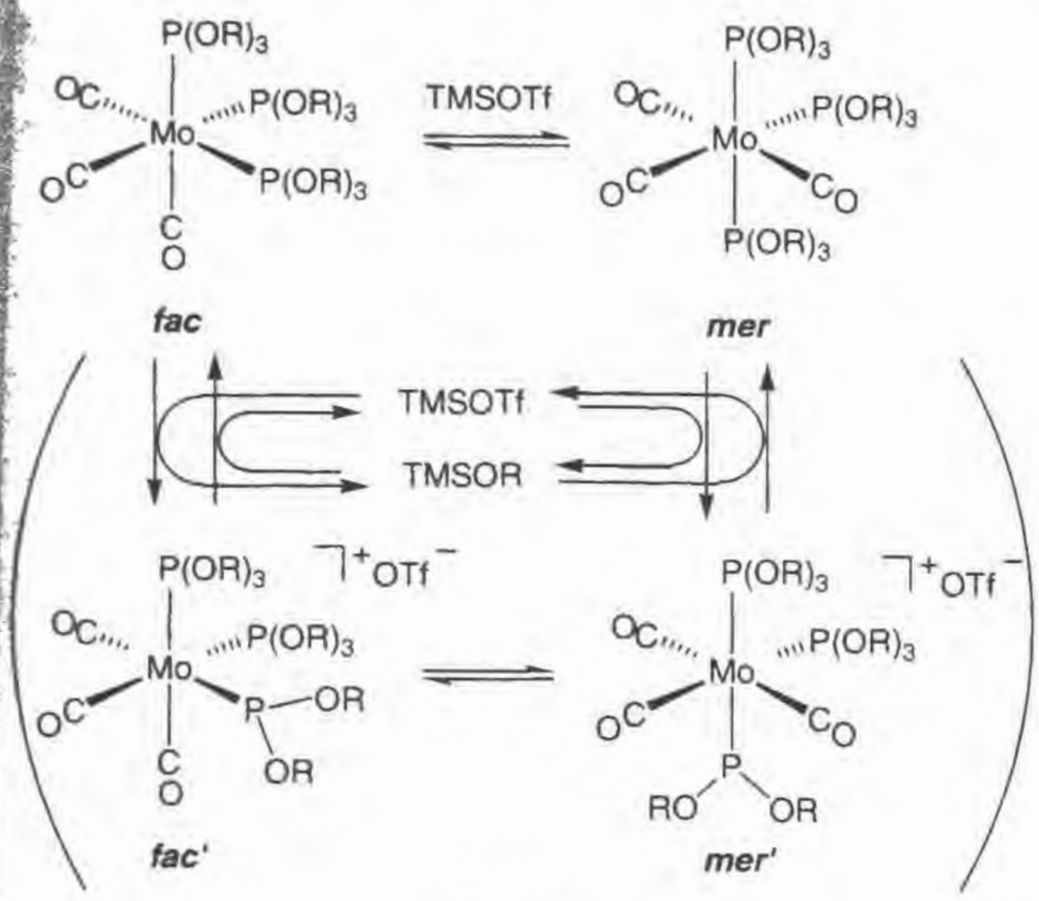

Scheme 1

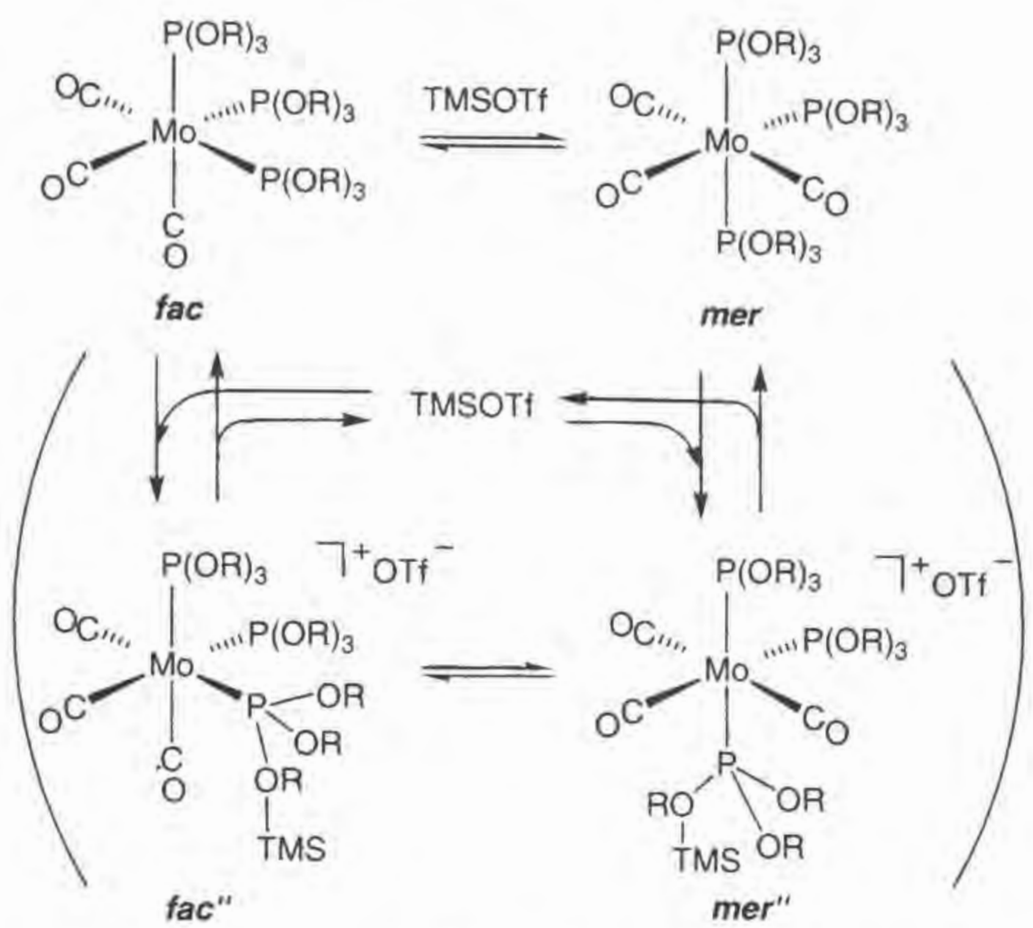

Scheme 2

of ***fac*-1** with 1 equiv of TMSOTf in the presence of 1 equiv of TMSOMe in CH_2Cl_2, the ^{31}P NMR spectra of the reaction mixture were measured and ***fac*-1** and ***mer*-1** were detected but *fac*- and *mer*-$Mo(CO)_3\{P(OPh)_3\}_2\{P(OPh)_2(OMe)\}$ were not detected at all. This indicates that the reaction of ***mer'*** with TMSOR to give ***mer*** in Scheme 1 does not proceed.

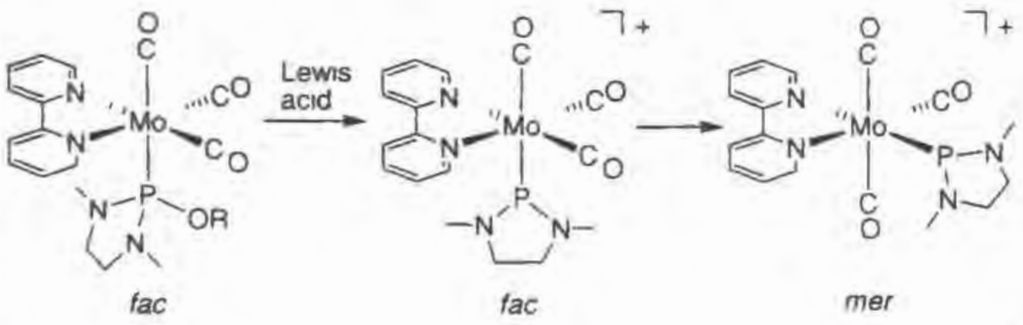

(4)

The other isomerization mechanism is shown in Scheme 2. The silicon atom in TMS^+ interacts with one oxygen in $P(OR)_3$ ligands to form ***fac''***, but does not abstract the OR group as an anion. The interaction weakens the coordination of the $P(OR)_3(TMS)$ ligand toward the central metal and makes the ligand bulky, thereby decreasing the isomerization energy barrier to give its *mer* isomer (***mer''***). Dissociation of TMS^+ from ***mer''*** gives *mer*-$Mo(CO)_3\{P(OR)_3\}_3$ with regeneration of TMSOTf. The similar isomerization mechanism has been proposed for the isomerization of $Mo(CO)_3\{P(OR)_3\}_3$ promoted by Me_3SiX (X = Cl, Br, I) [27].

There is a possibility that dissociation of one of the phosphites in $Mo(CO)_3\{P(OR)_3\}_3$ induces the isomerization and TMSOTf promotes the dissociation. To check the possibility, a crossover experiment was conducted. Both ***fac*-2** and ***fac*-3** were dissolved in CH_2Cl_2, TMSOTf was added, and the products were estimated from the ^{31}P NMR spectra of the resulting CH_2Cl_2 solution. Signals assignable to ***mer*-2** and ***mer*-3**, in addition to ***fac*-2** and ***fac*-3** were observed, but those due to phosphite exchange products such as *fac*- or *mer*-$Mo(CO)_3\{P(OMe)_3\}_2\{P(OEt)_3\}$ and OR exchange products such as *fac*- or *mer*-$Mo(CO)_3\{P(OMe)_3\}_2\{P(OMe)_2(OEt)\}$ were not detected. These results strongly suggest that neither phosphite dissociation nor OR^- abstraction shown in Scheme 1 is involved in the *fac–mer* isomerization. Therefore, we proposed the isomerization mechanism shown in Scheme 2, though the intermediates have not been observed.

2.4 Reaction of *cis*-$Mo(CO)_4L_2$ with TMSOTf

In addition to the isomerization of *fac*-$Mo(CO)_3\{P(OR)_3\}_3$ promoted by TMSOTf, the isomerization of *cis*-$Mo(CO)_4\{P(OR)_3\}_2$ was also investigated. The results were shown in Table 3. The *cis–trans* isomerization occurred in the presence of TMSOTf and did not in the absence of TMSOTf for ***cis*-5**, and ***cis*-6**, and TMSOTf worked as a catalyst. The ^{31}P NMR signals of ***trans*-5** and ***trans*-6** were observed at 173.4 and 155.1 ppm, respectively. In contrast, ***cis*-4** did not isomerize to ***trans*-4** even in the presence of TMSOTf. For the *cis–trans* isomerization, the reaction pathway similar to that for the *fac–mer* isomerization of $Mo(CO)_3\{P(OR)_3\}_3$ shown in Scheme 2 is proposed. Interaction of TMS^+ with an oxygen in the $P(OR)_3$ ligands may initiate the *cis–trans* isomerization. The basicity of the phosphite oxygen in *cis*-$Mo(CO)_4\{P(OR)_3\}_2$ is considered to be less than that in *fac*-$Mo(CO)_3\{P(OR)_3\}_3$ because the former complex has more CO ligands in number being a strong π-accepter ligand. Among ***cis*-4**, ***cis*-5**, and ***cis*-6**, ***cis*-4** has least oxygen basicity because of the sub-

Table 3
Isomerization of $Mo(CO)_4\{P(OR)_3\}_2$ by TMSOTf in CH_2Cl_2 at room temperature

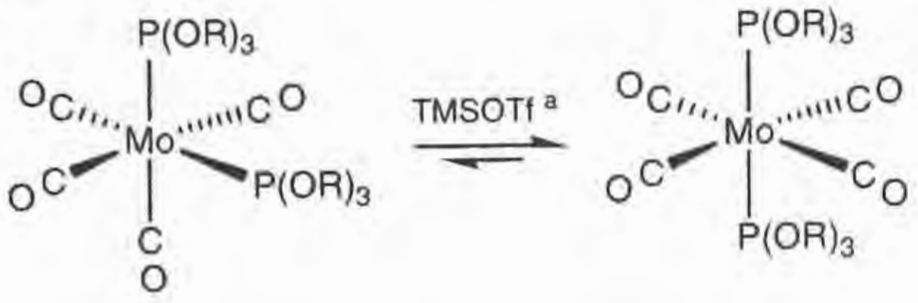

$P(OR)_3$			*cis trans*[b]
$P(OPh)_3$	***cis*-4**	***trans*-4**	no reaction
$P(OMe)_3$	***cis*-5**	***trans*-5**	1 0 9
$PPh_2(OMe)$	***cis*-6**	***trans*-6**	1 2 3

[a] 1 0, 0 5 and 0.1 equvalents based on the *cis* complex were used
[b] *cis*-*trans* equilibrium ratio after completion of the isomerization

stituents (Ph vs. Me). Therefore, ***cis*-4** may not have enough basicity on the oxygen to form an interaction with TMS^+.

2.5. Reaction of *fac*-$Mo(CO)_3L_3$ and *cis*-$Mo(CO)_4L_2$ with $BF_3 \cdot OEt_2$

TMSOTf and $BF_3 \cdot OEt_2$ are effective Lewis acids to obtain a cationic phosphenium complex by an OR anion abstraction from a diamino-substituted phosphite ligand in a transition metal complex. In contrast, TMSOTf does not abstract an OR anion from a $P(OR)_3$ ligand of *fac*-$Mo(CO)_3\{P(OR)_3\}_3$ and *cis*-$Mo(CO)_4\{P(OR)_3\}_2$, but promotes the *fac–mer* and *cis–trans* isomerization. Therefore, reactions of *fac*-$Mo(CO)_3\{P(OMe)_3\}_3$ (***fac*-2**) and *cis*-$Mo(CO)_4\{P(OMe)_3\}_2$ (***cis*-5**) with $BF_3 \cdot OEt_2$ were examined and it was found that $BF_3 \cdot OEt_2$ causes some complicated reactions in addition to isomerization.

The ^{31}P NMR spectrum of the reaction mixture of ***fac*-2** and an equimolar amount of $BF_3 \cdot OEt_2$ in CH_2Cl_2 showed several unidentified signals in addition to signals assignable to ***mer*-2**. These signals increased in intensity with time but the singlet due to the starting complex (***fac*-2**) still remained after several hours.

The reaction of ***cis*-5** with an equimolar amount of $BF_3 \cdot OEt_2$ in CH_2Cl_2 at room temperature was followed by the ^{31}P NMR measurement. After 4 h, in addition to a strong singlet due to ***cis*-5**, a doublet of doublet at 164.5 ppm (d, $^1J_{PF} = 1157.1$, and $^2J_{PP} = 46.9$ Hz) and a doublet at 163.4 ppm (d, $^2J_{PP} = 46.9$ Hz) were observed. The large coupling constant (1157.1 Hz) suggests the existence of a P–F bond and the small coupling constant (46.9 Hz) indicates that two phosphorus ligands are *cis* to each other. Therefore, the formation of *cis*-$Mo(CO)_4\{P(OMe)_3\}\{P(OMe)_2F\}$ was proposed. The similar OR/F substitution reaction has been reported [6,9,11]. The ^{31}P NMR spectrum after 24 h, signals due to *cis*-$Mo(CO)_4\{P(OMe)_3\}\{P(OMe)_2F\}$ increased in intensity and a new singlet at 173.4 ppm attributable to ***trans*-5** was observed. In addition, several unidentified signals were observed. Therefore, it was found in the reaction of ***cis*-5** with $BF_3 \cdot OEt_2$, relatively fast OMe/F substitution reaction and relatively slow *cis* to *trans* isomerization and some unidentified reactions take place.

3. Experimental

3 1 General remarks

All reactions were carried out under an atmosphere of dry nitrogen by using Schlenk tube techniques. CH_2Cl_2 was distilled from CaH_2, and hexane and THF were distilled from sodium metal. These were stored under nitrogen atmosphere. $Mo(CO)_3(NCMe)_3$ [30] and $Mo(CO)_4(nbd)$ [31] were prepared according to the literature methods. *Fac*-$Mo(CO)_3(L)_3$ and *cis*-$Mo(CO)_4(L)_2$ (L = phosphite) were prepared by the modification of the published procedures [28,29]. IR spectra were recorded on a Perkin–Elmer Spectrum One spectrometer. A JEOL JNM-AL400 spectrometer was used to obtain ^1H, ^{13}C, and ^{31}P NMR spectra. ^1H and ^{13}C NMR data were referenced to Me_4Si. ^{31}P NMR data were referenced to 85% H_3PO_4.

3 2. Preparation of *fac*-$Mo(CO)_3\{P(OPh)_3\}_3$ (***fac*-1**)

A THF solution (20 mL) containing $Mo(CO)_3(NCMe)_3$ (0.52 g, 1.72 mmol) and $P(OPh)_3$ (1.36 mL, 5.19 mmol) was stirred for 4 h at room temperature. After volatile materials were removed under reduced pressure, the resulting precipitate was washed with hexane a few times and dried in vacuo to give a white powder of ***fac*-1** (1.57 g, 1.41 mmol, 82%). ^1H NMR (δ, in $CDCl_3$): 6.98–7.18 (m, Ph). $^{13}C\{^1H\}$ NMR (δ, in $CDCl_3$): 121.9 (s, *p*-Ph), 124.3 (s, *m*-Ph), 129.4 (s, *o*-Ph), 152.1 (s, *ipso*-Ph), 212.2 (m, CO). $^{31}P\{^1H\}$ NMR (δ, in $CDCl_3$): 145.0 (s). IR (cm^{-1}, in $CHCl_3$): ν (CO) 1917, 1992.

3 3. Preparation of *fac*-$Mo(CO)_3\{P(OMe)_3\}_3$ (***fac*-2**)

A THF solution (20 mL) containing $Mo(CO)_3(NCMe)_3$ (0.55 g, 1.81 mmol) and $P(OMe)_3$ (0.65 mL, 5.51 mmol) was stirred for 4 h at room temperature. After volatile materials were removed under reduced pressure, the resulting precipitate was washed with hexane a few times and dried in vacuo to give a white powder of ***fac*-2** (0.92 g, 1.67 mmol, 92%). ^1H NMR (δ, in $CDCl_3$): 3.61 (d, $^3J_{PH} = 10.8$ Hz, OCH_3). $^{13}C\{^1H\}$ NMR (δ, in $CDCl_3$): 51.4 (m, OCH_3), 215.9 (m, CO). $^{31}P\{^1H\}$ NMR (δ, in $CDCl_3$): 168.0 (s). IR (cm^{-1}, in $CDCl_3$): ν (CO) 1880, 1967.

3 4. Preparation of *fac*-$Mo(CO)_3\{P(OEt)_3\}_3$ (***fac*-3**)

A THF solution (20 mL) containing $Mo(CO)_3(NCMe)_3$ (0.39 g, 1.30 mmol) and $P(OEt)_3$ (0.67 mL, 3.90 mmol) was stirred for 4 h at room temperature. After volatile materials were removed under reduced pressure, the resulting precipitate was washed with hexane a few times at −78 °C and

dried in vacuo to give a white powder of ***fac*-3** (0.61 g, 1.2 mmol, 92%). ^{1}H NMR (δ, in $CDCl_3$): 1.22 (m, 3H, OCH_2CH_3), 3.96 (m, 2H, OCH_2CH_3). $^{13}C\{^1H\}$ NMR (δ, in $CDCl_3$): 16.4 (m, OCH_2CH_3), 59.7 (s, OCH_2CH_3), 216.4 (m, CO). $^{31}P\{^1H\}$ NMR (δ, in $CDCl_3$): 161.2 (s). IR (cm^{-1}, in $CHCl_3$): ν (CO) 1860, 1963.

3.5 Preparation of *cis*-$Mo(CO)_4\{P(OPh)_3\}_2$ (***cis*-4**)

A CH_2Cl_2 solution (10 mL) containing $Mo(CO)_4$(nbd) (0.81 g, 2.46 mmol) and $P(OPh)_3$ (0.83 mL, 4.92 mmol) was stirred for 4 h at room temperature. After volatile materials were removed under reduced pressure, the resulting precipitate was washed with hexane a few times at −78 °C and dried in vacuo to give a white powder of ***cis*-4** (1.87 g, 2.68 mmol, 92%). ^{1}H NMR (δ , in $CDCl_3$): 7.18–7.36 (m, Ph). $^{13}C\{^1H\}$ NMR (δ, in $CDCl_3$): 121.6 (s, *p*-Ph), 124 9 (s, *m*-Ph), 129.8 (s, *o*-Ph), 151 4 (t, $^2J_{PC} = 4\ 2$ Hz, *ipso*-Ph), 205.5 (t, $^2J_{PC} = 13.3$ Hz, *cis*-CO), 209.5 (t, $^2J_{PC} = 17.4$ Hz, *trans*-CO) $^{31}P\{^1H\}$ NMR (δ, in $CDCl_3$): 151.4 (s). IR (cm^{-1}, in $CHCl_3$): ν (CO) 1940, 2046.

3 6 Preparation of *cis*-$Mo(CO)_4\{P(OMe)_3\}_2$ (***cis*-5**)

A CH_2Cl_2 solution (10 mL) containing $Mo(CO)_4$(nbd) (0.73 g, 2.21 mmol) and $P(OMe)_3$ (0.52 mL, 4.42 mmol) was stirred for 4 h at room temperature After volatile materials were removed under reduced pressure, the resulting precipitate was washed with hexane a few times at −78 °C and dried in vacuo to give a orange sticky powder of ***cis*-5** (0.97 g, 2.13 mmol, 96%). ^{1}H NMR (δ, in $CDCl_3$). 3.62 (s, OCH_3). $^{13}C\{^1H\}$ NMR (δ, in $CDCl_3$): 51 4 (s, OCH_3), 207.9 (t, $^2J_{PC} = 14.1$ Hz, *cis*-CO), 212.1 (t, $^2J_{PC} = 13.3$ Hz, *trans*-CO). $^{31}P\{^1H\}$ NMR (δ, in $CDCl_3$): 165.6 (s) IR (cm^{-1}, in $CHCl_3$): ν (CO) 2036, 1921.

3 7 Preparation of *cis*-$Mo(CO)_4\{PPh_2(OMe)\}_2$ (***cis*-6**)

A CH_2Cl_2 solution (10 mL) containing $Mo(CO)_4$(nbd) (0.63 g, 1.91 mmol) and $PPh_2(OMe)$ (0.76 mL, 3 82 mmol) was stirred for 3 h at room temperature After volatile materials were removed under reduced pressure, the resulting precipitate was washed with hexane a few times at −78 °C and dried in vacuo to give a white powder of ***cis*-6** (1.17 g, 1.82 mmol, 96%). ^{1}H NMR (δ, in $CDCl_3$): 3.27 (s, 3 H, OCH_3), 7.40–7.53 (m, 10H, Ph). $^{13}C\{^1H\}$ NMR (δ, in $CDCl_3$): 53.6 (s, OCH_3), 128.1 (s, *p*-Ph), 130.1 (s, *m*-Ph), 131.2 (t, $^2J_{PC} = 6.6$ Hz, *o*-Ph), 139.0 (t, $^2J_{PC} = 15.8$ Hz, *ipso*-Ph), 209.5 (t, $^2J_{PC} = 10.3$ Hz, *cis*-CO), 214.6 (t, $^2J_{PC} = 9.5$ Hz, *trans*-CO). $^{31}P\{^1H\}$ NMR (δ, in $CDCl_3$): 144.9 (s). IR (cm^{-1}, in $CHCl_3$): ν (CO) 2026, 1912.

3.8. Isolation of *mer*-$Mo(CO)_3\{P(OPh)_3\}_3$ (***mer*-1**)

A solution of ***fac*-1** (2.31 g, 2.08 mmol) and TMSOTf (0.38 mL, 2.08 mmol) in CH_2Cl_2 (20 mL) was stirred for 1 5 h at room temperature. After volatile materials were removed under reduced pressure, the resulting precipitate was washed with hexane (3 mL, 5 times) at −78 °C and dried in vacuo to give a white powder of a mixture of ***fac*-1** and ***mer*-1** (1:30). To obtain pure ***mer*-1**, the powder was washed with hexane/CH_2Cl_2 = 100/1 solution (5 mL, 20 times) at room temperature, and the powder was dried in vacuo (1.22 g, 1 10 mmol, 53%). ^{1}H NMR (δ, in $CDCl_3$) 6 83–7.25 (m, Ph). $^{13}C\{^1H\}$ NMR (δ, in $CDCl_3$). 121 6 (s, *p*-Ph), 124.2 (s, *m*-Ph), 129.4 (s, *o*-Ph), 151.9 (s, *ipso*-Ph), 208.0 (m, CO), 213 0 (m, CO). $^{31}P\{^1H\}$ NMR (δ, in $CDCl_3$): 148.6 (t, $^2J_{PP} = 46.9$ Hz, equatorial-P), 155.4 (d, $^2J_{PP} = 46\ 9$ Hz, apical-P). IR (cm^{-1}, in $CHCl_3$) ν (CO) 1931, 1813

3 9 X-ray crystal structure determination of ***mer*-1**

Crystals of ***mer*-1** suitable for an X-ray diffraction study were obtained through crystallization from CH_2Cl_2/hexane/benzene for a few days. The single crystal was mounted in a glass capillary. Data for ***mer*-1** were collected at −70 °C on Rigaku/MSC Mercury CCD area-detector diffractometer equipped with monochromated Mo Kα radiation. Calculations for ***mer*-1** were performed with the teXsan crystallographic software package of Molecular Structure Corporation. H atoms were refined using a riding model, with C–H = 0.95 Å, and fixed individual displacement parameters [U_{iso} (H) = U_{eq}(C)]. The crystal was formulated as ***mer*-1** $0.5CH_2Cl_2 \cdot 0.5C_6H_6$. The CH_2Cl_2 molecule was disordered in two positions with 50:50 probability in the unit cell.

Acknowledgements

This work was supported by a Grant-in-Aid for Science Research on Priority Area (No. 18033044, Chemistry of Coordination Space, and No. 19027047, Synergistic Effect of Elements) from the Ministry of Education, Culture, Sports, Science and Technology.

Appendix A. Supplementary material

X-ray crystallographic data in CIF format for ***mer*-1**. This material is available free of charge via the Internet at http://pubs.acs.org. Supplementary data associated with this article can be found, in the online version, at doi.10.1016/j.jorganchem.2008.02.024.

References

[1] A H Cowley, R A Kemp, Chem Rev 85 (1985) 367.
[2] (a) M Sanchez, M R Mazieres, L Lamande, R Wolf, in M Regitz, O.J Scherer (Eds), Multiple Bonds and Low Coordination in Phosphorus Chemistry, Thieme, New York, 1990 (Chapter D1).
(b) A Schmidpeter, in M Regitz, O J. Scherer (Eds), Multiple Bonds and Low Coordination in Phosphorus Chemistry, Thieme, New York, 1990 (Chapter D2).
[3] D. Gudat, Coord Chem Rev. 163 (1997) 71

[4] H. Nakazawa, J. Organomet. Chem. 611 (2000) 349
[5] H. Nakazawa, Adv. Organomet. Chem. 50 (2004) 107
[6] H. Nakazawa, M. Ohta, K. Miyoshi, H. Yoneda, Organometallics 8 (1989) 638
[7] H. Nakazawa, Y. Yamaguchi, K. Miyoshi, J. Organomet. Chem. 465 (1994) 193
[8] H. Nakazawa, Y. Yamaguchi, T. Mizuta, K. Miyoshi, Organometallics 14 (1995) 4137
[9] Y. Yamaguchi, H. Nakazawa, T. Itoh, K. Miyoshi, Bull. Chem. Soc. Jpn. 69 (1996) 983
[10] H. Nakazawa, Y. Yamaguchi, K. Miyoshi, Phosphorus, Sulfur, Silicon Relat. Elem. 109 (1996) 129
[11] H. Nakazawa, Y. Yamaguchi, K. Miyoshi, A. Nagasawa, Organometallics 15 (1996) 2517
[12] K. Takano, H. Tsumura, H. Nakazawa, M. Kurakata, T. Hirano, Organometallics 19 (2000) 3323
[13] H. Nakazawa, Y. Miyoshi, T. Katayama, T. Mizuta, K. Miyoshi, N. Tsuchida, A. Ono, K. Takano, Organometallics 25 (2006) 5913
[14] H. Nakazawa, M. Kishishita, S. Yoshinaga, Y. Yamaguchi, T. Mizuta, K. Miyoshi, J. Organomet. Chem. 529 (1997) 423
[15] H. Nakazawa, M. Kishishita, K. Miyoshi, Phosphorus, Sulfur, Silicon Relat. Elem. 144 (1999) 45
[16] H. Nakazawa, M. Kishishita, T. Ishiyama, T. Mizuta, K. Miyoshi, J. Organomet. Chem. 617–618 (2001) 453
[17] H. Nakazawa, Y. Yamashita, K. Miyoshi, Phosphorus, Sulfur, Silicon Relat. Elem. 177 (2002) 1533
[18] H. Nakazawa, Y. Yamaguchi, T. Mizuta, S. Ichimura, K. Miyoshi, Organometallics 14 (1995) 4635
[19] H. Nakazawa, Y. Yamaguchi, K. Miyoshi, Organometallics 15 (1996) 1337
[20] H. Nakazawa, Y. Yamaguchi, K. Kawamura, K. Miyoshi, Organometallics 16 (1997) 4626
[21] K. Kawamura, H. Nakazawa, K. Miyoshi, Organometallics 18 (1999) 1517
[22] K. Kawamura, H. Nakazawa, K. Miyoshi, Organometallics 18 (1999) 4785
[23] H. Nakazawa, M. Kishishita, T. Nakamoto, N. Makanura, T. Ishiyama, K. Miyoshi, Chem. Lett. (2000) 230
[24] A.M. Bond, R. Colton, S.W. Feldberg, P.J. Mahon, T. Whyte, Organometallics 10 (1991) 3320
[25] J.-C. Rousche, G.R. Dobson, Inorg. Chim. Acta 28 (1978) L139
[26] J.A.S. Howell, P.C. Yates, N.F. Ashford, D.T. Dixon, R. Warren, J. Chem. Soc., Dalton Trans. 20 (1996) 3959
[27] K. Fukumoto, H. Nakazawa, Organometallics 26 (2007) 6505
[28] E.C. Alyea, G. Ferguson, S.-Q. Song, Acta Crystallogr. C 51 (1995) 2238
[29] G.R. Dobson, A.J. Rettenmaier, Inorg. Chim. Acta 6 (1972) 507
[30] D.P. Tate, W.R. Knipple, J.M. Augl, Inorg. Chem. 1 (1962) 433
[31] M.A. Bennett, L. Pratt, G. Wilkinson, J. Chem. Soc. (1961) 2037

Journal of the American Chemical Society

Communication

N#CN Bond Cleavage of Cyanamides by a Transition-Metal Complex

Kozo Fukumoto, Tsukuru Oya, Masumi Itazaki, and Hiroshi Nakazawa

J. Am. Chem. Soc., **2009**, 131 (1), 38-39 • DOI: 10.1021/ja807896b • Publication Date (Web): 10 December 2008

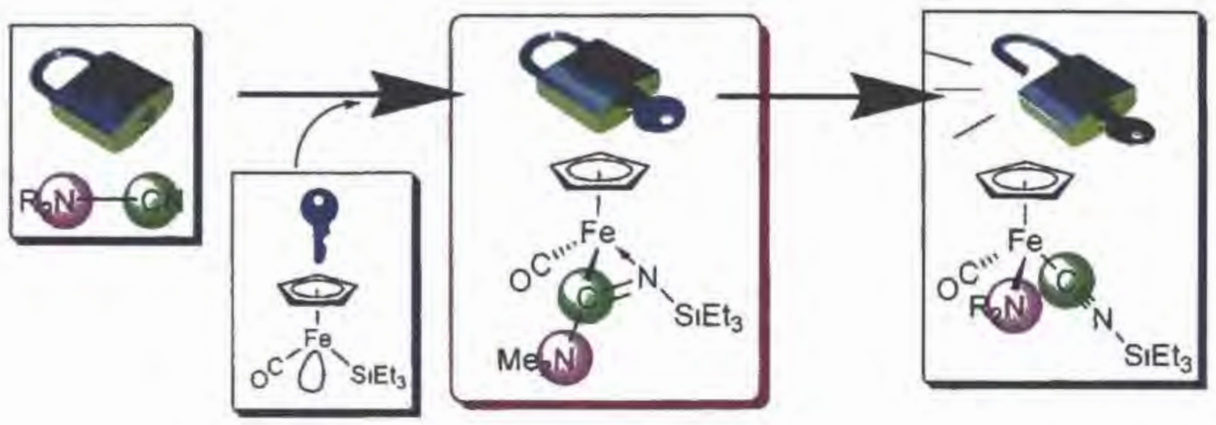

More About This Article

Additional resources and features associated with this article are available within the HTML version:

- Supporting Information
- Access to high resolution figures
- Links to articles and content related to this article
- Copyright permission to reproduce figures and/or text from this article

View the Full Text HTML

Journal of the American Chemical Society is published by the American Chemical Society 1155 Sixteenth Street N.W. Washington, DC 20036

J|A|C|S COMMUNICATIONS

Published on Web 12/10/2008

N−CN Bond Cleavage of Cyanamides by a Transition-Metal Complex

Kozo Fukumoto, Tsukuru Oya, Masumi Itazaki, and Hiroshi Nakazawa*

Department of Chemistry, Graduate School of Science, Osaka City University, Sumiyoshi-ku, Osaka 558-8585, Japan

Received October 6, 2008, E-mail nakazawa@sci osaka-cu ac jp

In the last two decades, considerable efforts have been devoted to cleavage of unreactive bonds such as carbon−hydrogen,[1] carbon−carbon,[2] carbon−nitrogen,[3] and carbon−oxygen [4] Direct cleavage of these bonds provides several advantages in organic syntheses, including atom efficiency, low environmental load, and the potential for unusual chemoselectivity

Scheme 1. Reaction Pathway of Me−CN Bond Cleavage

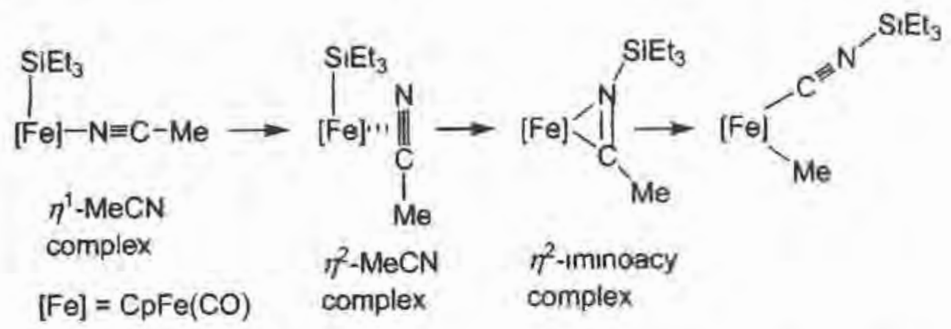

We recently reported reactions of C−CN bond cleavage of organonitriles promoted using a silyl−iron complex [2d] The essence of the reaction mechanism for Me−CN bond cleavage is depicted in Scheme 1 Acetonitrile coordinates to a 16e silyl−iron complex $Cp(CO)Fe(SiEt_3)$ produced from $Cp(CO)_2Fe(SiEt_3)$ (**1**) in a photoreaction to give an η^1-MeCN complex, which is converted into an η^2-MeCN complex Then, silyl migration from Fe to the nitrile nitrogen atom occurs to form η^2-iminoacyl complex, followed by C−C bond cleavage on the coordination sphere to give a methylsilylisocyanide complex The η^2-coordination of acetonitrile through C≡N π-bond induces silyl migration, which then causes C−CN bond cleavage The reaction sequences stimulate us to examine the possibility of R_2N−CN (cyanamide) bond cleavage by a silyl−iron complex because the replacement of the R group in RCN by an NR_2 group yields cyanamide The R_2N−CN bond is known to be strong and not broken readily For example, the N−CN bond length in Me(p-C_6H_4Cl)N−CN is reported to be 1 331 Å, which lies just between that of a normal N−C single bond (1.47 Å) and that of an N=C double bond (1.27 Å) [5] The von Braun reaction is the only reaction known to date to cleave R_2N−CN bond [6] However, it requires harsh reaction conditions (strong acid or base conditions) Herein, we describe the first R_2N−CN bond cleavage reaction by a transition-metal complex, isolation of an intermediate, and establishment of a catalytic cycle involving R_2N−CN bond cleavage.

A solution of an equimolar amount of dimethylcyanamide and the silyl−iron complex **1** in toluene was irradiated with a 400-W medium pressure mercury arc lamp (Pyrex filtered) at room temperature for 12 h The ^{1}H NMR spectrum and the GC analysis of the reaction mixture showed formation of Et_3SiCN. The yield was 51% (entry 1 in Table 1), showing that the Me_2N−CN bond cleavage could be attained at room temperature using a silyl−iron complex.

Results of reactions with other cyanamides are presented in Table 1 Although the yields of Et_3SiCN are less than 50%, these N−CN bonds are cleaved (entries 2−6) The reaction of H_2NCN is noteworthy (entry 6). The H_2N−CN bond has a double bond character because H_2N−CN (cyanamide) is a tautomer of HN=C=NH (carbodiimide) Therefore H_2N−CN bond is stronger than other R_2N−CN The first H_2N−CN bond cleavage is attainable in our reaction conditions, although the efficiency remains insufficient

Table 1. Photoreaction of Cyanamides With $Cp(CO)_2Fe(SiEt_3)$[e]

$$R_2N{-}CN + Cp(CO)_2Fe(SiEt_3) \xrightarrow[\text{in toluene}]{h\nu \text{ at r t}} Et_3SiCN$$

entry	substrates	time (h)	yield (%)[a]
1	Me_2NCN	12	51
2	$^nHex_2NCN$	12	30
3	*N*-cyanopiperidine	12	41
4	*N*-cyanomorpholine	12	32
5	*N*-cyanopyrrolidine	12	26
6	H_2NCN	12	20[b]
7	$Me_2N(BH_3)CN$	24	14
8	$Me_2N(BF_3)CN$	24	0
9	$C_5H_{10}N(BH_3)CN$	24	18

[a] Yield of Et_3SiCN obtained by GC [b] In 1,2-dichloroethane

Cyanamide has a lone pair of electrons on the amino nitrogen in addition to the cyano nitrogen. Coordination of cyanamide to the 16e Fe species, $Cp(CO)Fe(SiEt_3)$, through the amino nitrogen, may reduce the activity of the iron complex toward R_2N−CN bond cleavage Derivation of cyanamide into the borane adduct at the amino nitrogen, $R_2N(BX_3)CN$ (X = H, F),[7] might engender more effective R_2N−CN bond cleavage because of masking of the lone pair electrons on the amino nitrogen The results (Table 1, entries 7−9) showed that the introduction of borane into cyanamide did not facilitate R_2N−CN bond cleavage, instead, it reduced the activity, presumably because of steric hindrance.

Reaction sequences resembling those in Scheme 1 are expected for the reaction of **1** with cyanamide. We attempted to isolate the *N*-silylated η^2-amidino iron intermediate, but the reaction of **1** with Me_2NCN was unsuccessful However, reactions with Me_2NCN of $(C_5R_5)Fe(CO)(py)(SiR'R''_2)$ (py = pyridine), considered as a synthon of a 16e complex $(C_5R_5)Fe(CO)(SiR'R''_2)$,[8] led to isolation of *N*-silylated η^2-amidino iron complexes (Scheme 2). Heating a solution containing **2** and Me_2NCN in benzene at 50 °C for 10 h yielded **3** quantitatively according to the NMR measurements, but the isolation as a solid failed In contrast, a reaction of **4** with Me_2NCN yielded **5**, which can be isolated as a dark-red powder in 85% yield. The unprecedented η^2-amidino complex was confirmed using X-ray analysis (Scheme 2).[8] The iron takes a distorted three-legged piano-stool structure with an η^2-amidino fragment. The bond distance of N1−C2 (1.327 Å) is shorter than that of a typical N−C single bond (e.g., C3−N1 = 1.455 Å, C4−N1 = 1 458 Å) and is

10.1021/ja807896b CCC: $40.75

rather similar to that of an *N*=C double bond (e.g., N2−C2 = 1.303 Å). The sum of angles around N1 is 359.9°. These structural characters are consistent with sp^2 hybridization of N1. The C3−N1−C2−N2 fragment is nearly planar with a torsion angle of 2.6(4)°. Both ^{1}H and ^{13}C NMR spectra show that the structure in a solid state is maintained in solution. Two NCH_3 resonances were observed at room temperature in ^{1}H and ^{13}C NMR, reflecting that the C2−N1 bond does not rotate freely at room temperature.

Scheme 2. Synthesis of *N*-Silylated η^2-Amidino Iron Complexes

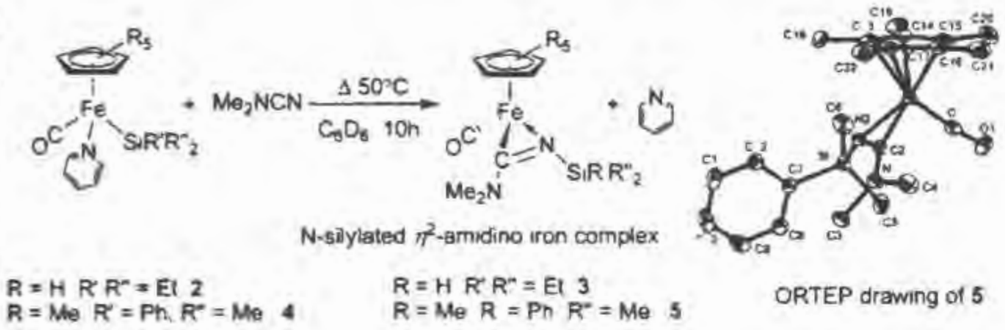

Complexes **3** and **5** were subjected to a thermal reaction. Although **5** produced a small amount of $PhMe_2SiCN$ on heating in toluene at 110 °C for 24 h, **3** gave Et_3SiCN in 62% yield on heating in benzene at 70 °C for 24 h. The results show that an *N*-silylated η^2-amidino complex is an intermediate in the N−CN bond cleavage of cyanamide.

Scheme 3. Proposed Catalytic Cycle

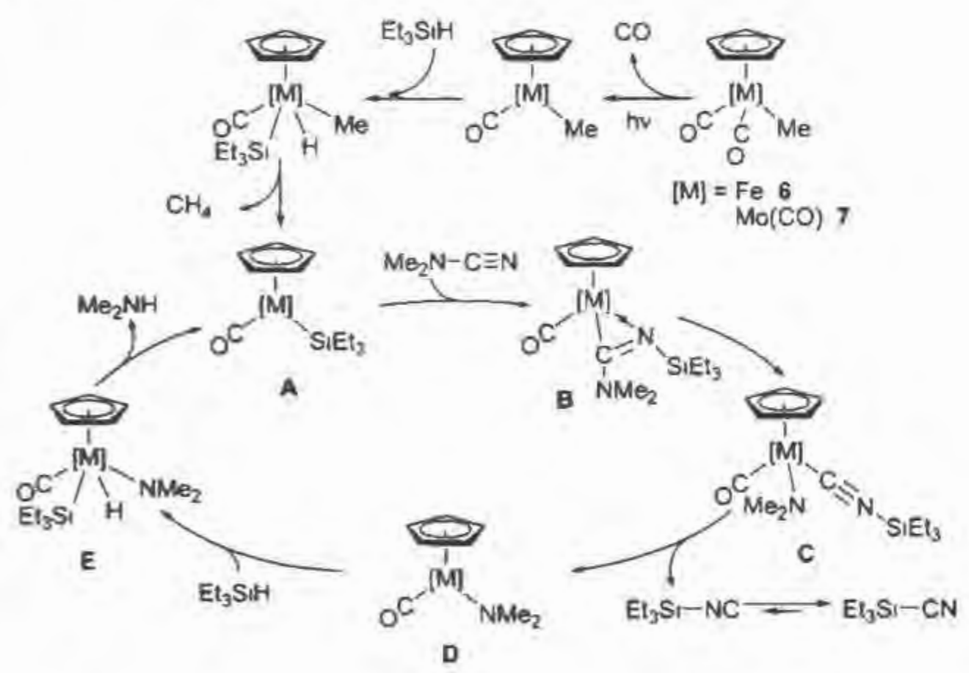

Next, we attempted to extend the stoichiometric R_2N−CN bond cleavage to a catalytic reaction. We envision a catalytic cycle for Fe and Mo complexes shown in Scheme 3 based on that of R−CN bond cleavage.[9] A 16e silyl complex **A** reacts with Me_2NCN to give an *N*-silylated η^2-amidino complex **B**, followed by N−CN bond cleavage to give **C**, and dissociation of silyl isocyanide to give a 16e amido complex **D**. It may react with Et_3SiH to produce **E**, then reductive elimination of Me_2NH regenerates **A** to complete the catalytic cycle. To produce 16e intermediate **A**, $CpMo(CO)_3$-Me (**7**) or $CpFe(CO)_2Me$ (**6**) seem to be good precursors because successive CO dissociation, Et_3Si−H oxidative addition, and CH_4 reductive elimination will give **A**.

Results of reactions of Me_2NCN and Et_3SiH in the presence of a catalytic amount of Fe complex **6** or Mo complex **7** are presented in Table 2. Entry 1 there shows that the Fe complex does not work as a catalyst, whereas the Mo complex does, under photoirradiation conditions (entry 2). The Mo complex shows catalytic activity even under thermal conditions (entries 4−6).

In conclusion, this paper describes the first example of inert N−CN bond cleavage by a transition metal complex. An *N*-silylated η^2-amidino complex can be isolated. It was shown to be an intermediate in the reaction pathway. Catalytic N−CN bond cleavage reaction was also attained using a methyl molybdenum complex. Studies are underway to design transition-metal catalysts to improve activity and to elucidate the reaction mechanism.

Table 2. Catalytic Cleavage[a] Under Photolysis or Heating

$$Me_2NCN + Et_3SiH \xrightarrow[\text{in toluene}]{\text{cat. 6 or 7}} Et_3SiCN$$

entry	cat.	[M] [N] [Si][b]	conditions	temp/°C	time/h	TON[c]
1	**6**	1 10 10	hν	25	24	0.4
2	**7**	1 10 10	hν	25	24	1.4
3	**6**	1 1 1	Δ	80	12	0
4	**7**	1 1 1	Δ	100	12	0.52
5[d]	**7**	1 10 1000	Δ	100	48	7.9
6[d]	**7**	1 1000 5000	Δ	100	120	32.3

[a] No Me_2N−CN bond cleavage took place in the absence of **6** or **7**. [b] Molar ratio of a transition metal complex, Me_2NCN, and Et_3SiH. [c] Calculated from the isolated Et_3SiCN. The values are based on the concentration of a transition metal complex. [d] In free solvent.

Acknowledgment. This work was supported by a Grant-in-Aid for Science Research on Priority Area (No. 20036043, Synergistic Effect of Elements) from the Ministry of Education, Culture, Sports, Science and Technology.

Supporting Information Available: Detailed experimental procedures and the characterization of products. This material is available free of charge via the Internet at http://pubs.acs.org.

References

(1) See, for example, (a) Ritleng, V.; Sirlin, C.; Pfeffer, M. *Chem. Rev.* **2002**, *102*, 1731–1770. (b) Dyker, G. *Angew. Chem. Int. Ed.* **1999**, *38*, 1698–1712. (c) Naota, T.; Takaya, H.; Murahashi, S.-I. *Chem. Rev.* **1998**, *98*, 2599–2660. (d) Zhang, Y.; Li, C.-J. *Angew. Chem., Int. Ed.* **2006**, *45*, 1949–1952. (e) Ma, K.; Piers, W. E.; Parvez, M. *J. Am. Chem. Soc.* **2006**, *128*, 3303–3312. (f) Kakiuchi, F.; Kan, S.; Igi, K.; Chatani, N.; Murai, S. *J. Am. Chem. Soc.* **2003**, *125*, 1698–1699. (g) Goosen, L. J. *Angew. Chem., Int. Ed.* **2002**, *41*, 3775–3778. (h) Arndtsen, B. A.; Bergman, R. G.; Mobley, T. A.; Peterson, T. H. *Acc. Chem. Res.* **1995**, *28*, 154–162. (i) Crabtree, R. H. *J. Organomet. Chem.* **2004**, *689*, 4083–4091.

(2) See for example: (a) Jun, C.-H. *Chem. Soc. Rev.* **2004**, *33*, 610–618. (b) Rybtchinski, B.; Milstein, D. *Angew. Chem. Int. Ed.* **1999**, *38*, 870–883. (c) Storsberg, J.; Yao, M.-L.; Ocal, N.; De Meijere, A.; Adam, A. E. W.; Kaufmann, D. E. *Chem. Commun.* **2005**, 5665–5666. (d) Nakazawa, H.; Kawasaki, T.; Miyoshi, K.; Suresh, C. H.; Koga, N. *Organometallics* **2004**, *23*, 117–126. (e) Chianese, A. R.; Zeglis, B. M.; Crabtree, R. H. *Chem. Commun.* **2004**, 2176–2177. (f) Terao, Y.; Wakui, H.; Satoh, T.; Miura, M.; Nomura, M. *J. Am. Chem. Soc.* **2001**, *123*, 10407–10408.

(3) (a) Lei, Y.; Wrobleski, A. D.; Golden, J. E.; Powell, D. R.; Aubé, J. *J. Am. Chem. Soc.* **2005**, *127*, 4552–4553. (b) Fran, L.; Yang, L.; Guo, C.; Foxman, B. M.; Ozerov, O. V. *Organometallics* **2004**, *23*, 4778–4787. (c) Yao, M.-L.; Adiwidjaja, G.; Kanfmann, D. E. *Angew. Chem., Int. Ed.* **2002**, *41*, 3375–3378. (d) Niklas, N.; Heinemann, F. W.; Hampel, F.; Alsfasser, R. *Angew. Chem., Int. Ed.* **2002**, *41*, 3386–3388.

(4) See for example: (a) Maercker, A. *Angew. Chem. Int. Ed. Engl.* **1987**, *26*, 972–989. (b) Kabalka, G. W.; Yao, M.-L.; Borella, S.; Goins, L. K. *Organometallics* **2007**, *26*, 4112–4114. (c) Szu, P.-h.; He, X.; Zhao, L.; Liu, H.-w. *Angew. Chem., Int. Ed.* **2005**, *44*, 6742–6746. (d) Casado, F.; Pisano, L.; Farriol, M.; Gallardo, I.; Marquet, J.; Melloni, G. *J. Org. Chem.* **2000**, *65*, 322–331.

(5) Cunningham, I. D.; Light, M. E.; Hursthouse, M. B. *Acat Crystallogr., Sect. C Cryst. Struct. Commun.* **1999**, *55*, 1833–1835.

(6) Vliet, E. B. *Org. Synth.* **1941**, *1*, 201–202.

(7) Syntheses of boran adduct of cyanamide and confirmation of the adduct at the amino nitrogen have been reported: Henneike, H. F.; Drago, R. S. *Inorg. Chem.* **1968**, *7*, 1908–1915.

(8) Selected bond lengths (Å) and angles (deg): C2−N1, 1.327(3); C2−N2, 1.303(2); C3−N1, 1.455(3); C4−N1, 1.458(3); C2−N1−C3, 123.4(2); C2−N1−C4, 119.5(2); C3−N1−C4, 117.0(2); Fe1−C2−N1, 149.40(17); Fe1−C2−N2, 78.31(15); N1−C2−N2, 132.3(3); Fe1−N2-Si1, 134.04(12); Fe1−N2−C2, 63.04(13); Si1−N2−C2, 141.24(19).

(9) (a) Nakazawa, H.; Kamata, K.; Itazaki, M. *Chem. Commun.* **2005**, 4004–4006. (b) Nakazawa, H.; Itazaki, M.; Kamata, K.; Ueda, K. *Chem.−Asian J.* **2007**, *2*, 882–888.

JA807896B